Oligosaccharide Analogues of Polysaccharides

Part 20[1])

NMR Analysis of Templated Cellodextrins Possessing Two Parallel Chains: A Mimic for Cellulose I?

by **Bruno Bernet**, **Jinwang Xu**, and **Andrea Vasella***

Laboratorium für Organische Chemie, ETH-Zentrum, Universitätstrasse 16, CH-8092 Zürich

Für *Albert*, den Meister des Komplexen an sich

Naphthalene-1-ethanol and naphthalene-1,8-diethanol carrying one or two glycosidically bonded cellodextrin chains, **T-x** and **T-x-x**, resp. (**x** = 1–4, 8) were analyzed by NMR spectroscopy. For solutions in (D_6)DMSO and (D_5)pyridine, analysis was based on a comparison of chemical shifts, coupling constants, temperature dependence of OH signals, and ROESY spectra of the singly and doubly substituted **T-x** and **T-x-x**. The characteristic strong intrachain inter-residue O(3)–H···O(5′) H-bond of celluloses was detected in the singly and doubly substituted naphthalenes. Also detected was a weakly persistent flip-flop H-bond between HO(2′) and HO(6). Weak interchain interactions were, however, observed only for the units closest to the link of **T-x-x** in (D_6)DMSO and for parallel units of **T-1-1** and **T-3-3** in (D_5)pyridine. Interchain interactions in **T-x-x** are stronger in (D_5)pyridine than in (D_6)DMSO and decrease with increasing distance from the link. The solid-state CP/MAS ^{13}C-NMR spectra of **T-x-x** were compared with those of **T-x** and of celluloses. The spectrum of **T-8** and, surprisingly, also of **T-8-8** strongly resembles that of cellulose II and not that of cellulose I_β, evidencing that a flexible template possessing parallel cellodextrin chains does not impose sufficient constraints on the structure of supramolecular assemblies to mimic cellulose I_β, but leads to a valuable mimic of cellulose II.

Introduction. – There are at least four polymorphs of celluloses, namely cellulose I–IV [2–4]. The two most common polymorphs are cellulose I, the native form, and cellulose II, the mercerised or regenerated form. Cellulose II is the most stable polymorph. There are two allomorphs of cellulose I. Cellulose I_α predominates in algal celluloses [5][6] and cellulose I_β in plant celluloses. Cellulose I_β is more stable than cellulose I_α [7]. Common to all celluloses is the $^4C_1$ conformation of all 1,4-linked β-D-glucopyranosyl moieties and the intrachain inter-residue O(3)–H···O(5′) H-bond[2]). Alternating glucopyranosyl units are rotated by *ca.* 180° relative to each other; thus, cellobiosyl moieties are the repeating unit of celluloses. Current three-dimensional structures of celluloses are mainly based on limited X-ray-diffraction data of polycrystalline samples (a few tens of reflections) and computer modeling. Additional models for cellulose II are derived from the crystal structure of β-cellotetraose hemihydrate and from a neutron-diffraction analysis of deuteriated cellulose II fibres (see below).

---

[1]) Part 19: [1].

[2]) For convenience, the O-atoms of the glucosyl units are numbered in the same way as the corresponding C-atoms (*e.g.*, O(3) is O–C(3)). Atoms of a vicinal glucopyranosyl unit are primed.

Crystalline cellulose I_α is reported to possess a triclinic unit cell (space group $P1$; $a = 6.74$, $b = 5.93$, $c = 10.36$ Å; $\alpha = 117$, $\beta = 113$, $\gamma = 81°$) consisting of a single chain [6] (*Fig. 1, a*). The cellobiosyl moieties of neighbouring parallel chains are staggered by $c/4$ (*ca.* 2.6 Å; *Fig. 1, b*). The conformation of the chain and the H-bond network have, however, not been elucidated.

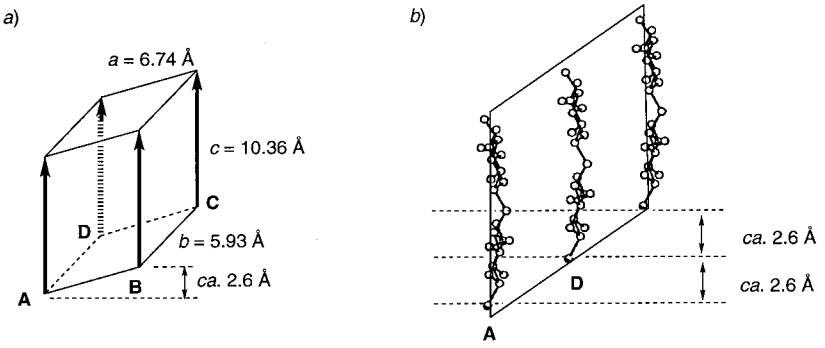

Fig. 1. *Crystal structure of cellulose* I_α. a) *Three-dimensional view according to* Sugiyama et al. [6] (arrow heads indicate reducing ends). b) *Schematic drawing of three parallel cellulose chains in the* bc *plane.*

The X-ray crystal structure of cellulose I_β [8–11] and cellulose II [12][13] has been discussed in detail. Both cellulose I_β (space group $P2_1$; $a = 8.20$, $b = 7.78$, $c = 10.34$ Å; $\gamma = 96.5°$; values of ramie cellulose [9]; *Fig. 2*) and cellulose II (space group $P1$; $a = 8.01$, $b = 9.04$, $c = 10.36$ Å; $\gamma = 117.1°$ [12]; *Fig. 3*) are monoclinic and their unit cell contains two independent chains.

In cellulose I_β (*Fig. 2, a*), the chains are positioned in the screw axis of the unit cell in a parallel array, and the centre chain **E** is staggered by $c/4$ (*ca.* 2.6 Å) with respect to the origin chain **A**. The CH_2OH groups in all chains adopt the *tg* conformation. The chains are H-bonded in two dimensions to form sheets in the *ac* plane, *i.e.*, between the chains **A** and **B**, **C** and **D**, and **E** and **F** (*Fig. 2, b*). No H-bonding is possible along the *b* axis (*bc* plane) and along the unit-cell diagonals (110 and $1\bar{1}0$ planes); in other words, there is no H-bonding between **A** and **D**, or **B** and **E**, or **A** and **E**. The intrasheet H-bond network is the same for the origin chains **A**/**B** and the centre chains **E**/**F** and is shown in *Fig. 2, c* and *d*. It consists of two intrachain inter-residue H-bonds (O(3)–H $\cdots$ O(5′) and O(2′)–H $\cdots$ O(6)), and two interchain intrasheet H-bonds in the *ac* plane of the unit cell (O($6_{\mathbf{A}}$)–H $\cdots$ O($3_{\mathbf{B}}$) and O($6'_{\mathbf{B}}$)–H $\cdots$ O($3'_{\mathbf{B}}$) for the origin chains, and O($6_{\mathbf{F}}$)–H $\cdots$ O($3_{\mathbf{E}}$), and O($6'_{\mathbf{E}}$)–H $\cdots$ O($3'_{\mathbf{F}}$) for the centre chains). All OH groups are involved in H-bonding. HO(2) acts as the H-donor in an intrachain, inter-residue H-bond to HO(6′). HO(3) and HO(6) are both H-donors and H-acceptors: HO(3) donates an intrachain inter-residue H-bond to O(5′) and accepts an interchain H-bond from HO(6), and HO(6) accepts an intrachain, inter-residue H-bond and donates an interchain H-bond.

According to the X-ray analysis [12][13], the centre chain **E** of cellulose II is antiparallel to the origin chains **A** to **D** with a $c/4$ phase shift (2.2 Å between C(1) of chain **A** and C(4) of chain **E**; *Fig. 3, a*). The calculated distances are 4.4 Å between the chains **A** and **E**, and 7.4 Å between the chains **B** and **E** [14] (*Fig. 3, b*). The X-ray data

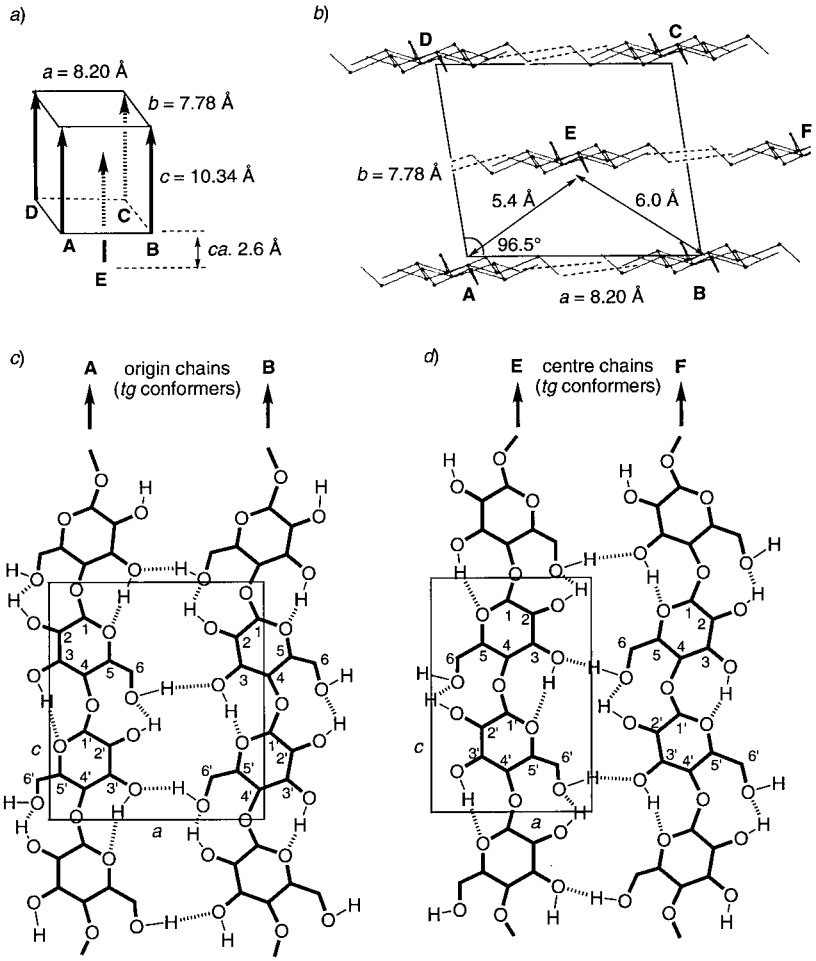

Fig. 2. *Crystal structure of cellulose* I_β. a) *Three-dimensional view of the unit cell* (arrow heads indicate reducing ends). The axis connecting the two external glycosidic oxygen atoms of the cellobiosyl residue in chain **E** is located on the cross point of the two diagonals. b) *Unit cell viewed perpendicular to the* ab *plane* (along the fiber axis *c*) [9]. The dashed lines indicate intermolecular H-bonding. The distances between **A** and **E** and between **B** and **E** are obtained by calculation [14]. c) *Schematic view of the origin chains* **A** *and* **B** *in the* ac *plane.* d) *Schematic view of the centre chains* **E** *and* **F** *in a plane parallel to the* ac *plane.* Intrasheet H-bonds in *c* and *d* indicated by hashed lines.

led to the conclusion that the CH_2OH groups of the centre chains adopt a *tg* conformation as in cellulose I_β, while those of the origin chains adopt a *gt* conformation. However, solid-state CP/MAS ^{13}C-NMR spectroscopy evidenced the *gt* conformation of all glucosyl units of cellulose II [15] (see also *Sect. 5* of *Results*). The similarity of the crystal structures of β-cellotetraose hemihydrate and cellulose II [16][17], on the one hand, and molecular-dynamics calculations of cellulose II [18], on the other hand, led to new models of cellulose II possessing the *gt* conformation in both the origin and the

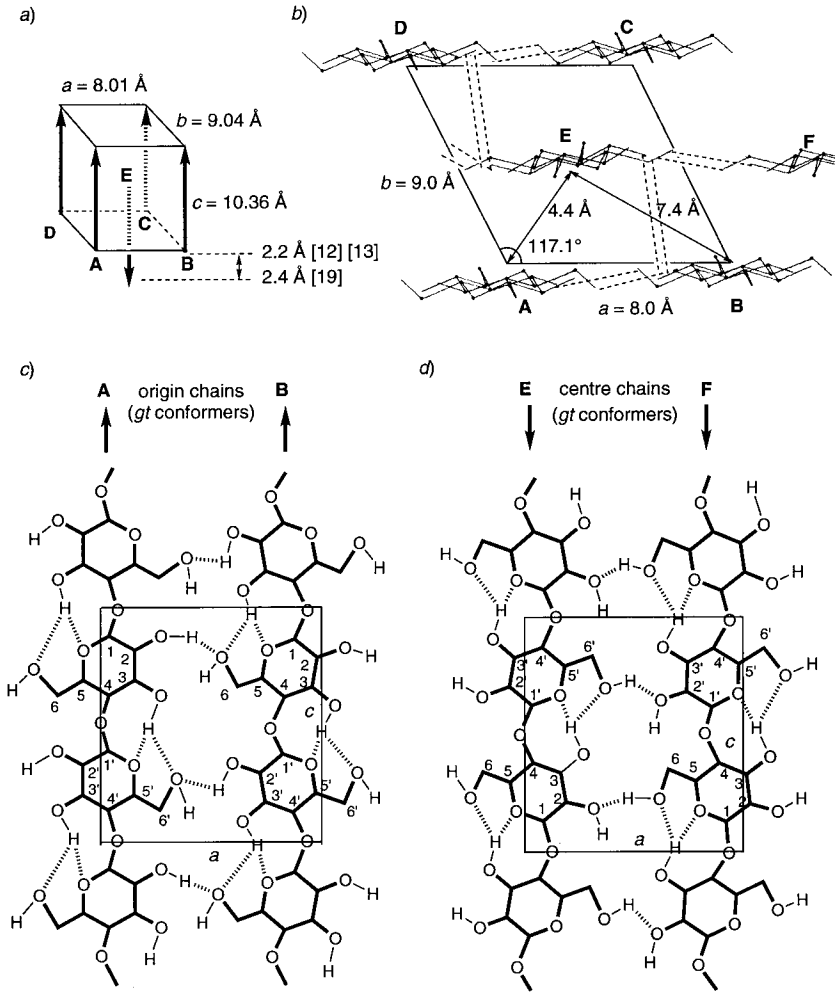

Fig. 3. *Crystal structure of cellulose II*. a) *Three-dimensional view of the unit cell* (arrow heads indicate reducing ends). The axis connecting the two external glycosidic O-atoms of the cellobiosysl residue in chain **E** is located on the cross point of the two diagonals. b) *Unit cell viewed perpendicular to the* ab *plane* (along the fiber axis *c*) [12]. The dashed lines indicate intermolecular H-bonding. The distances between **A** and **E** and between **B** and **E** have been obtained by calculation [14]. c) *Schematic view of the origin chains* **A** *and* **B** *in the* ac *plane*. d) *Schematic view of the centre chains* **E** *and* **F** *in a plane parallel to the* ac *plane*. Intrasheet H-bonds, as proposed by *Langan et al*. [19] are indicated in *c* and *d* by hashed lines.

centre chains. A recent neutron-diffraction analysis of deuteriated cellulose II fibers by *Langan et al*. [19] confirmed the unit-cell parameters of the X-ray analysis. Refinement of the data from the diffraction analysis, however, led to a model possessing exclusively the *gt* conformation that is paralleled by a slightly enhanced phase shift between the origin and centre chains (2.4 instead of 2.2 Å), and a completely different H-bonding network. Particularly, the *gt* conformation does not allow the inter-residue

O(2)–H···O(6′) H-bond which is characteristic for cellulose I_β (see above). The H-bonding network derived from the neutron diffraction is substantially different from the network postulated for the other two models postulating a *gt* conformation (see [19]), and its compatibility with the CP/MAS ^{13}C-NMR data [15] justifies a more detailed discussion.

The *gt* conformation of the origin and centre chains of *Langan*'s model [19] favours an inter-residue bifurcated H-bond with HO(3) as the H-donor and O(5′) and O(6′) as H-acceptors (*Fig. 3*, *c* and *d*). The O(3)···O(5′) distance is shorter (2.84 Å for the origin and 2.91 Å for the centre chains) than the O(3)···O(6′) distance (3.32 Å for the origin and 3.09 Å for the centre chains), evidencing asymmetric bifurcated H-bonds. HO(2) and HO(6) do not form an intramolecular H-bond; they are involved in intermolecular H-bonds to both the origin and centre chains. HO(2) is the H-donor of the intrasheet H-bond to HO(6) between the origin chains ($O(2_{\mathbf{A}})$–H···$O(6_{\mathbf{B}})$ and ($O(2'_{\mathbf{B}})$–H···$O(6'_{\mathbf{A}})$ H-bonds in *Fig. 3*, *c*), and the H-acceptor of a similar H-bond between the centre chains ($O(6_{\mathbf{F}})$–H···$O(2_{\mathbf{E}})$ and ($O(6'_{\mathbf{E}})$–H···$O(2'_{\mathbf{F}})$ H-bonds in *Fig. 3*, *d*). Intersheet H-bonds occur along the unit-cell (110) diagonal plane between the chains **D**, **E**, and **B** (*Fig. 4*). There is a H-bond between the HO(2) groups with HO(2) of the centre chains as H-donor and HO(2) of the origin chains as the H-acceptor, and a

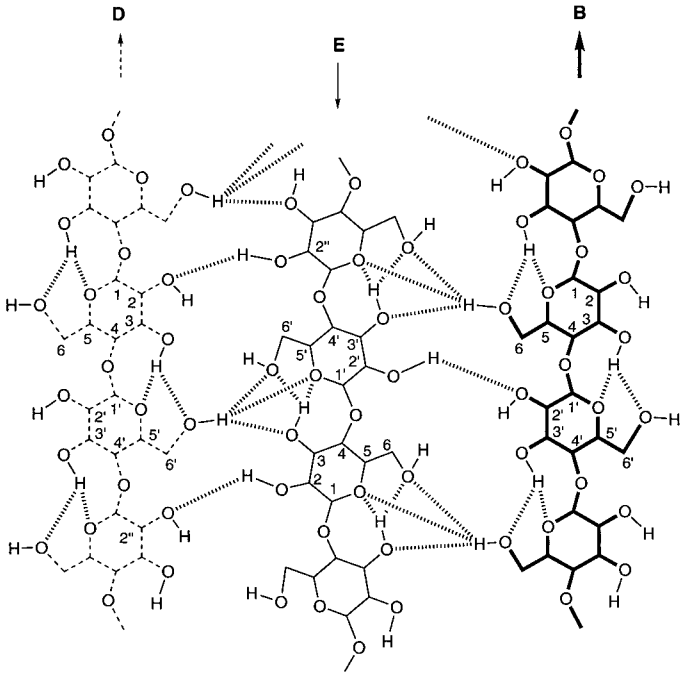

Fig. 4. *Schematic view of the chains* **D**, **E**, *and* **B** *of cellulose II in the (110) plane*. The different lines of the backbone (**B**: bold, **E**: normal, and **D**: dashed lines) indicate the increasing distance from the viewer. The sheets are parallel with an angle of *ca*. 32° to the (110) plane. Intramolecular and intermolecular intersheet H-bonds, as proposed by *Langan et al.* [19] are indicated by hashed lines (intermolecular intrasheet H-bonds are omitted for clarity).

tetravalent H-bond [20] with HO(6) of the origin chains as H-donor and O(3), O(5′), and O(6′) of the centre chains as H-acceptors. Thus, O(5′) and O(6′) act as H-acceptors of both the inter-residue H-bond of HO(3) and the intersheet H-bond of HO(6). There are no intersheet H-bonds along the *bc* plane (between chains **A** and **D**) and the $1\bar{1}0$ diagonal plane (between chains **A** and **E**).

According to *Langan*'s model [19], cellulose II differs from cellulose I_β mainly by the antiparallel orientation of the origin and centre chains, the *gt* conformation, and the intersheet H-bonds.

So far, no model compound is known for native celluloses. The parallel orientation of the origin and centre chains that is specific for native celluloses might be enforced by attaching two parallel cellodextrin chains to a template[3]). However, even a parallel orientation of the chains will not necessarily lead to a model of native celluloses, since parallel chains are also found within the sheets of cellulose II (see *Fig. 3*).

We have described the design and synthesis of the templated cellodextrins **T-x** and **T-x-x** (**x** = 1–4, 8; *Fig. 5*; see *Sect. 1* of *Results* for the nomenclature) as potential model compounds for native celluloses [1]. The rather flexible template should allow for the required distance between the origin and centre chains of cellulose I_β (5.4 Å between **A** and **E**; 6.0 Å between **B** and **E**; *Fig. 2*, *b*). It should also allow for at least a partial phase shift between the origin and centre chains.

Since the centre chain **E** forms H-bonds with the origin chains **B** and **D** in cellulose II, but not in cellulose I, we have analyzed the interchain H-bonding of **T-x-x** in solution[4]); we have also compared the CP-MAS solid-state ^{13}C-NMR spectra of **T-x-x** and **T-x** with those of cellulose I_α, I_β, and II.

Results and Discussion. – 1. *Nomenclature for the Templated Cellodextrins and Their Glucopyranosyl Units.* To facilitate a comparison of the NMR data, the model compounds possessing one or two cellodextrin chains are represented by **T-x** and **T-x-x**, respectively, with **x** and **x-x** denoting the number of glucosyl residues in the single- and double-chain compounds (*Fig. 5*,*a*). The glucopyranosyl units of **T-x** and **T-x-x** (**x** = 2–4, 8) are labelled *a*, *b*, *b*′, and *c* (*Fig. 5*, *b*): unit *a* is the terminal moiety of the oligosaccharide (*i.e.*, the one most remote from the naphthalene moiety); unit *b* is the internal glucosyl residue next to *a*, while the other internal units in the tetra- and octaoses are labelled *b*′; unit *c* is the residue closest to the naphthalene moiety. The units of the glucosides **T-1** and **T-1-1** are not labelled, but included in the unit *a* family. The labels of the glycosyl residues reflect regularities in the NMR spectra, as discussed below.

2. *Conformation of the CH_2CH_2O Moiety of* **T-x** *and* **T-x-x**. Force-field calculations have shown that small energy barriers[5]) allow an easy interconversion of the conformers of 1-(2-methoxethyl)naphthalene and 1,8-bis(2-methoxethyl)naphthalene

---

[3]) There are many examples where two peptide chains have been attached to a template to study their interaction (for leading refs., see [21][22]).

[4]) To the best of our knowledge, no investigations of H-bond interactions between templated oligosaccharide chains have been published, although lactosyl moieties have been attached to glycerol [23] and TRIS [24] and cellobiosyl moieties to threitols [25].

[5]) The barriers amount to 2.7 and 4.5 kcal/mol for rotation about the $Ar-CH_2$ bond of the mono- and the dimethyl ether, respectively, and to 2 kcal/mol for rotation about the CH_2-CH_2 bond.

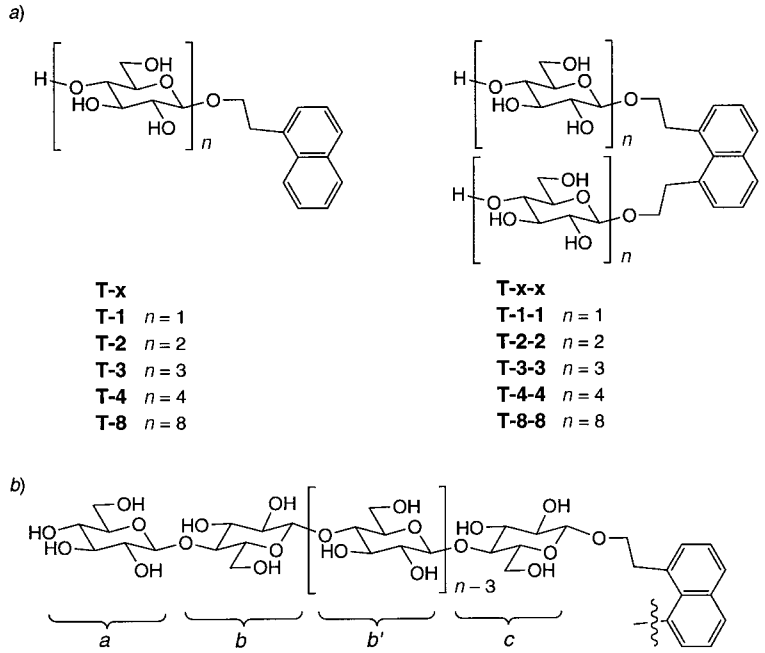

Fig. 5. a) *Labelling of the single- and double-chain glucosides and cellodextrins.* b) *Labelling of the glucopyranosyl units of* **T-x** *and* **T-x-x** (**x** = 2–4, 8).

[1]. As expected from their stereotopic relation, the benzylic and the homobenzylic H-atoms of both compounds each resonate as a *triplet* with $J(CH_2,CH_2) = 7.2$ Hz. This does not allow to assign a preferred conformation, and to detect differences between the single and double chained compounds.

The H-atoms of the individual CH_2 groups of the CH_2CH_2O moieties of **T-x** and **T-x-x** (**x** = 1–4, 8) are diastereotopic; the CH_2CH_2O groups should give rise to an *ABXY* system. The two CH_2CH_2O groups of **T-x-x** are homotopic, and one expects a single *ABXY* system, as long as there are no significantly strong interchain H-bonds. In all cases, we have only observed a single *ABXY* system. Hindered rotation about the CH_2-CH_2 bond(s) of **T-x** and **T-x-x**, conditioned by interchain H-bonding, should be indicated by the vicinal couplings between the CH_2 groups. Such a hindered rotation about the CH_2-O, CH_2-CH_2, and $CH_2-C(Ar)$ bonds of **T-x** and **T-x-x** may enhance the shift difference for individual homobenzylic and benzylic CH_2 groups.

The homobenzylic H-atoms of **T-x** and **T-x-x** are geminal to an *O*-substituent and resonate at lower field than the benzylic H-atoms (*ca.* 4.1–3.8 *vs. ca.* 3.5–3.2 ppm; *Table 1*). The chemical-shift difference between the diastereotopic H-atoms of the homobenzylic CH_2 groups is about the same for **T-x** and **T-x-x**; it depends on the solvent and decreases from 0.38–0.33 ppm in (D_5)pyridine, *via* 0.27–0.22 ppm in (D_6)DMSO to 0.24–0.14 ppm in D_2O. The shift differences of the single-chained **T-x** and the double-chained **T-x-x** in a given solvent differ little and indicate similar surroundings of the homobenzylic H-atoms.

Table 1. *^{1}H-NMR Chemical Shifts and Coupling Constants for the CH_2CH_2 Moieties of* **T-x** *and* **T-x-x** (**x** = 1–4, 8)

	Solvent	δ(ArCH$_2$C*H*) [ppm] (multiplicity, *J* [Hz])	δ(ArCH$_2$C*H*′) [ppm] (multiplicity, *J* [Hz])	$\Delta\delta$(ArCH$_2$CH_2) [ppm]	δ(ArCH_2) (multiplicity, *J* or $\Delta\delta^{t7}$) [Hz])
T-1	D_2O	4.14 (*dt*, *J* = 10.2, 7.2)	3.94 (*dt*, *J* = 10.2, 7.3)	0.20	3.36 (*t*, *J* ≈ 7.3)
	(D_6)DMSO	4.02 (*ddd*, *J* = 9.8, 8.1, 7.0)	3.80 (*ddd*, *J* = 9.7, 8.4, 6.8)	0.22	3.38–3.31 (*AB* of *ABMX*, 50)
	(D_5)pyridine	4.40 (*ddd*, *J* = 9.5, 8.3, 7.8)	4.02 (*ddd*, *J* = 9.7, 8.4, 7.1)	0.38	3.53–3.44 (*AB* of *ABMX*, 45)
T-2	D_2O	4.07 (br. *q*, *J* ≈ 8.0)	3.86 (*dt*, *J* ≈ 9.5, 7.2)	0.21	3.41–3.37[a])
	(D_6)DMSO	4.03 (*ddd*, *J* = 9.8, 8.1, 7.1)	3.80 (*ddd*, *J* = 9.7, 8.3, 6.6)	0.23	3.37–3.27[a])
	(D_5)pyridine	4.34 (br. *q*, *J* ≈ 8.1)	3.98 (*dt*, *J* ≈ 9.5, 6.7)	0.36	3.53–3.44 (*AB* of *ABMX*, 46)
T-3	D_2O	4.18 (*dt*, *J* = 10.2, 7.2)	3.99 (*dt*, *J* = 10.4, 7.3)	0.19	3.40 (*t*, *J* ≈ 7.2)
	(D_6)DMSO	4.03 (*ddd*, *J* = 9.6, 8.2, 6.7)	3.80 (*ddd*, *J* = 9.8, 8.2, 6.8)	0.23	3.42–3.26[a])
	(D_5)pyridine	4.38–4.30[a])	4.04–3.97[a])	0.34	3.54–3.45 (*AB* of *ABMX*, 45)
T-4	D_2O	4.17 (*dt*, *J* ≈ 10.0, 7.3)	3.98 (*dt*, *J* ≈ 10.2, 7.1)	0.19	3.50–3.36[a])
	(D_6)DMSO	4.02 (*ddd*, *J* = 9.8, 8.1, 6.8)	3.82–3.72[a])	0.25	3.41–3.27[a])
	(D_5)pyridine	4.33 (*ddd*, *J* = 9.7, 7.8, 7.0)	4.02–3.95[a])	0.35	3.53–3.43 (*AB* of *ABMX*, 52)
T-8	(D_6)DMSO	4.03 (*ddd*, *J* = 9.7, 8.4, 7.0)	3.83–3.66[a])		3.44–3.26[a])
T-1-1	D_2O	4.00 (*dt*, *J* = 9.9, 7.5)	3.80–3.73[a])	0.24	3.44 (*t*, *J* ≈ 7.5)
	(D_6)DMSO	3.95 (*td*, *J* ≈ 9.7, 6.3)	3.68 (*td*, *J* ≈ 9.7, 6.8)	0.27	3.525–3.43 (*AB* of *ABMX*, 48)
	(D_5)pyridine	4.30 (*td*, *J* ≈ 9.2, 6.8)	3.93 (*td*, *J* ≈ 9.6, 6.4)	0.37	3.75–3.65 (*AB* of *ABMX*, 49)
T-2-2	D_2O	4.03 (*dt*, *J* ≈ 9.8, 7.5)	3.82–3.76[a])	0.21	3.51–3.41[a])
	(D_6)DMSO	3.95 (*td*, *J* ≈ 9.7, 6.2)	3.74–3.66[a])	0.25	3.53–3.39 (*AB* of *ABMX*, 69)
	(D_5)pyridine	4.26–4.22[a])	3.94–3.88[a])	0.33	3.73–3.63 (*AB* of *ABMX*, 49)
T-3-3	D_2O	4.02 (*dt*, *J* = 10.0, 7.5)	3.83–3.77[a])	0.22	3.51–3.41[a])
	(D_6)DMSO	3.95 (*td*, *J* ≈ 9.6, 5.9)	3.80–3.66[a])		3.53–3.39 (*AB* of *ABMX*, 70)[a])[b])
	(D_5)pyridine	4.34–4.23[a])	3.93 (*td*, *J* ≈ 9.5, 6.7)	0.35	3.75–3.65 (*AB* of *ABMX*, 49)
T-4-4	D_2O	4.01 (*dt*, *J* ≈ 9.9, 7.4)	3.82–3.76[a])	0.22	3.49–3.38[a])
	(D_6)DMSO	3.95 (*td*, *J* ≈ 9.6, 6.3)	3.81–3.66[a])		3.63–3.24[a])
T-8-8	(D_6)DMSO	3.99–3.92[a])	3.82–3.66[a])		3.63–3.24[a])

[a]) Signal partially overlapped by other signals. [b]) Estimated value (similar signal pattern as **T-2-2** in (D_6)DMSO).

The benzylic H-atoms of **T-x** and **T-x-x** appear either as a *triplet* or as an *AB* system additionally split by couplings with the homobenzylic H-atoms (*Table 1*). The isochronous benzylic H-atoms of **T-1**, **T-3**, and **T-1-1** in D_2O resonate as a *triplet*. The benzylic H-atoms of **T-x** (**x** = 1 – 4) and **T-x-x** (**x** = 1 – 3)[6]) in (D_5)pyridine and **T-1-1** in (D_6)DMSO resonate as an *AB* system with a nearly constant $\Delta\delta^t$ value of *ca.* 50 Hz[7]), while the benzylic H-atoms of **T-2-2** and **T-3-3** in (D_6)DMSO show an *AB* system with a larger $\Delta\delta^t$ value of *ca.* 70 Hz. This indicates a similar conformation for **T-x-x** (**x** = 1 – 3) in (D_5)pyridine and a different conformation for **T-1-1** *vs.* **T-x-x** (**x** = 2, 3)[6]) in (D_6)DMSO induced by interchain interactions of the cellobiosyl and cellotriosyl moieties.

The vicinal couplings between the homobenzylic and the benzylic H-atoms of **T-x** vary between 6.6 and 7.8 Hz, independently of the solvent, and evidence similar conformational equilibria (*Table 1*). The vicinal couplings of **T-x-x**, however, show a characteristic dependence on the solvent. In D_2O, the coupling values of **T-x-x** are *ca.* 7.5 Hz as for **T-x**. For **T-x-x** in (D_6)DMSO and (D_5)pyridine, however, one observes a large and a medium vicinal coupling (*ca.* 9.5 and 5.9 – 6.8 Hz). This difference between **T-x** and **T-x-x** is best rationalised by assuming a preferred antiperiplanar arrangement of the CH_2-C_{Ar} and the CH_2-O bond of **T-x** in all solvents, and of **T-x-x** in D_2O, while a synclinal arrangement of these bonds is preferred by **T-x-x** in (D_6)DMSO and (D_5)pyridine. This evidences an interaction between the chains of **T-x-x** in (D_6)DMSO and (D_5)pyridine, but not in D_2O.

In the ^{13}C-NMR spectra, the signal of the homobenzylic C-atom of **T-x** (**x** = 1 – 4, 8) in D_2O appears at 70.2 – 70.3 ppm, 1.1 – 1.3 ppm downfield to the corresponding signal of **T-x** in (D_6)DMSO (*Table 2*). Constant downfield shifts are observed for the homobenzylic C-atom of **T-x-x** in both solvents relative to those of **T-x** ($\Delta\delta$ *ca.* 1.0 ppm in D_2O and 1.2 ppm in (D_6)DMSO). The benzylic C-atom of **T-x-x** in D_2O and (D_6)DMSO resonates at 36.48 – 36.59 ppm, 4.2 – 4.3 ppm downfield to the benzylic C-atom of **T-x** in D_2O, and 3.6 – 3.85 ppm downfield to the benzylic C-atom of **T-x** in (D_6)DMSO. Such $\Delta\delta$ values are characteristic for 1-mono- and 1,8-disubstituted naphthalene derivatives and are also observed for 1-(2-methoxyethyl)naphthalene and 1,8-bis(2-methoxyethyl)naphthalene in $CDCl_3$ ($\Delta\delta(ArCH_2CH_2) = 0.7$, $\Delta\delta(ArCH_2) =$ 3.9 ppm) [1].

Thus, the ^{1}H-NMR data of the homobenzylic and benzylic H-atoms of **T-x-x** evidence a conformational difference relative to **T-x** in (D_6)DMSO and (D_5)pyridine, but not in D_2O. The small difference between the $\Delta\delta$ values for the homobenzylic and benzylic C-atoms of **T-x-x** and **T-x** in (D_6)DMSO and D_2O ($\Delta\Delta\delta < 0.7$ ppm) do not disagree with this conformational difference.

3. *Analysis of Melting Points, Solubility, and Chromatographic Behaviour of* **T-x** *and* **T-x-x**. Melting points, solubility, and chromatographic behaviour of **T-x** and **T-x-x** should be influenced by H-bonds. As expected, the melting points increase with

---

[6]) Overlapping signals for **T-x-x** (**x** = 2 – 4) in D_2O prevented an analogous analysis.

[7]) The chemical-shift difference $\Delta\delta^t$ between the terminal lines of the *AB* system was used for the analysis. The identical $\Delta\delta^t$ value for **T-1-1** in (D_6)DMSO and in (D_5)pyridine cannot be taken as evidence of a similar conformation since this value is influenced by the solvent.

Table 2. *^{13}C-NMR Chemical Shifts* [ppm] *for the CH_2CH_2 Moieties of* **T-x** *and* **T-x-x** (**x** = 1–4, 8). In parentheses: $\Delta\delta = \delta$(**T-x-x**) – δ(**T-x**).

Compound	Solvent	$\delta(ArCH_2CH_2)$ ($\Delta\delta$)	$\delta(ArCH_2)$ ($\Delta\delta$)
T-1	D_2O	70.20	32.38
	(D_6)DMSO	69.01	32.74
T-2	D_2O	70.24	32.38
	(D_6)DMSO	69.13	32.68
T-3	D_2O	70.29	32.39
	(D_6)DMSO	69.09	32.65
T-4	D_2O	70.19	32.74
	(D_6)DMSO	69.09	32.65
T-8	(D_6)DMSO	[a])	32.24
T-1-1	D_2O	71.19 (0.99)	36.59 (4.21)
	(D_6)DMSO	70.23 (1.22)	36.58 (3.84)
T-2-2	D_2O	71.25 (1.01)	36.58 (4.20)
	(D_6)DMSO	70.29 (1.16)	36.48 (3.80)
T-3-3	D_2O	71.22 (0.93)	36.56 (4.17)
	(D_6)DMSO	70.26 (1.17)	36.48 (3.83)
T-4-4	D_2O	71.14 (0.95)	36.53 (4.29)
	(D_6)DMSO	70.31 (1.22)	36.25 (3.60)
T-8-8	(D_6)DMSO	70.35	36.56 (3.82)

[a]) Hidden by the noise.

increasing chain length of **T-x** and **T-x-x** (*Table 3*). The double-chain compounds **T-x-x** possess higher melting points than their single-chain analogues **T-x**.

T-x-x (**x** = 1–4) show a higher solubility in H_2O than **T-x**; this is particularly evident for **T-3-3** and **T-4-4** *vs.* **T-3** and **T-4** (54–56 *vs. ca.* 3 g/l; *Table 3*). This may be taken as evidence against strong interchain H-bonds of **T-x-x** (**x** = 1–4). The poor solubiliy of **T-x** (**x** = 1–4) in H_2O presumably reflects the influence of the lipophilic template moiety, as evidenced by a comparison with the solubility of cellobiose (210 g/l at 25° [26]), cellotriose (very soluble in cold H_2O [27]), and cellotetraose (130 g/l in warm H_2O

Table 3. *Melting Points, Solubility, and Chromatographic Behaviour of* **T-x** *and* **T-x-x** (**x** = 1–4, 8)

	Mol. mass [g/mol]	M.p. [°]	Solubility in H_2O at 24° [g/l]	Solubility in DMSO at 24° [g/l]	R_f[a])	t_R[b]) [min]
T-1	334	122–124	26	> 40	0.18	11.5
T-2	496	186–189	28	> 40	0.21	10.8
T-3	658	249–255	*ca.* 3	> 40	0.23	10.1
T-4	820	290	*ca.* 3	> 40	0.25	9.7
T-8	1468	> 300	0	*ca.* 3		
T-1-1	540	184–187	48	> 40	0.31	6.1
T-2-2	864	199–201	53	> 40	0.36	5.6
T-3-3	1188	> 300	56	> 40	0.38	5.4
T-4-4	1512	> 300	54	> 40	0.40	5.1
T-8-8	2810	> 300	0	*ca.* 3		

[a]) Reversed-phase TLC (H_2O/MeOH 1:1). [b]) Reversed-phase analytical HPLC (H_2O/MeOH 1:1; flow rate: 1 ml/min).

[27]). Like cellulose, the octaosides **T-8** and **T-8-8**, are insoluble in H_2O, sparingly soluble in pure *N*,*N*-dimethylacetamide (DMA; <3 g/l), and better soluble in the complex solvent DMA/LiCl (>20 g/l of **T-8** or **T-8-8** in DMA containing 30 g/l of LiCl as compared to 150 g/l of cellulose [28]). In DMSO, **T-x** and **T-x-x** (**x** = 1–4) are well soluble (>40 g/l), while the octaosides **T-8** and **T-8-8** are sparingly soluble (*ca.* 3 g/l).

The chromatographic behaviour of **T-x** and **T-x-x** (**x** = 1–4) on reversed-phase silica gel is as expected, with the more highly glucosylated compounds migrating faster (*Table 3*).

4. *Analysis of the NMR Spectra of* **T-x** *and* **T-x-x** *in Solution.* Considering the strong influence of solvents on H-bonding, we analyzed the NMR spectra of **T-x** and **T-x-x** in D_2O, (D_6)DMSO, and (D_5)pyridine, choosing a protic solvent and two aprotic solvents with different polarities. Unless indicated otherwise, the concentration of **T-x** was 20 mM, and of **T-x-x** was 10 mM, leading to similar concentrations of the cellodextrin units.

4.1. *In D_2O.* Under standard conditions at room temperature in D_2O, OH signals can not be observed due to a fast H/D exchange[8]). As discussed above, the analysis of the ^{1}H-NMR data of the CH_2CH_2O groups suggests weak interchain H-bonds for solutions of **T-x-x** in (D_6)DMSO and (D_5)pyridine, but not in D_2O. Nevertheless, we recorded standard D_2O spectra of the H_2O soluble **T-x** and **T-x-x** (**x** = 1–4) at 500 MHz, to characterise these compounds [1]. Spectra of *ca.* 3 mM saturated solutions were recorded of the sparingly soluble **T-3** and **T-4**. The absence of OH signals facilitated the assignment of the rather well-separated CH signals (*Table 4*). The assignment is based on homodecoupling experiments for **T-1**, **T-2**, and **T-1-1**, and on a comparison with the spectra of methyl β-cellobioside [35] and cellodextrins [36]. The coupling constants for **T-x** and **T-x-x** (**x** = 1–4) are characteristic for the β-D-configuration and the $^4C_1$-conformation of all glucopyranosyl moieties ($J(1,2) = 7.6–8.0$, $J(2,3) \approx J(3,4) \approx J(4,5) = 8.7–9.3$ Hz; see [1]). The relative chemical shifts for the diastereotopic H–C(6) (see [37][38]) of all units are identical, and the vicinal coupling constants with H–C(5) are similar ($J(5,6) = 1.0–2.1$ and 4.5–5.8 Hz), indicating more or less similar conformational equilibria (*gg*/*gt ca.* 2 : 1).

The signals for H–C(1*a*) to H–C(4*a*) of **T-2** are shifted slightly downfield as compared to the corresponding signals of **T-1** ($\Delta\delta = 0.04–0.06$ ppm), whereas the signals for H–C(5*a*) to H–C(6*a*) resonate at the same field (*Table 4*). Glucosylation leads to a downfield shift of H–C(4*c*) of **T-2** (0.15 ppm relative to δ(H–C(4)) of **T-1**). H–C(3*c*) and both H–C(6*c*) of **T-2** resonate at lower field ($\Delta\delta = 0.03–0.06$ ppm) than the corresponding signals of unit *a*, while H–C(1*c*) and H–C(2*c*) resonate at higher field ($\Delta\delta = 0.09$ and 0.02 ppm, respectively). Signals of **T-3** and **T-4** that appear at similar positions as for **T-2** ($\Delta\delta \leq 0.06$ ppm) were assigned to units *a* and *c*. The signals of the internal units *b* and *b*′ are slightly shifted downfield ($\Delta\delta \leq 0.07$ ppm) relative to the corresponding signals of unit *c*. H–C(1*c*) of **T-3** and **T-4** resonates at *ca.* 4.45 ppm, at a similar position than the other H–C(1) of **T-3** and **T-4**, but *ca.* 0.13 ppm downfield

---

[8]) Only strong intramolecular H-bonds survive in aqueous solutions. They can be detected under appropriate conditions, *e.g.*, in the presence of a cosolvent, at low temperature ($-5°$ to $-20°$), and by special NMR techniques [29–32]. A relevant example is given by the interresidue O(3)–H···O(5′) H-bonds of methyl β-cellobioside [33] and methyl β-lactoside [31], which persist in H_2O to *ca.* 50% [34].

Table 4. *Selected ^{1}H-NMR Chemical Shifts* [ppm] *for* **T-x** *and* **T-x-x** (**x** = 1–4, 8) *in D_2O.* Acetone (2.15 ppm) as internal reference.

	Unit	H–C(1)	H–C(2)	H–C(3)	H–C(4)	H–C(5)	H–C(6)
T-1[a])		4.37	3.19	3.39	3.30	3.31	3.80, 3.66
T-2[a])	*a*	4.41	3.24	3.43	3.36	3.36–3.28	3.81, 3.66
	c	4.32	3.22	3.49	3.51	3.36–3.28	3.84, 3.70
T-3	*a*	4.43[b])	3.25	3.44	3.35	3.42	3.84, 3.67
	b	4.44[b])	3.28	3.55	3.60	3.56–3.52	3.90, 3.75
	c	4.45[b])	3.23	3.53	3.57	3.47	3.86, 3.71
T-4	*a*	4.42[b])	3.25	3.44	3.35	3.50–3.36	3.85, 3.67
	b	4.46[b])	3.28[b])	3.64–3.52	3.64–3.52	3.64–3.52	3.91, 3.75
	b′	4.45[b])	3.30[b])	3.64–3.52	3.64–3.52	3.64–3.52	3.91, 3.75
	c	4.44[b])	3.23	3.64–3.52	3.64–3.52	3.50–3.36	3.85, 3.71
T-1-1[a])		4.27	3.17	3.36	3.30	3.26	3.78, 3.61
T-2-2	*a*	4.42	3.24	3.44	3.35	3.41	3.83, 3.67
	c	4.32	3.22	3.51	3.55	3.43–3.37	3.85, 3.70
T-3-3	*a*	4.43[b])	3.25	3.44	3.35	3.42	3.82, 3.67
	b	4.44[b])	3.29	3.55	3.60	3.56–3.52	3.90, 3.75
	c	4.30	3.22	3.51	3.57	3.43–3.38	3.85, 3.70
T-4-4	*a*	4.44[b])	3.25	3.45	3.35	3.49–3.38	3.83, 3.68
	b	4.45[b])	3.29[b])	3.64–3.53	3.64–3.53	3.64–3.53	3.91, 3.76
	b′	4.46[b])	3.30[b])	3.64–3.53	3.64–3.53	3.64–3.53	3.91, 3.76
	c	4.31	3.23	3.51	3.64–3.53	3.49–3.38	3.85, 3.71

[a]) Assignment based on homonuclear decoupling experiments. [b]) Assignment may be interchanged.

to H–C(1*c*) of **T-2**. Since the signal of H–C(1*c*) of **T-x-x** (**x** = 2–4) appears at the same position as H–C(1*c*) of **T-2** and **T-2-2**, the downfield shift of H–C(1*c*) of **T-3** and **T-4** is surprising. A possible rationalisation may be aggregate formation in the nearly saturated solutions of **T-3** and **T-4**. Apart from this difference between the chemical shifts of H–C(1*c*) of **T-x-x** and **T-x** (**x** = 3, 4), and that for H–C(1*a*) of **T-1-1** and **T-1** ($\Delta\delta = 0.10$ ppm), only $\Delta\delta$ values ≤ 0.05 ppm are observed for corresponding CH signals of **T-x-x** and **T-x** (**x** = 1–4).

4.2. *In DMSO.* The chemical shift of OH groups (δ(OH)), the vicinal coupling constant (J(H,OH)), and the temperature dependence of OH signals ($\Delta\delta$(OH)/ΔT) are useful parameters for the investigation of H-bonds of solutes in (D_6)DMSO [34][39]. Fully solvated OH groups, acting as H-donors in an intermolecular H-bond to (D_6)DMSO, are characterised by a downfield shift, a medium J(H,OH) value (4.5–5.5 Hz for equatorial OH groups, 4.2–4.4 Hz for axial OH groups), and a strong temperature dependence ($|\Delta\delta(\mathrm{OH})/\Delta T| > 4.5$ ppb/K). OH Groups acting as H-donors in an intramolecular H-bond are readily detected by an upfield shift, a J(H,OH) value deviating from the J(H,OH) value of a fully solvated OH group, and a weak temperature dependence ($|\Delta\delta(\mathrm{OH})/\Delta T| < 3$ ppb/K). Since the δ(OH) values are also influenced by electronic, configurational, and conformational factors, $\Delta\delta$(OH) values must be interpreted relative to an appropriate reference; increments for the calculation of δ(OH) values for fully solvated OH groups are given in [34][39]. The δ(OH) values for OH groups of monosaccharides or of terminal units of oligosaccharides are useful references for the interpretation of δ(OH) values for OH groups of internal units of oligosaccharides.

The H-bonding of β-cellobiose and methyl β-cellobioside [33] in (D_6)DMSO has been analysed [34]. Except for HO(3), all OH groups are more or less fully solvated. A completely persistent inter-residue O(3)–H···O(5′) H-bond of methyl β-cellobioside is evidenced by J(3,OH) = 1.7 Hz, δ(HO(3)) = 4.68 ppm, and $\Delta\delta$(HO(3))/ΔT = −2.6 ppb/K. This inter-residue H-bond leads to an higher acidity of the OH groups of the H-accepting (upstream) unit and to a downfield 'protonation shift' of *ca.* 0.1 ppm for HO(3′), HO(4′), and HO(6′). The stronger downfield shift of 0.2 ppm for HO(2′) both of β-cellobiose and methyl β-cellobioside indicates a weakly persistent O(6)–H···O(2′) H-bond, either unidirectional or of the flip-flop type.

^{1}H-NMR Spectra of 20 mM solutions of **T-x** (**x** = 1–4), of 10 mM solutions of **T-x-x** (**x** = 1–4), and of *ca.* 3 mM solutions of **T-8** and **T-8-8** in (D_6)DMSO were recorded at 500 MHz and 298 K. The chemical shifts and coupling constants of 0.97 and 73 mM solutions of **T-4**, and of 0.55 and 33 mM solutions of **T-4-4** are independent of the concentration, indicating the absence of intermolecular carbohydrate-carbohydrate associations in (D_6)DMSO, and evidencing that there are no chemical-shift changes due to a solute-solute association in the (D_6)DMSO solutions used for the NMR measurements.

The CH and OH resonances of **T-1** and **T-1-1** were assigned by successive spin decouplings, starting from H–C(1*a*). The assignment of the **T-4** and **T-4-4** signals is based on ^{1}H,^{1}H COSY, ^{1}H,^{13}C COSY, TOCSY, and ROESY experiments. The OH signals show intensity reductions upon addition of D_2O. The signals of the terminal unit *a* were easily differentiated from the signals of the other units, as the terminal unit possesses four OH groups. The signals for unit *b* were assigned by starting with HO(3*b*), which exhibits a ROE with H–C(1*a*). Similarly, resonances for unit *c* were assigned from ROEs between *H*–C(1*c*) and $ArCH_2CH_2$. The resonances for the other **T-x** and **T-x-x** (**x** = 2, 3, 8) were assigned by comparison with **T-4** and **T-4-4**. The assignments for **T-1**, **T-1-1**, **T-2**, and **T-2-2** agree well with the assignments for methyl β-D-glucopyranoside [40] and methyl β-cellobioside [35], respectively.

The CH signals of **T-x** and **T-x-x** strongly overlap with each other and with the signal of HDO, except for the CH signals of the terminal unit *a* and some signals of the unit *c* of **T-2** and **T-2-2**. The chemical shifts of the corresponding CH signals of unit *a* for all **T-x** and **T-x-x** are nearly identical ($\Delta\delta \leq 0.02$ ppm). Thus, these data do not evidence interchain H-bonds. In contrast to the CH signals, the OH signals of **T-x** and **T-x-x** are well-resolved, allowing a complete assignment. The δ(OH) and J(H,OH) values of **T-x** and **T-x-x** are listed in *Table 5*.

H-Bonding of the single-chain glycosides **T-x** (**x** = 1–4, 8) will be discussed first (*Fig. 6* and *Table 5*). The δ(OH) and J(H,OH) values of **T-1** are similar to those of methyl β-D-glucopyranoside [40] ($\Delta\delta$(OH) < 0.05 ppm, ΔJ(H,OH) ≤ 0.2 Hz) and evidence fully solvated OH groups. In the absence of intramolecular H-bonds, glycosylation at O(4) of **T-1** should lead to a downfield shift ('alkylation shift') of 0.2 ppm for HO(3*c*), and of 0.1 ppm for HO(2*c*) and HO(6*c*) of **T-2** [39]. While this is found for HO(2*c*) and HO(6*c*) that resonate 0.15 and 0.1 ppm, respectively, downfield to the corresponding OH of **T-1**, HO(3*c*) of **T-2** appears at 4.67 ppm, 0.45 ppm upfield to the expected value. This upfield shift and J(3*c*,OH) < 1.5 Hz evidence a completely persistent interresidue O(3*c*)–H···O(5*a*) H-bond of **T-2**. δ(HO(2*a*)), δ(HO(3*a*)), δ(HO(4*a*)), and δ(HO(6*a*)) values are similar to those of methyl β-cellobioside

Table 5. *^{1}H-NMR δ(OH) Values* [ppm] *of* **T-x** *and* **T-x-x** (**x** = 1–4, 8) *in (D$_6$)DMSO*. In parentheses, *J*(H,OH) values [Hz].

	T-1	**T-2**	**T-3**	**T-4**	**T-8**
HO(2*a*)	4.974 (4.8)	5.199 (4.8)	5.200 (5.0)	5.201 (5.0)	5.205 (5.0)
HO(3*a*)	4.910 (4.8)	4.983 (4.9)	4.990 (5.0)	4.993 (5.0)	5.000 (4.8)
HO(4*a*)	4.874 (5.2)	4.958 (5.5)	4.960 (5.5)	4.964 (5.4)	4.970 (5.3)
HO(6*a*)	4.466 (5.9)	4.576 (5.5)	4.565 (5.9)	4.570 (5.6)	4.569 (5.9)
HO(2*b*)			5.365 (5.0)	5.368 (5.0)[a])	5.37 (4.9)
HO(3*b*)			4.712 (1.8)	4.723 (1.6)	4.726[c])
HO(6*b*)			4.638 (5.9)	4.641 (6.0)[b])	4.67–4.63
HO(2*b*′)				5.373 (5.0)[a])	5.373 (4.9)
HO(3*b*′)				4.643 (1.5)	4.67–4.63
HO(6*b*′)				4.650 (6.5)[b])	4.67–4.63
HO(2*c*)		5.127 (5.0)	5.128 (5.0)	5.132 (5.0)	5.131 (5.0)
HO(3*c*)		4.667[c])	4.595 (1.6)	4.600 (1.6)	4.600[c])
HO(6*c*)		4.566 (5.9)	4.561 (6.0)	4.570 (5.6)	4.569 (5.9)
	T-1-1	**T-2-2**	**T-3-3**	**T-4-4**	**T-8-8**[d])
HO(2*a*)	4.982 (4.5)	5.197 (4.9)	5.203 (4.6)	5.200 (4.9)	5.200 (5.0)
HO(3*a*)	4.900 (4.7)	4.979 (5.0)	4.994 (5.0)	4.992 (4.9)	4.994 (4.8)
HO(4*a*)	4.861 (4.8)	4.958 (5.5)	4.962 (5.4)	4.963 (5.4)	4.962 (5.4)
HO(6*a*)	4.421 (5.8)	4.580 (5.4)	4.567 (5.3)	4.570 (5.3)	4.565 (5.3)
HO(2*b*)			5.362 (4.3)	5.363 (4.9)[a])	5.37 (4.9)
HO(3*b*)			4.714[c])	4.722 (1.6)	4.722[c])
HO(6*b*)			4.645 (5.4)	4.638 (6.4)[b])	4.69–4.61
HO(2*b*′)				5.369 (5.0)[a])	5.37 (4.9)
HO(3*b*′)				4.640 (1.5)	4.722[c])
HO(6*b*′)				4.653 (5.7)[b])	4.69–4.61
HO(2*c*)		5.146 (5.2)	5.147 (5.0)	5.146 (5.1)	5.146 (5.3)
HO(3*c*)		4.669 (1.3)	4.598	4.600[c])	4.596[c])
HO(6*c*)		4.530 (6.0)	4.529 (6.0)	4.530 (6.0)	4.527 (6.0)

[a])[b]) Entries may be interchanged. [c]) Broad *s* ($J < 1.5$ Hz). [d]) Additional signals for OH groups of unit *c* (see *Discussion*).

($\Delta\delta(\mathrm{OH}) \leq 0.05$ ppm). The fully solvated HO(2*a*), HO(3*a*), HO(4*a*), HO(6*a*), and HO(2*c*) groups of **T-3**, **T-4**, and **T-8** resonate at the same position as the corresponding OH of **T-2** ($\Delta\delta(\mathrm{OH}) \leq 0.012$ ppm), whereas the intramolecularly H-bonded HO(3*c*) of **T-3**, **T-4**, and **T-8** is shifted upfield by 0.07 ppm relative to HO(3*c*) of **T-2**.

The chemical shifts of the OH groups of the internal units of **T-3**, **T-4**, and **T-8** may be calculated either from the δ(OH) values of unit *c* or of unit *a*. Unit *c* is a H-donor in a strong inter-residue H-bond, whereas the internal untis *b* and *b*′ act both as H-donors and as H-acceptors. One expects a downfield shift of 0.2 ppm for HO(2*b*) and HO(2*b*′) and of 0.1 ppm for HO(3*b*), HO(3*b*′), HO(6*b*), and HO(6*b*′), as compared to the corresponding OH signals of unit *c* ('protonation shift'). Such downfield shifts are, indeed, observed: 0.24 ppm for HO(2*b*) and HO(2*b*′), 0.12–0.14 ppm for HO(3*b*) and HO(3*b*′), and 0.08 ppm for HO(6*b*) and HO(6*b*′). The glucosyl residue at O(4*b*) and O(4*b*′) should lead to a downfield shift ('alkylation shift') of *ca*. 0.1 ppm for HO(2*b*), HO(2*b*′), HO(6*b*), and HO(6*b*′), relative to the corresponding OH groups of unit *a*.

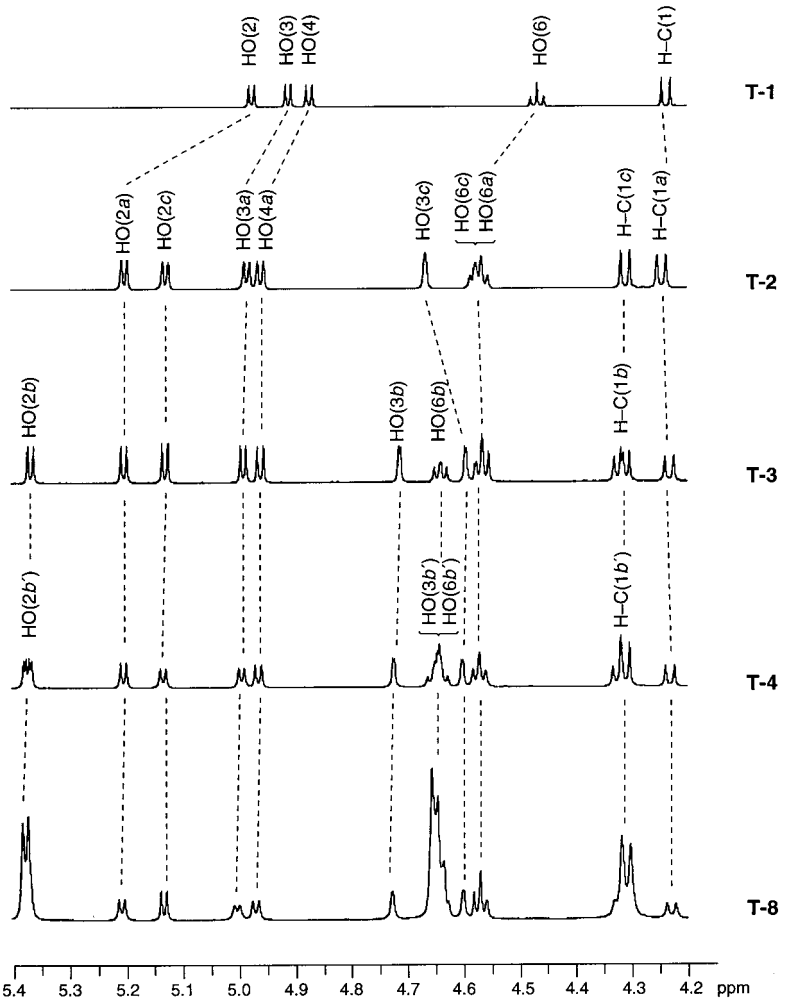

Fig. 6. *^{1}H-NMR Spectra of* **T-x** (**x** = 1–4, 8) *in (D$_6$)DMSO* (500 MHz, 25°) *showing the OH and H–C(1) signals* (concentration for **T-x** (**x** = 1–4) 20 mM and for **T-8** *ca.* 3 mM)

Such downfield shifts are observed: 0.17 ppm for HO(2*b*) and HO(2*b*′), and 0.075 ppm for HO(6*b*) and HO(6*b*′).

The ^{1}H-NMR spectra of **T-2**, **T-3**, **T-4**, and **T-8** clearly evidence the inter-residue O(3)–H···O(5′) H-bonds and thereby the determining factor for the conformational rigidity of celluloses. There is also the same evidence for weakly persistent inter-residue O(6)–H···O(2′) H-bonds as for β-cellobiose and methyl β-cellobioside. Further evidence for flip-flop inter-residue H-bonds between HO(6) and HO(2′) is found in the ROESY spectra (see below).

The identical shifts for corresponding OH groups of **T-x** (**x** = 3, 4, 8) show the absence of an enhanced acidity of the OH groups of higher cellodextrins that might be

caused by co-operative inter-residue H-bonds, and the δ(OH) values of the completely solvated OH groups of **T-x** (**x** = 2–4, 8) are characteristic for OH groups attached to unit *a*, *b*/*b*′, or *c*, independently of **x**. The δ(OH) values for HO(3) of **T-x** (**x** = 2–4, 8) depend on the complete H-bonding of both units that are bridged by the O(3)–H⋯O(5′) H-bond. HO(3*c*) of **T-x** (**x** = 3, 4, 8) resonates at highest field (4.60 ppm) and HO(3*b*) at lowest field (4.72 ppm) of all HO(3) in an inter-residue H-bond. The upfield shift of HO(3*c*) reflects the absence of a partial protonation of unit *c* by HO(3) of a neighbouring unit. The relative chemical shifts of HO(3*b*) and HO(3*b*′) are rationalised by the σ-acceptor properties of their O(4) substituents. For unit *b*, it is a glucosyl, for unit *b*′ a cellobiosyl unit. The σ-acceptor properties of the monosaccharide unit should be lower than those of the disaccharide unit and further reduced by the strong intermolecular H-bonds of four OH groups to (D_6)DMSO. The difference in the σ-acceptor properties of unit *a* on *b* and of the combined units *a* and *b* on *b*′ leads to the observed stronger deshielding of HO(3*b*).

The analysis of the ^{1}H-NMR spectra of **T-x** carrying a single cellodextrin chain serves as background for the analysis of **T-x-x** carrying two such chains. Since the design of the model compounds **T-x-x** is such that no (intramolecular) interchain H-bonds should be formed in the solid state, we expected at best weak interchain H-bonds in solution, *i.e.*, small differences of J(H,OH) and δ(OH) values between **T-x-x** and **T-x**. A comparison of the data for **T-x-x** an **T-x** (**x** = 1–4) shows that there are indeed only small changes of J(H,OH) ($\Delta J \leq 0.7$ Hz) and δ(OH) ($\Delta\delta \leq 0.045$ ppm; *Table 5*). However, inspection of *Fig. 7* and *Table 5* denotes a conspicuous *systematic* shift for HO(6*c*) and HO(2*c*) of **T-x-x** relative to **T-x**. The *upfield* shift of HO(6*c*) is particularly obvious (0.03–0.045 ppm), but even the small *downfield* shift of HO(2*c*) (0.01–0.02 ppm) has to be contrasted with very small $\Delta\delta$ values for the other OH signals of **T-x-x** *vs.* **T-x** (**x** = 2–4, 8)[9]. One also notes a systematic, small *upfield* shift of the H–C(1) signals (up to 0.01 ppm). Thus, interchain interactions appear to be restricted to the unit *c* closest to the naphthalene moiety. The *upfield* shift of HO(6*c*) and the *downfield* shift of HO(2*c*) point to a weakly persistent interchain O(6*c*)–H⋯O(2*c**) H-bond[10]).

Surprisingly, the spectrum of **T-8-8** (viewed against the spectra **T-8** and **T-4-4**) shows additional OH signals (*Fig. 8*). To exclude the possibility that the additional signals are due to impurities, we acetylated **T-8-8** with Ac_2O in *N*,*N*-dimethylacetamide/LiCl. This led to a single peracetate. Deacetylation of the isolated peracetate with NH_3 in MeOH transformed it quantitatively back into **T-8-8**, which exhibits the same ^{1}H-NMR spectrum as the original sample. Differences between the spectra of **T-8-8** and **T-8** are restricted to the signals for HO(2*c*), HO(3*c*), and HO(6*c*); corresponding OH signals of the units *a*, *b*, and *b*′ of **T-8-8**, **T-8**, and **T-4-4** appear at the same position. In the spectrum of **T-8-8**, the *doublet* for HO(2*c*) at 5.15 ppm integrates for only 0.4 H. Three additional *doublets* ($J \approx 5.0$ Hz), marked with roman numerals (I–III), are observed at 5.32 (HO(2c^{I}), 0.3 H), 5.10 (HO(2c^{II}), 0.15 H), and 4.77 ppm (HO(2c^{III}), 0.15 H). A further *doublet* of very weak intensity is visible at 4.75 ppm. Since no other *doublets*

---

[9]) The upfield shift of HO(3) and HO(4) for **T-1-1** *vs.* **T-1** (0.01 ppm) probably reflects the absence of intrachain H-bonds.

[10]) The O-atoms of the second chain are marked with an asterisk.

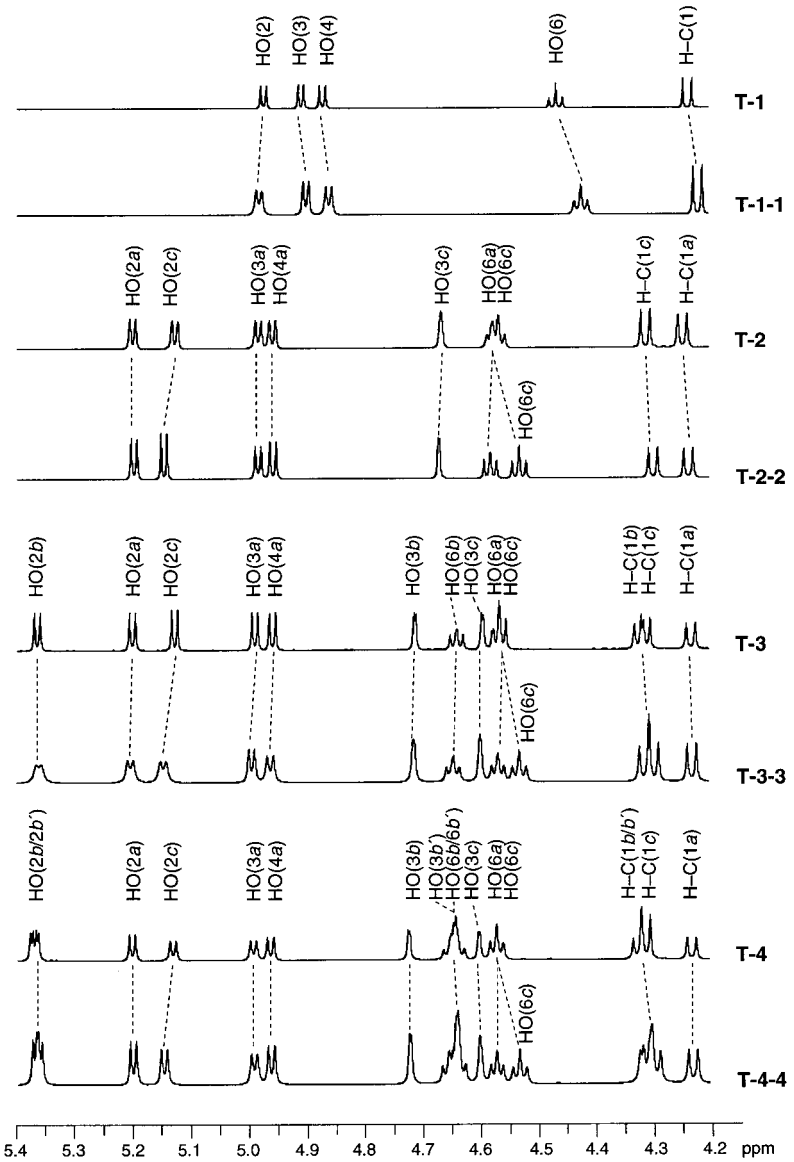

Fig. 7. *Comparison of the* ^{1}*H-NMR spectra of* **T-x** (**x** = 1–4; 20 mM) *and* **T-x-x** (**x** = 1–4; 10 mM) *in* (D_6)*DMSO* (500 MHz, 25°)

appear in this region of the spectrum, the *doublet* at 4.75 ppm is presumably also due to HO(2*c*). Similarly, the broad *singulet* for HO(3*c*) at 4.60 ppm integrates for only 0.4 H. An additional broad *singulet* is observed at 4.46 ppm (HO(3c^1), *ca.* 0.2 H). The *triplet* at 4.57 ppm in the spectrum of **T-8**, integrating for 2 H (HO(6*a*) and HO(6*c*)), corresponds to three signals in the spectrum of **T-8-8**. The *triplet* at 4.565 ppm

integrating for one H is assigned to HO(6*a*). The second signal consists of two overlapping *triplets* ($J \approx 6.0$ Hz) and appears at 4.53 ppm (0.55 H). A third signal appears at 4.44 ppm (t, $J = 6.0$ Hz, *ca.* 0.2 H). These two signals are assigned to HO(6*c*)/HO(6c^{I}) and HO(6c^{II}). The *multiplet* at 4.69–4.61 ppm in the spectrum of **T-8**,

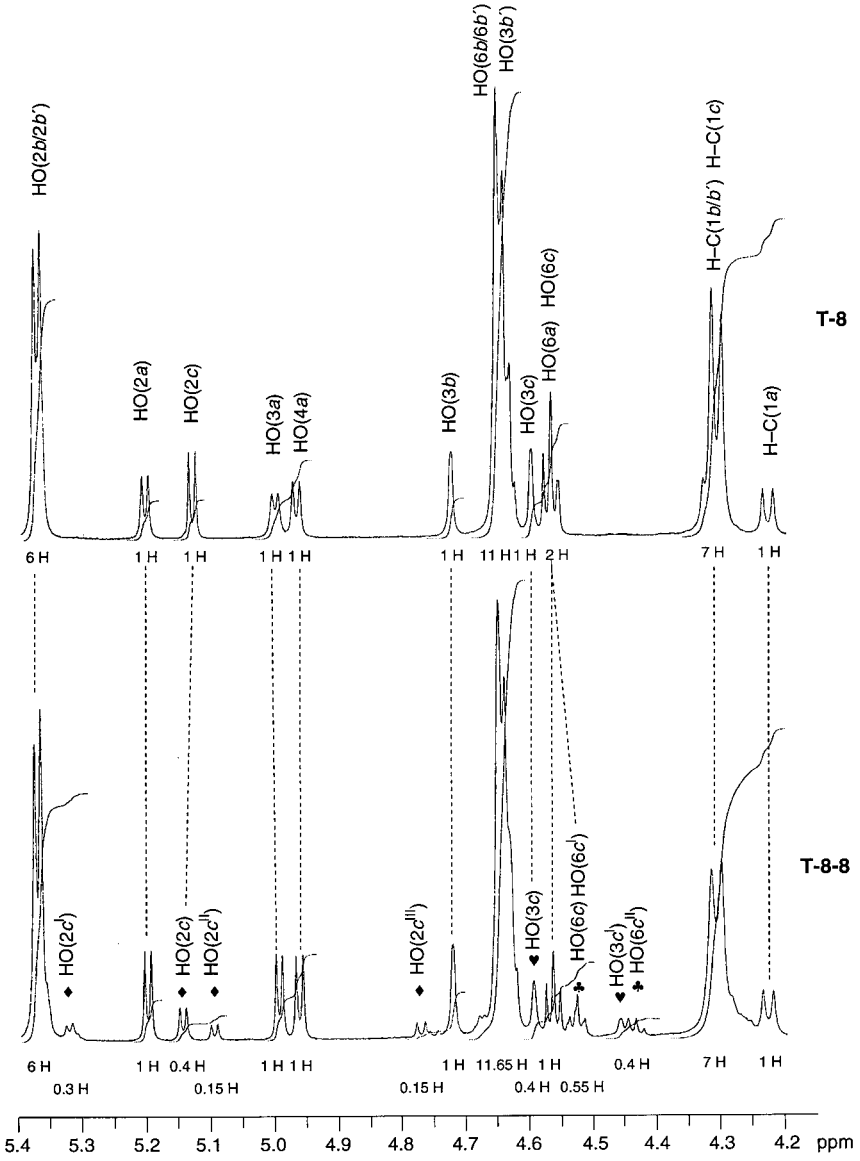

Fig. 8. *^{1}H-NMR Spectra of* **T-8** (3 mM) *and* **T-8-8** (3 mM) in *(D_6)DMSO* (500 MHz, 25°) *showing the OH and H–C(1) signals.* Integrals are given below the spectra. Signals for OH of the unit *c* of **T-8-8** are marked with ◆ (HO(2*c*)), ♥ (HO(3*c*)), and ♣ (HO(6*c*)); additional signals are indexed with roman numerals.

integrating for 11 H, comprises the signals of the five HO(3*b*′) and the six HO(6*b*/*b*′). Integration of the corresponding signal in the spectrum of **T-8-8** (11.65 H) accounts for additional signals of HO(2*c*) and HO(6*c*) that are partially visible at 4.68 ppm. Unfortunately, corroboration of this assignment by saturation-transfer experiments failed due to saturation transfer (*via* adventitious H_2O?) to all OH groups. The signals for HO($2c^{I}$) and HO($2c^{II}$) are still visible in a spectrum recorded at 95°. Other additional signals are then hidden, but visible in the spectra recorded at intermediate temperatures.

The interpretation of these data is difficult. Intermolecular interactions, as suggested by the observation that HO(2*c*) of **T-8** and **T-8-8** resonates at the same field, are not in keeping with the observation that the spectrum of **T-8-8** is not affected by lowering the concentration from 3 to 1.5 mM. Interchain H-bonding, leading to several species, is suggested by the observation that only OH signals of the unit *c* are affected, similarly to what was observed in the spectra of **T-x-x** (**x** = 2–4).

The temperature dependence of the chemical shifts of the OH signals is another useful parameter for determining intramolecular H-bonds in dilute (D_6)DMSO solutions (see [34][39] and refs. cit. there). As a rule, OH signals are shifted upfield with increasing temperature. For solutions in (D_6)DMSO, $|\Delta\delta/\Delta T| \leq 3$ ppb/K have been attributed to intramolecularly H-bonded OH, while $|\Delta\delta/\Delta T| > 4.5$ ppb/K are characteristic for OH groups which are intermolecularly H-bonded to (D_6)DMSO.

The $\Delta\delta/\Delta T$ values of **T-x** and **T-x-x** (**x** = 1–4) were deduced from spectra recorded in the range from 298 to 333 K in 5 K steps, and those of **T-8** and **T-8-8** from spectra recorded in the range from 298 to 338 K in 10 K steps. A linear temperature dependence is observed for all OH and H–C(1) signals (*Table 6*). The latter are used as internal reference, showing a very weak temperature dependence ($\Delta\delta/\Delta T \leq 1.0$ ppb/K).

Table 6. $\Delta\delta/\Delta$T *Values for OH and H–C(1)* [ppb/K] *of* **T-x** *and* **T-x-x** (**x** = 1–4, 8) *in (*D_6*)DMSO*[a])

	T-1	**T-1-1**	**T-2**	**T-2-2**	**T-3**	**T-3-3**	**T-4**	**T-4-4**	**T-8**	**T-8-8**
HO(2*a*)	−7.0	−7.4	−5.2	−5.2	−5.3	−5.6	−5.5	−5.4	−5.8	−5.2
HO(2*b*)					−5.2	−5.6	−5.6	−5.6	−6.0	−5.5
HO(2*b*′)							−5.6	−5.6	−6.0	−5.5
HO(2*c*)			−6.7	−7.4	−6.4	−7.5	−6.7	−7.4	−6.8	−7.1
HO(3*a*)	−6.4	−6.5	−6.1	−5.7	−6.3	−6.3	−6.3	−6.3	−6.3	−5.9
HO(3*b*)					−2.0	−2.2	−2.0	−2.0	−2.2	−2.2
HO(3*b*′)							−2.3	−2.2	−2.4	−2.2
HO(3*c*)			−2.0	−2.4	−1.9	−2.1	−2.0	−2.1	−1.7	−2.2
HO(4*a*)	−5.6	−5.4	−5.3	−5.4	−5.5	−5.6	−5.4	−5.6	−5.7	−5.2
HO(6*a*)	−5.6	−5.3	−5.0	−5.2	−4.9	−4.7	−4.6	−4.6	−5.0	−4.5
HO(6*b*)					−4.3	−4.6	−4.2	−4.8	−4.7	−4.4
HO(6*b*′)							−4.7	−4.7	−4.7	−4.4
HO(6*c*)			−4.6	−5.3	−4.9	−5.1	−5.1	−4.9	−5.0	−4.2
H–C(1*a*)	0.5	0.5	0.9	0.9	0.9	1.0	0.9	0.7	0.8	1.0
H–C(1*b*)					0.7	0.7	0.8	0.8	0.8	1.0
H–C(1*b*′)							0.2	0.7	0.8	1.0
H–C(1*c*)			0.3	0.0	0.2	0.0	0.0	0.0	0.6	1.0

[a]) Deduced from the ^{1}H-NMR spectra recorded at 298 to 333 K in 5 K intervals of 20 mM solution of **T-x** (**x** = 1–4) and of 10 mM solution of **T-x-x** (**x** = 1–4), and from 298 to 338 K in 10 K intervals of *ca.* 3 mM solution of **T-8** and **T-8-8**.

As expected, the chemical shifts of HO(3*b*), HO(3*b*′), and HO(3*c*) of **T-x** and **T-x-x** (**x** = 2–4, 8) engaged in persistent interresidue H-bonds show a weak dependence upon the temperature ($\Delta\delta$(OH)/ΔT between −1.7 and −2.4 ppb/K; *Table 6*). The other OH groups show $\Delta\delta$(OH)/ΔT values in the range of −4.2 to −7.4 ppb/K. Among them, HO(2*c*) of **T-x-x** are most sensitive ($\Delta\delta$(OH)/ΔT between −7.1 and −7.4 ppb/K) and slightly more so than HO(2*c*) of **T-x** ($\Delta\delta$(OH)/ΔT between −6.7 and −6.8 ppb/K). This agrees with the weakly persistent interchain O(6*c*)–H···O(2*c**) H-bond that will enhance the acidity of HO(2*c*) of **T-x-x**, and thereby the interaction with (D_6)DMSO. Concomitantly, the $\Delta\delta$(OH)/ΔT value for HO(6*c*) should be smaller for **T-x-x** than for **T-x**. This is so for **T-4-4** and **T-8-8**, but not for **T-2-2** and **T-3-3**, evidencing a dependence on the number of chains and on the chain length of the interresidue O(6*c*)–H···O(2′) flip-flop H-bond and of the interchain O(6*c*)–H···O(2*c**) H-bond of **T-x-x**; *i.e.*, of the conformation of the CH_2OH group of unit *c*.

SIMPLE ^{1}H-NMR Experiments [41] allow to detect strongly persistent intramolecular H-bonds between OH groups (see [39][42] and refs. cit. therein). Titration [43] of **T-1-1** in (D_6)DMSO with D_2O, and of **T-4** and **T-4-4** in (D_6)DMSO with CD_3OD did not lead to split OH signals. The absence of SIMPLE effects is not surprising, since only the ring O-atoms of **T-4** and **T-4-4** (and not OH groups) act as H-acceptors in strong H-bonds, while the other intramolecular H-bonds of **T-1-1**, **T-4**, and **T-4-4** are too weakly persistent to be detected by this method.

Relative distances between OH groups of **T-x** and **T-x-x** were estimated on the basis of ROESY spectra [44][45]. ROESY Experiments have not only the advantage of being better adapted to the mass of **T-x** and **T-x-x**, they also allow to distinguish ROE cross-peaks from those due to exchange between OH protons and the residual H_2O in (D_6)DMSO, and to identify spin-diffusion effects in large molecules [46][11])[12]).

The ROESY spectra of **T-4** and **T-4-4** were recorded under identical conditions. Signal overlap prevents the assignment of the cross peaks involving CH groups other than H–C(1). We have, therefore, limited the analysis to interactions between H–C(1) and OH groups and between OH groups. Expanded parts of the spectra are depicted in *Fig. 9*, *a* (**T-4**) and *b* (**T-4-4**).

The ROESY spectrum of **T-4** (*Fig. 9*, *a*) shows four cross-peaks diagnostic for H–C(1)/OH interactions, but none for OH/OH interactions. The cross-peaks between H–C(1*a*) and HO(3*b*), between H–C(1*b*) and HO(3*b*′), and between H–C(1*b*′) and HO(3*c*) are consistent with the orientation of HO(3*b*), HO(3*b*′), and HO(3*c*) dictated

---

[11]) The cross-peak in a ROESY spectrum may arise from a 'true' ROE or from relayed ROEs, such as TOCSY/ROE and exchange/ROE [47]. The ROESY spectrum of a three-spin system (H_a, H_b, and H_c) with a ROE between H_a and H_b, and a coupling between H_b and H_c may show cross-peaks not only between H_a and H_b, but also between H_a and H_c (TOCSY/ROE). An exchange-relayed ROE can occur if there is a ROE between H_a and H_b, and if the proton-exchange rates between H_b and H_c are similar to or faster than the cross-relaxation rates, leading to a cross-peak between H_a and H_c, even if H_a and H_c are remote from each other (exchange/ROE). The cross peak between H_a and H_c due to an exchange/ROE is necessarily smaller than the corresponding exchange cross-peak between H_a and H_b. The cross-peaks due to the TOCSY effect or due to proton exchange exhibit the same phase as the diagonal peaks and have therefore an opposite phase as the 'true' ROE cross peaks. TOCSY/ROE and exchange/ROE cross-peaks, however, have the same phase as 'true' ROE cross peaks and may lead to misinterpretation.

[12]) For applications of ROESY spectroscopy to the structure determination and conformational analysis of carbohydrates, see [35][45][48].

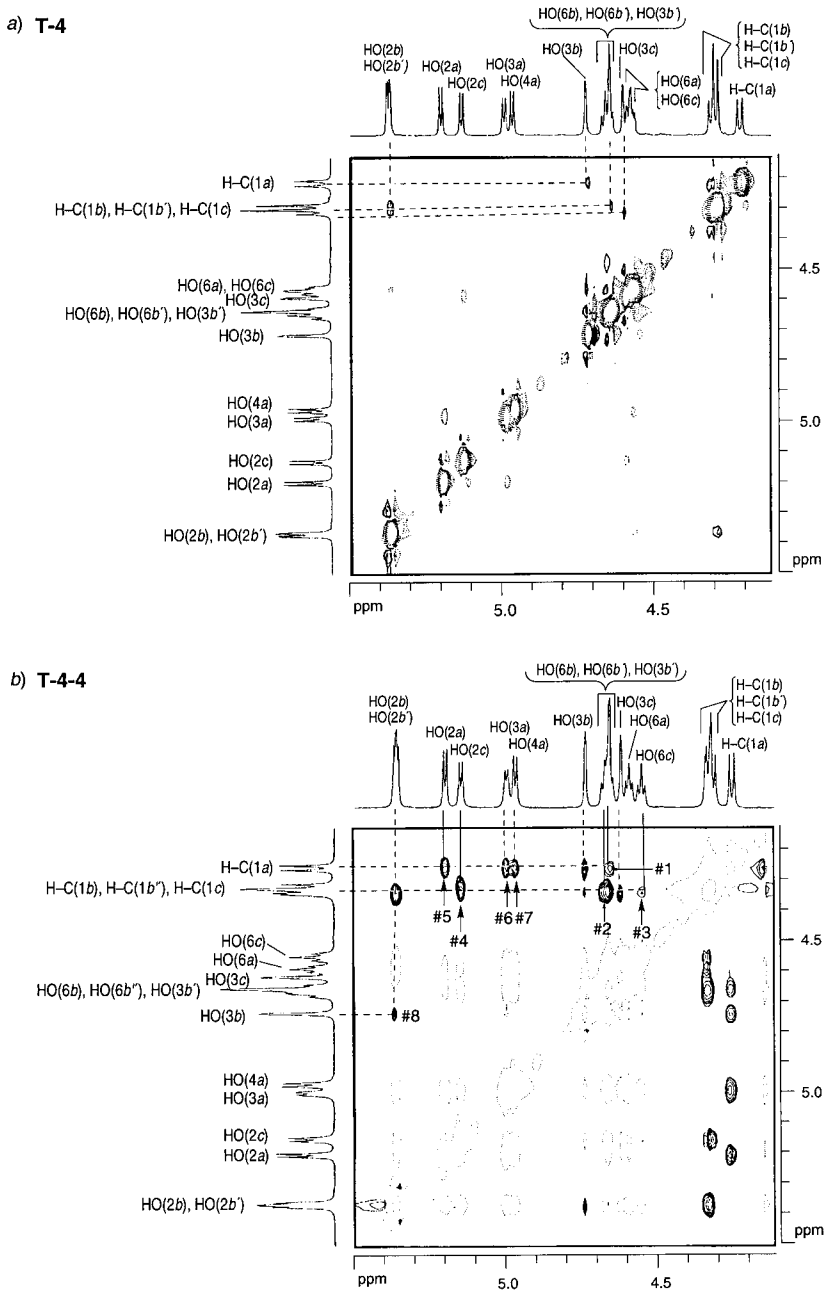

Fig. 9. *Expansions of the ROESY spectra of* a) **T-4** *and* b) **T-4-4** *in (D_6)DMSO, showing the cross-peaks between H–C(1) and OH, and between OH signals.* Positive cross-peaks (solid contours) are due to ROE or TOCSY/ROE and negative cross-peaks (dashed contours) to TOCSY or H/H exchange. Additional positive cross-peaks in **T-4-4** are marked with #1 to #8.

by the interresidue O(3*b*)–H···O(5*a*), O(3*b*′)–H···O(5*b*), and O(3*c*)–H···O(5*b*′) H-bonds (*Fig. 10*). The single cross-peak between the overlapping signals for H–C(1*b*), H–C(1*b*′), and H–C(1*c*), and the overlapping signals for HO(2*b*) and HO(2*b*′) is assigned to two intra-residue interactions, one between H–C(1*b*) and HO(2*b*), and one between H–C(1*b*′) and HO(2*b*′). These interpretations are rationalised by two weakly persistent interresidue H-bonds, one between HO(2*b*) and HO(6*b*′), and one between HO(2*b*′) and HO(6*c*). MM3* Force-field calculations [49] of the intraresidue distance between *H*–C(1) and *HO*(2) yield a value of *ca.* 1.7 Å, when HO(2*b*) and HO(2*b*′) act as H-donors in these inter-residue H-bonds, and a value of $\geq$ 3.4 Å, when they act as H-acceptors. Taken together, ROEs, δ(HO(2*b*)), and δ(HO(2*b*′)) are in agreement with a minor contribution of the inter-residue H-bonded conformer depicted in *Fig. 10* to the equilibrium between H-bonded and solvated conformers.

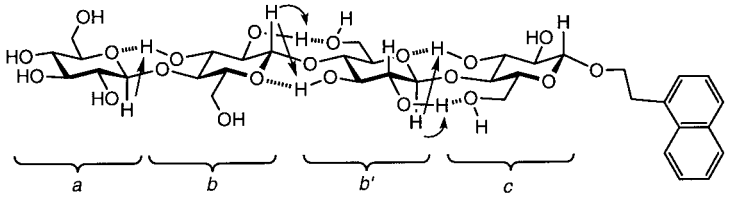

Fig. 10. *Assignment of inter-residue H-bonds* (dashed lines) *based on the interpretation of the ROEs between the H–C(1) and OH signals of* **T-4** (ROEs indicated by arrows)

There are no analogous cross-peaks between the H–C(1*a*) and HO(2*a*) signals nor between the H–C(1*c*) and HO(2*c*) signals, evidencing a different orientation of HO(2*a*) and HO(2*c*) *vs.* HO(2*b*) and HO(2*b*′). An inter-residue H-bond analogous to that between HO(2*b*) and HO(6*b*′) is not possible for HO(2*c*). A different orientation of HO(2*a*) is correlated with the fact that unit *a* is not glucosylated, and that HO(3*a*) is not involved in an intramolecular H-bond. Either of these differences to units *b* and *b*′, *viz.* the expected lower acidity of HO(2*a*) and the lack of a defined orientation of HO(3*a*) may influence the strength and orientation of a H-bond between HO(2*a*) and HO(6*b*). One also expects a higher flexibility for the terminal unit *a* of the cellodextrin chain that may weaken any inter-residue H-bond between the units *a* and *b*, as discussed above in the context of the relative chemical shifts for HO(3*a*), HO(3*b*), HO(3*b*′), and HO(3*c*).

Intrachain cross peaks corresponding to those of **T-4** are also visible in the ROESY spectrum of **T-4-4** (*Fig. 9*, *b*). In addition, there are seven cross-peaks between H–C(1) and OH groups (marked in *Fig. 9*, *b*, with #1 – #7), and one between OH groups (#8), as follows: #1 between the signal for H–C(1*a*) and the overlapping signals for HO(6*b*), HO(6*b*′), and HO(3*b*′), #2 between the overlapping signals for H–C(1*b*), H–C(1*b*′), and H–C(1*c*), and the overlapping signals for HO(6*b*), HO(6*b*′), and HO(3*b*′), #3 and #4 between the overlapping signals for H–C(1*b*), H–C(1*b*′), and H–C(1*c*), and the signals of both HO(6*c*) and HO(2*c*), #5, #6, and #7 between the signal of H–C(1*a*) and each signal of HO(2*a*), HO(3*a*), and HO(4*a*), and #8 between the signal for HO(3*b*) and the overlapping signals for HO(2*b*) and HO(2*b*′). These additional cross-peaks indicate an interaction between the two chains. They can not arise from intermolecular

interactions considering that the δ(OH) and J(H,OH) values do not depend upon the concentration (see above). The relatively strong intensities of these cross-peaks indicate that they are due to intra- or interchain ROEs or TOCSY/ROEs.

Cross-peak #1 can not be due to spin coupling as there is no corresponding TOCSY cross-peak. The other cross-peaks #2–#8 are paralleled by TOCSY-type cross-peaks, indicating that they could arise wholly or partly from spin coupling. Since cross-peaks #1, #2, and #4–#7 are strong, they most probably express the effects both of spatial proximity and spin coupling.

Cross-peak #1 must arise from either an intra- or interchain interaction between H–C(1*a*) and HO(6*b*), since H–C(1*a*) is too far removed from HO(6*b*′) and HO(3*b*′) to allow an interchain interaction.

Cross-peak #2 possesses the highest intensity in the region between 5.5 and 4.2 ppm. It may *a priori* arise from two sets of nine (intra- and interchain) interactions, some of which can be eliminated on the basis of the distance between the partners. No intrachain interactions are possible between H–C(1*b*) and HO(6*b*), H–C(1*b*′) and HO(6*b*), H–C(1*b*′) and HO(6*b*′), H–C(1*b*′) and HO(3*b*′), H–C(1*c*) and HO(6*b*), H–C(1*c*) and HO(6*b*′), and H–C(1*c*) and HO(3*b*′). Of the remaining two possible intrachain interactions, the one between H–C(1*b*) and HO(3*b*′) is also observed in the ROESY spectrum of **T-4**, while the interaction between H–C(1*b*) and HO(6*b*′) is new. Of the possible interchain interactions, those between H–C(1*b*′) and HO(3*b*′*), H–C(1*b*′) and HO(6*b**), H–C(1*c*) and HO(6*b**), H–C(1*c*) and HO(6*b*′*), and H–C(1*c*) and HO(3*b*′*) can also be excluded. Among the remaining possible interactions, those between H–C(1*b*) and HO(3*b*′), and between H–C(1*b*) and HO(6*b*′) may correspond to intra- or interchain interactions, while those between H–C(1*b*) and HO(6*b**), and between H–C(1*b*′) and HO(6*b*′*) can only reflect interchain interactions.

Cross peak #3 is too strong to be due to spin coupling between H–C(1) and HO(6) alone. It must reflect additional effects that may result from an interchain interaction between H–C(1*c*) and HO(6*c**) and/or an intra- or interchain interaction between H–C(1*b*′) and HO(6*c*).

Thus, cross peaks #1–#3 indicate the proximity of H–C(1) and HO(6) of two glucosyl moieties that either belong to a cellobiosyl unit within one chain (**B** in *Fig. 11*), or between glucosyl units belonging to different chains of the same molecule (*Fig. 12*). The interchain interactions may either involve 'diagonal' glucosyl moieties (*e.g.*, between H–C(1*b*) and HO(6*b*′*); **C** and **D** in *Fig. 12*) or 'parallel' glucosyl moieties (*e.g.*, between H–C(1*b*) and HO(6*b**); **E** and **F** in *Fig. 12*).

Cross-peak #4 may arise either from an intra- or an interchain interaction between H–C(1*c*) and HO(2*c*).

Cross-peaks #5, #6, and #7 are restricted to interactions involving unit *a*. Cross-peak #5 may arise from an intra- and/or an interchain interaction between H–C(1*a*) and HO(2*a*). Cross-peak #6 indicates an interaction between H–C(1*a*) and HO(3*a*). These H-atoms are too far removed from each other to give rise to a ROE, and cross peak #6 must be due to a TOCSY/ROE[11]). This is evidenced by two additional cross-peaks (outside of the expanded part of the spectrum of **T-4-4** in *Fig. 9*, *b*), a strong one between H–C(1*a*) and H–C(3*a*), and a negative one between H–C(3*a*) and HO(3*a*), typical for a TOCSY effect. Cross-peak #7 indicates an interaction between H–C(1*a*)

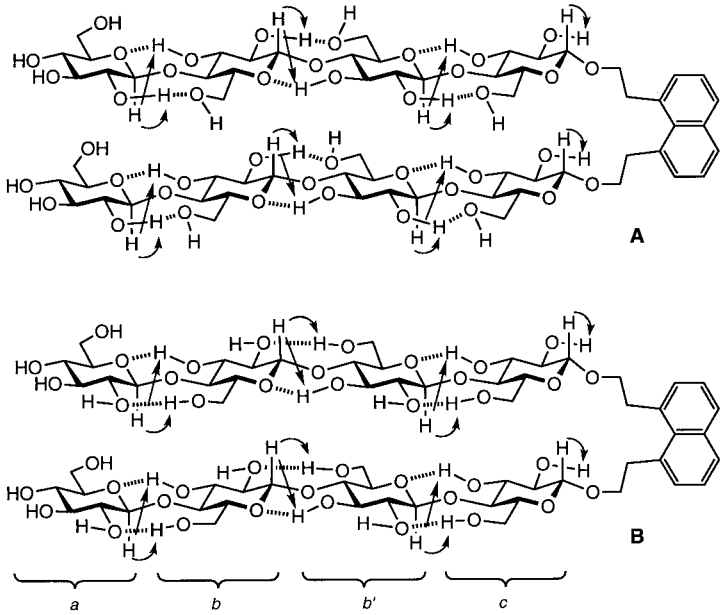

Fig. 11. *Assignment of inter-residue H-bonds* (dashed lines) *based on the interpretation of the ROEs between the H–C(1) and OH signals of* **T-4-4** (ROEs indicated by arrows) *by inter-residue O(3)–H···O(5) and O(2)–H···O(6) H-bonds* (**A**) *or by inter-residue O(3)–H···O(5) and O(6)–H···O(2) H-bonds* (**B**)

and HO(4*a*) that are also too far removed from each other for a ROE. However, cross-peak #7 is stronger than expected for a TOCSY/ROE, and yet difficult to be rationalised in another way[13]).

Cross peak #8 between the signal for HO(3*b*) and the overlapping signal for HO(2*b*) and HO(2*b*′) is the only positive cross-peak between OH signals. It must reflect an interaction between HO(3*b*) and HO(2*b*), but can not arise from a 'true' intraresidue ROE, as the H···H distance is too large also for this interaction. The cross peak is probably due a TOCSY/ROE transmitted *via* H–C(3*b*), although an interchain interaction between HO(3*b*) and HO(2*b**) can not be excluded.

As discussed above, a weakly persistent interchain O(6*c**)–H···O(2*c*) H-bond of **T-4-4** is evidenced by δ(OH) and $\Delta\delta$(OH)/ΔT values. The only indirect evidence for this H-bond in the ROESY spectrum of **T-4-4** is found in the cross peak #4 which evidences a different orientation of HO(2*c*) in **T-4-4** and in **T-4**.

In summary, of the eight cross peaks that are found in the spectrum of **T-4-4**, but not of **T-4**, #1–#5 may be due to either intra- or interchain interactions of H–C(1) and OH groups; *i.e.*, *they are indirectly or directly diagnostic of interchain interactions, such as have been evidenced by the analysis of coupling constants and chemical-shift values for*

---

[13]) Cross peak #7 may arise from a ROE between H–C(1*a*) and H–C(3*a*), and/or H–C(5*a*), a TOCSY effect between H–C(3*a*) and/or H–C(5*a*) on one side, and H–C(4*a*) on the other side, and a TOCSY effect between H–C(4*a*) and HO(4*a*). Such a 'TOCSY/TOCSY/ROE' ought to lead to a cross peak of weak intensity between the signals of H–C(1*a*) and HO(4*a*), unless the double path (*via* H–C(3*a*) and H–C(5*a*)) should enhance it.

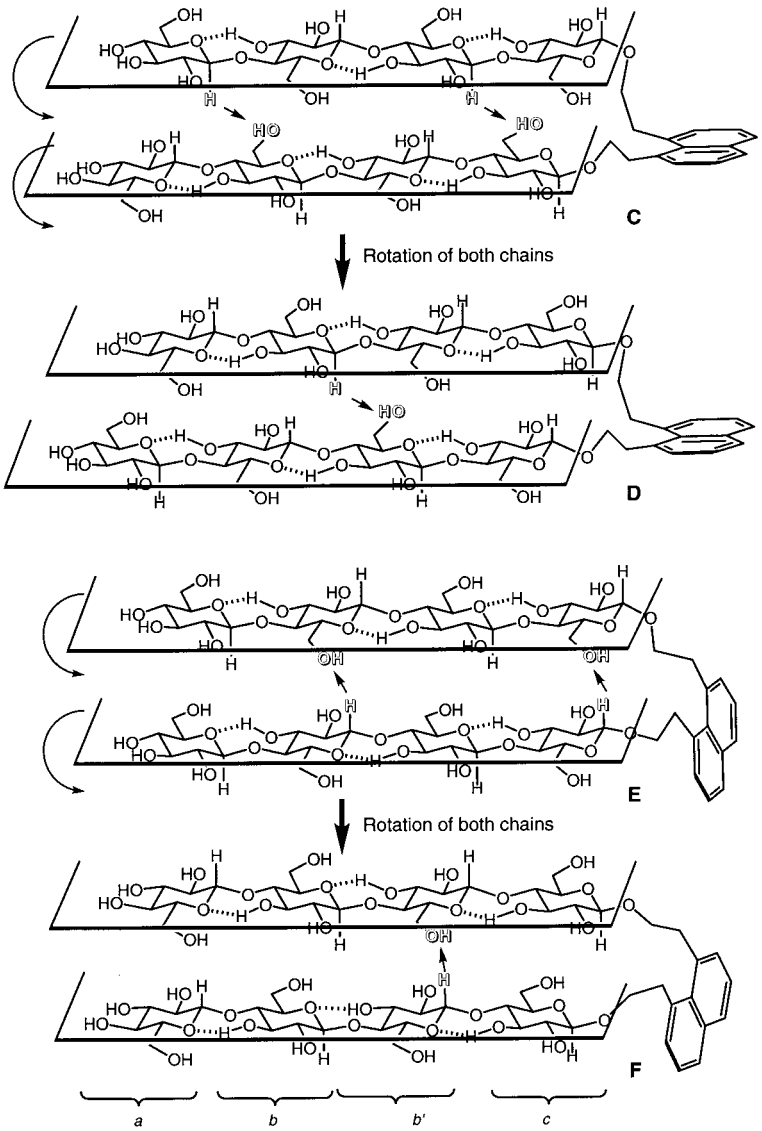

Fig. 12. *Rationalisations of the cross-peaks #1 – #5 in the ROESY spectrum of* **T-4-4** *by interchain interactions between 'diagonal'* (**C** and **D**) *or 'parallel' units* (**E** and **F**; ROEs marked by arrows between shadowed partners). The schematic drawing is intended to illustrate the planes in which the two tetraosyl chains are located, without defining their exact position in these planes.

the units c *and* c*. The distinction between intra- and interchain interactions requires a more detailed interpretation of cross peaks #1 – #5.

Cross-peak #5 is best interpreted as the result of an intrachain interaction, denoting an interresidue O(2*a*)H···O(6*b*) H-bond in **T-4-4**. Analogous H-bonds between all other neighbouring units have been detected in the spectra of **T-4** and **T-4-4**; that such a

H-bond is also visible between the two units farthest removed from the link between the cellodextrin chains of **T-4-4** is most readily interpreted as resulting from a reduced flexibility of the chains in **T-4-4**, as conditioned by the (weak) interchain interactions of units *c* and *c** (**A** in *Fig. 11*). Cross-peaks #1–#3 evidence the proximity of H–C(1) and HO(6′) of neighbouring units. It is tempting to interpret them as the result of intrachain flip-flop H-bonds between HO(2) and HO(6′) of a cellobiosyl unit (*cf.* **B** in *Fig. 11*)[14]). Since the spectrum of **T-4** shows cross-peaks that denote HO(2) only as H-bond donor, the second chain of **T-4-4** either strengthens the H-bonds between two neighbouring units, or shifts the flip-flop equilibrium.

These cross-peaks #1–#5 can also be interpreted as resulting from interchain interactions between either 'diagonal' or 'parallel' glucosyl units. An interaction between H–C(1*a*) and HO(6*b**) (cross peak #1) is only possible between diagonally oriented glucosyl units as in conformer **C** (*Fig. 12*). The required conformation of **T-4-4** may also lead to an interaction between H–C(1*b*′) and HO(6*c**) (cross-peak #3), but not that between H–C(1*b*) and HO(6*b*′*) (cross-peak #2). To explain cross-peak #2, one must assume a rotation of both chains of conformer **C** leading to an equilibrium between conformers **C** and **D** (*Fig. 12*). Conformers **E** and **F** that lead to interactions between parallel glucosyl units can not be excluded, but do not rationalise the interaction between H–C(1*b*′) and HO(6*c**) (cross-peak #1), since the corresponding interaction is geometrically not feasible. None of conformers **C**–**F**, however, rationalises the interchain O(2*c*)–H···O(6*c**) H-bond, evidenced by the analysis of the δ(OH) and $\Delta\delta$(OH)/ΔT values, and no conformer is apparent that could rationalise all observations on the basis of interchain interactions.

These considerations most probably mean that there is only an interchain interaction between *c* and *c**, restricting the conformational freedom of **T-4-4** as compared to **T-4**. The additional interactions in **T-4-4** must be due to strengthened intrachain, inter-residue H-bonds.

The intrachain inter-residue O(3)–H···O(5′) and O(2′)–H···O(6) H-bonds of **T-4-4** correspond to the intramolecular H-bonds in cellulose I_β in the solid state, as derived from X-ray diffraction data [9]. The intrachain inter-residue O(6)–H···O(2′) H-bonds of **T-4-4** do not correspond to an intramolecular H-bond in either cellulose I_β or cellulose II. *The structure of* **T-4-4** *in (D$_6$)DMSO may be taken as evidence that dissolution of celluloses proceeds by first breaking the inter- and intrachain H-bonds between HO(2) and HO(6).*

The cross-peaks between H–C(1) and OH groups in the ROESY spectra of **T-8** and **T-8-8** are similar to those in the spectra of **T-4** and **T-4-4**, respectively, suggesting that the chain length has only a slight effect on the intra- or interchain interactions.

4.3. *In Pyridine.* Weak intramolecular H-bonds should be more easily detectable in solvents that are weaker H-bond acceptors than DMSO, such as pyridine, THF, or dioxane[15]) [50]. Among them, (D$_5$)pyridine proved the best solvent for **T-x** and **T-x-x** (**x** = 1–4). (D$_5$)Pyridine has been used for structural analyses of glucose [51],

---

[14]) For flip-flop H-bonds between OH groups of monosaccharides in (D$_6$)DMSO, see [39].

[15]) The ability of solvents to act as an H-acceptor in a solute-to-solvent H-bond is defined by the β scale. The β value is 0.76 for DMSO, 0.64 for pyridine, 0.55 for THF, and 0.37 for dioxane [50].

cellobiosides [52–56], and a cellotrioside [57]. To the best of our knowledge, no analysis of intra- *vs.* intermolecular H-bonding in this solvent has been published.

^{1}H-NMR Spectra were recorded of 20 mM solutions of **T-x** (**x** = 1–4) and 10 mM solutions of **T-x-x** (**x** = 1–4) in (D_5)pyridine (same concentration as of the (D_6)DMSO solutions). **T-8** and **T-8-8** are insoluble in pyridine. The CH and OH resonances in the ^{1}H-NMR spectra of **T-1**, **T-2**, **T-1-1**, and **T-2-2** in (D_5)pyridine were assigned by homodecoupling experiments. The assignment of the resonances for **T-3-3** is based on ^{1}H,^{1}H-COSY, ^{1}H,^{13}C-COSY, and TOCSY experiments, and on the assumption that the chemical shift for H–C(1*c*) of **T-3-3** is similar to that for H–C(1*c*) of **T-2-2**. The resonances of **T-3** were assigned on the basis of a TOCSY experiment and of a comparison with **T-3-3**. The signals for **T-4** and **T-4-4** strongly overlap and do not allow an unambiguous assignment. *Table 7* lists selected chemical shifts and coupling constants for **T-x** and **T-x-x** (**x** = 1–3), revealing that the solvent change did not affect the ring conformation of the glucopyranosyl units.

The OH groups of **T-1**, **T-1-1**, **T-3**, and **T-3-3** resonate as sharp signals, as shown in *Fig. 13*, while the OH groups of **T-2**, **T-2-2**, **T-4**, and **T-4-4** appear as broad *singulet*s, preventing a precise analysis.

To detect intra- and intermolecular H-bonds, we have examined the J(H,OH) and δ(OH) values of **T-1**, **T-3**, **T-1-1**, and **T-3-3** in (D_5)pyridine, following our established procedure [34][39]. We first checked for the three relevant ranges of J(H,OH) values: those for freely rotating secondary OH groups (J = 3.5–5.5 Hz), and those that significantly deviate from these values by either small (J < 3.0 Hz) or large coupling constants (J > 6.0 Hz). Inspection of *Table 7* reveals that there are no large J(H,OH) values that might have indicated interchain H-bonds, while J(3*b*,OH) and J(3*c*,OH) of **T-3** and **T-3-3** are small with a value of 1.7–1.8 Hz, equal to what was found in (D_6)DMSO and typical for the persistent interresidue O(3*b*)–H···O(5*a*) and O(3*c*)–H···O(5*b*) H-bonds. The J(H,OH) values of the other secondary OH groups, however, are slightly, but significantly, smaller for solutions in (D_5)pyridine (3.9–4.5 Hz) than in (D_6)DMSO (4.3–5.5 Hz). That this is also the case for **T-1** evidences a small contribution to the conformational equilibrium of intramolecularly H-bonded species possessing H-bonds between neighbouring equatorial OH groups (J(H,OH) for such H-bonded conformers is *ca.* 2 Hz [58]). This finding confirms the expectation that weak H-bonds are more persistent in (D_5)pyridine than in (D_6)DMSO. In contradistinction to solutions in (D_6)DMSO, where the signals for the primary OH groups appear as *triplet*s, some of the primary OH groups of **T-3** and **T-3-3** resonate in (D_5)pyridine as *doublet*s of *doublet*s.

The change from (D_6)DMSO to (D_5)pyridine usually leads to a downfield shift of the CH and especially of the OH signals due to the anisotropy effect of the pyridine ring [59]. The presence of signals for both intramolecularly H-bonded and solvated OH groups allows an assessment of the influence of H-bonds on the chemical shifts of OH groups. We were interested to learn whether an intramolecular O–H···OR H-bond (R = H, alkyl, or alkoxyalkyl) leads to an upfield shift of the OH signal, as in (D_6)DMSO, or to a downfield shift, as in $CDCl_3$ [39]. A qualitative comparison of the chemical-shift values of all OH signals for **T-1** and **T-3**, and also for **T-1-1** and **T-3-3** in (D_5)pyridine shows that HO(3*b*) and HO(3*c*) of **T-3** and **T-3-3**, involved in completely persistent interresidue H-bonds, resonate at the highest field (6.39/6.37 and 6.19/

Table 7. *Selected ^{1}H-NMR* ((D$_5$)pyridine) *Chemical Shifts* [ppm] *and Coupling Constants* [Hz] *of* **T-x** *and* **T-x-x** (**x** = 1–3). Concentration for **T-x** 20 mM and for **T-x-x** 10 mM.

	T-1	**T-1-1**	**T-2**		**T-2-2**		**T-3**			**T-3-3**		
Unit			*a*	*c*	*a*	*c*	*a*	*b*	*c*	*a*	*b*	*c*
H–C(1)	4.93	4.90	5.20	4.86	5.18	4.84	5.15	5.19	4.86	5.14	5.17	4.84
H–C(2)	4.09	4.04	4.11	4.08	4.09	4.04	4.10	4.11	4.07	4.09	4.09	4.04
H–C(3)	4.27	4.25	4.28	4.22	4.25	4.20	4.23–4.18	4.26	4.26	4.34–4.23	4.34–4.23	4.23–4.18
H–C(4)	4.25	4.21	4.34	4.20	4.32	4.18	4.23–4.18	4.34	4.31	4.34–4.23	4.34–4.23	4.23–4.18
H–C(5)	3.97	3.96	4.01	3.90	4.00	3.94–3.88	4.04–3.97	4.04–3.97	3.89	4.03–3.97	4.03–3.97	3.90
H–C(6)	4.56	4.54	4.54	4.54	4.52	4.53	4.57–4.47	4.57–4.47	4.57–4.47	4.57–4.45	4.57–4.45	4.57–4.45
H′–C(6)	4.39	4.38	4.31	4.48	4.28	4.46	4.34–4.29	4.57–4.47	4.57–4.47	4.45	4.57–4.45	4.57–4.45
HO(2)	7.22	7.13	[a])	[a])	[a])	[a])	7.52	7.77	7.36	7.50	7.71	7.26
HO(3)	7.17	7.14	[a])	[a])	[a])	[a])	7.31	6.39	6.19	7.30	6.37	6.21
HO(4)	7.15	7.12	[a])	–	[a])	–	7.23	–	–	7.22	–	–
HO(6)	6.41	6.31	[a])	[a])	[a])	[a])	6.51	6.51	6.46	6.46	6.45	6.40
J(1,2)	7.7	7.7	7.8	7.8	7.9	7.8	7.8	7.9	7.9	7.9	8.0	7.8
J(2,3)	8.9	8.4	8.7	8.0	8.5	8.6	8.8	9.1	9.1	8.3	8.3	8.7
J(3,4)	8.9	8.9	8.8	8.9	8.9	8.7	[b])	9.3	9.4	[b])	[b])	[b])
J(4,5)	9.2	9.6	9.2	9.2	9.0	8.7	9.5	9.3	9.4	[b])	[b])	9.8
J(5,6)	2.4	2.5	2.4	3.5	2.6	4.7	2.9	[b])	[b])	2.7	[b])	5.6
J(5,6′)	5.4	5.5	5.9	2.8	5.6	2.6	3.6	[b])	[b])	5.7	[b])	5.6
J(6,6′)	11.7	11.8	11.6	12.1	11.4	12.2	[b])	[b])	[b])	12.0	[b])	[b])
J(2,OH)	4.3	4.5	[b])	[b])	[b])	[b])	4.5	4.3	4.3	4.2	4.4	4.4
J(3,OH)	4.0	3.9	[b])	[b])	[b])	[b])	3.9	1.7	1.8	3.9	1.8	1.8
J(4,OH)	4.1	4.4	[b])	–	[b])	–	4.4	–	–	4.4	–	–
J(6,OH)	6.2	6.3	[b])	[b])	[b])	[b])	6.3	6.3	4.6, 6.5	6.0	4.4, 6.4	5.7, 7.5

[a]) Broad signals. [b]) Not determined.

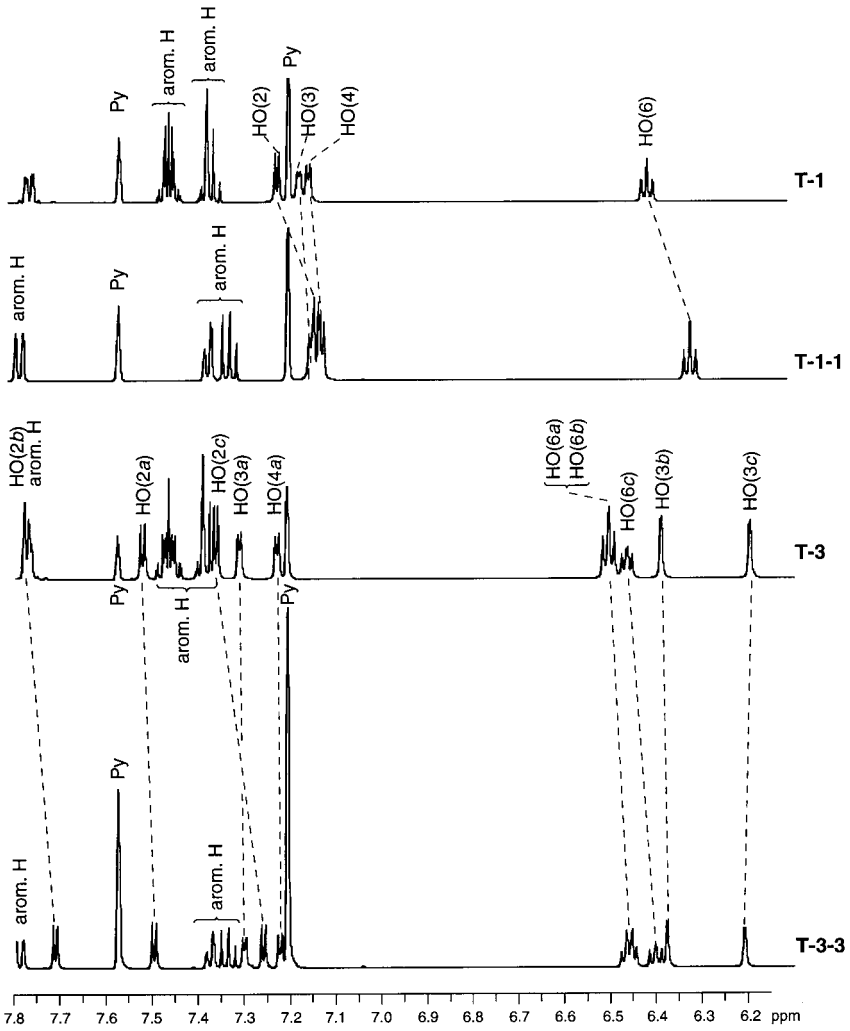

Fig. 13. *^{1}H-NMR Spectra of* **T-x** (**x** = 1, 3; 20 mM) *and* **T-x-x** (**x** = 1, 3; 10 mM) *in (D$_5$)pyridine* (500 MHz, 25°) *showing signals for the OH groups and the naphthalene moiety*

6.21 ppm; *Table 7* and *Fig. 13*). Thus, in (D$_5$)pyridine, as in (D$_6$)DMSO, an intramolecularly O–H···OR H-bonded OH group resonates at higher field than a corresponding solvated OH group. The upfield shift of HO(3*b*) and HO(3*c*) of **T-3** and **T-3-3** as related to δ(HO(3)) of **T-1** and **T-3** is larger in (D$_5$)pyridine (*ca.* 0.75 and 0.95 ppm) than in (D$_6$)DMSO (*ca.* 0.2 and 0.3 ppm), probably due to the anisotropy effect of pyridine. Qualitatively, the relative chemical shift of the other OH signals of **T-1** and **T-3**, and of **T-1-1** and **T-3-3** in (D$_5$)pyridine is the same as in (D$_6$)DMSO.

An analysis of interresidue H-bonds between HO(2) and HO(6′) of **T-3** and **T-3-3** in (D$_5$)pyridine requires a detailed evaluation of the J(H,OH) and δ(OH) values. Such H-

bonds are possible between units *c* and *b*, and *b* and *a*; they cannot involve HO(2*c*) and HO(6*a*). A comparison of *J*(2,OH) and *J*(6,OH) values of **T-1** and **T-3** shows no systematic differences that could evidence inter-residue H-bonds between HO(2) and HO(6′). This may either be taken as evidence for the absence of such H-bonds or for a rapid flip-flop equilibrium. Since intramolecular H-bonds tend to be stronger in (D_5)pyridine than in (D_6)DMSO, and since flip-flop H-bonds were evidenced for the **T-x-x** compounds in (D_6)DMSO, a similar flip-flop equilibrium for the single-chain **T-3** in (D_5)pyridine is a more likely explanation.

The analysis of the δ(OH) values is more complex, since the effect of neighbouring units and of H-bonding have to be taken into account [34]. The difference between the δ(OH) values of **T-1** and of unit *a* of **T-3** is expected to show the influence of the O(3*b*)–H···O(5*a*) H-bond. Similarly for what we have discussed for the spectra in (D_6)DMSO, one expects a downfield shift of the OH signals of unit *a*, expressing the increased acidity resulting from the partial inter-residue proton transfer from HO(3*b*). This 'protonation shift' is observed (*Table 7*). The $\Delta\delta$ value for HO(2*a*) as compared to the $\Delta\delta$ values for the other OH groups of unit *a* is larger (0.30 *vs.* 0.08–0.14 ppm) than what has been observed for the spectrum in (D_6)DMSO (0.22 *vs.* 0.08–0.10 ppm), possibly resulting from a stronger partial O(6*b*)–H···O(2*a*) H-bond.

The $\Delta\delta$ value for HO(2*c*) of **T-3** *vs.* HO(2) of **T-1** (0.14 ppm) must reflect the influence of attaching a glucosyl unit to HO(4) ('alkylation shift'). It is very similar to the $\Delta\delta$ value in (D_6)DMSO (0.15 ppm). The $\Delta\delta$ value for HO(6*c*) of **T-3** *vs.* HO(6) of **T-1**, however, is 0.05 ppm in (D_5)pyridine as compared to 0.10 ppm in (D_6)DMSO; *i.e.*, the deshielding of HO(6*c*) ('alkylation shift') is weaker than expected from the comparison to the $\Delta\delta$ value for HO(2*c*) and to the $\Delta\delta$ values in (D_6)DMSO, in agreement with the additional effect of an interresidue H-bond between HO(6*c*) and HO(2*b*), with HO(6*c*) acting predominantly as H-donor. This interpretation is in keeping with the couplings of HO(6*c*) that appear as *doublet*s of *doublet*s, and not as *triplet*s.

The chemical shift of HO(2*b*) and HO(6*b*) must reflect a combination of the effects of units *a* and *c*. One expects a $\Delta\delta$ value of 0.44 ppm for HO(2*b*) and of 0.15 ppm for HO(6*b*) ('alkylation' and 'protonation shifts'); compared to the experimental values of 0.55 and 0.10 ppm this appears to confirm that HO(6*c*) acts predominantly as H-donor to HO(2*b*) and HO(6*b*), similarly to HO(2*a*). HO(6*b*) of **T-3** resonates as a *triplet* with $J = 6.3$ Hz, while HO(6*c*) shows two different coupling constants ($J = 6.5$ and 4.6 Hz). In summary, the analysis of *J*(H,OH) and δ(OH) values for **T-3** *vs.* **T-1** suggests rapid interresidue flip-flop H-bonds between HO(6*c*) and HO(2*b*), and between HO(6*b*) and HO(2*a*), with the primary OH groups acting preferentially as H-bond donors.

As in (D_6)DMSO, the $\Delta\delta$ values for corresponding CH signals of **T-x** and **T-x-x** (**x** = 1–3) in (D_5)pyridine are small ($\leq$0.05 ppm). A closer inspection of the δ(CH) and δ(OH) values of **T-1-1** and those of **T-1** shows a weak upfield shift of 0.01–0.05 ppm for all CH (*Table 7* and *Fig. 13*). An upfield shift (0.03 ppm) is also observed for HO(3) and HO(4). The weak upfield shift of 0.09–0.10 ppm for HO(2) and HO(6) suggests an interchain flip-flop H-bond. An analogous comparison of the δ(CH) and δ(OH) values of **T-3-3** with those of **T-3** leads to a similar result. Stronger upfield shifts are only observed for HO(2) and HO(6): 0.10 ppm for HO(2*c*), 0.06 ppm for HO(2*b*), 0.06 ppm for HO(6*c*) and HO(6*b*), and 0.05 ppm for HO(6*a*). These values evidence interchain

(flip-flop) H-bonds between HO(2) and HO(6*) with a persistence that decreases with increasing distance of the units from the link. This interpretation is corroborated by two different J(6,OH) values for units *c* and *b* of **T-3-3**.

The temperature dependence of the OH and H–C(1) signals of **T-x** and **T-x-x** (**x** = 1 and 3) was determined in the range of 298 to 333 K in 5 K steps. It increases from −0.8 to −2.3 ppb/K for all H–C(1) *via* −7.5 to −8.6 ppb/K for HO(3*b*) and HO(3*c*) to −11.7 to −15.6 ppb/K for all other OH groups (*Table 8*), suggesting a typical $\Delta\delta$(OH)/ΔT value for a completely intramolecularly H-bonded OH of −7 to −9 ppb/K. The slightly weaker temperature dependence for HO(2) and HO(6) of **T-1-1** than for the corresponding OH of **T-1** ($\Delta\Delta\delta$(OH)/ΔT = 0.8–0.9 ppb/K) agrees with a weakly persistent interchain flip-flop H-bond between HO(2) and HO(6*). However, HO(2*c*) and HO(6*c*) of **T-3-3** show a stronger temperature dependence than the corresponding OH of **T-3** ($\Delta\Delta\delta$(OH)/ΔT = 1.0 and 1.8 ppb/K, resp.), whereas HO(2*b*), HO(6*b*), HO(2*a*), and HO(6*a*) of **T-3-3** show only a slightly stronger temperature dependence ($\Delta\Delta\delta$(OH)/ΔT = 0.3–0.5 ppb/K). The distinctly stronger temperature dependence of HO(2*c*) of **T-3-3** suggests that it acts predominantly as H-acceptor of a weakly persistent interstrand O(6*c**)–H···O(2*c*) H-bond. The temperature dependencies of HO(6*c*), HO(2*b*), HO(6*b*), and HO(2*a*) of **T-3-3** may be influenced by both intra- and interchain interactions and can not be interpreted easily.

Table 8. *$\Delta\delta/\Delta T$ Values for OH and H–C(1)* [ppb/K] *of* **T-x** *and* **T-x-x** (**x** = 1, 3) *in (D$_5$)Pyridine*[a])

	T-1	**T-1-1**	**T-3**	**T-3-3**
HO(2*a*)	−15.6	−14.5	−11.9	−12.3
HO(2*b*)			−12.2	−12.7
HO(2*c*)			−15.6	−16.6
HO(3*a*)	−14.8	−14.6	−14.0	−14.4
HO(3*b*)			−7.5	−7.7
HO(3*c*)			−7.7	−8.6
HO(4*a*)	−14.3	−14.2	−13.0	−13.8
HO(6*a*)	−15.6	−14.8	−12.1	−12.4
HO(6*b*)			−12.1	−12.4
HO(6*c*)			−11.7	−13.5
H–C(1*a*)	−1.9	−1.3	−1.7	−2.3
H–C(1*b*)			−2.0	−2.2
H–C(1*c*)			−0.9	−0.8

[a]) Deduced from the ^{1}H-NMR spectra recorded at 298 to 333 K in 5 K intervals of 20 mM soln. of **T-x** (**x** = 1, 3) and of 10 mM soln. of **T-x-x** (**x** = 1, 3).

Unfortunately, strong saturation transfer and TOCSY effects (strong negative cross-peaks for CH and OH signals) prevent a straightforward interpretation of the ROESY spectra of **T-3** and **T-3-3** in (D$_5$)pyridine.

Thus, the main difference between **T-x-x** in (D$_6$)DMSO and (D$_5$)pyridine is the enhanced interchain interaction in (D$_5$)pyridine. While this interaction in (D$_6$)DMSO is only evidenced for units *c*/*c**, it is also apparent for units *b*/*b** and *a*/*a** of **T-3-3** in (D$_5$)pyridine. This may be taken to indicate that interchain interactions will be stronger

in the solid state so that **T-x-x** may not be a suitable model for cellulose I. Unfortunately, **T-4-4** and **T-8-8** did not, in our hands, led to crystals suitable for X-ray analysis. We have, therefore, measured solid-state CP/MAS ^{13}C-NMR spectra of **T-x** and **T-x-x** (**x** = 1–4, 8).

5. *Determination of H-Bonds in the Solid State of* **T-x** *and* **T-x-x**. The differences in the conformation and packing of the chains in cellulose I_α, I_β[16]), and cellulose II are reflected in their solid-state CP/MAS ^{13}C-NMR spectra [5][60–64] (*Fig. 14*). C(1) of cellulose I_β and cellulose II give rise to two signals of aproximately equal intensity at 105.2–108.3 ppm, whereas C(1) of cellulose I_α resonate as a single peak at 106.3 ppm. C(4) of all three polymorphs appear as a more or less well-resolved double peak between 88.7 and 91.0 ppm. C(2), C(3), and C(5) (78.0–72.0 ppm) appear as three peaks in the spectrum of cellulose II and as four peaks in the spectra of cellulose I_α and I_β, with characteristic intensity ratios. C(6) of cellulose II and cellulose I_β give rise to two signals, and C(6) of cellulose I_α to a single one. The chemical shifts of C(6) of cellulose I_α and I_β (66.1–66.5 ppm) have been taken to reveal a *tg*, and those for cellulose II (63.6 and 64.2 ppm) a *gt* conformation [15]. This is in contradiction to the

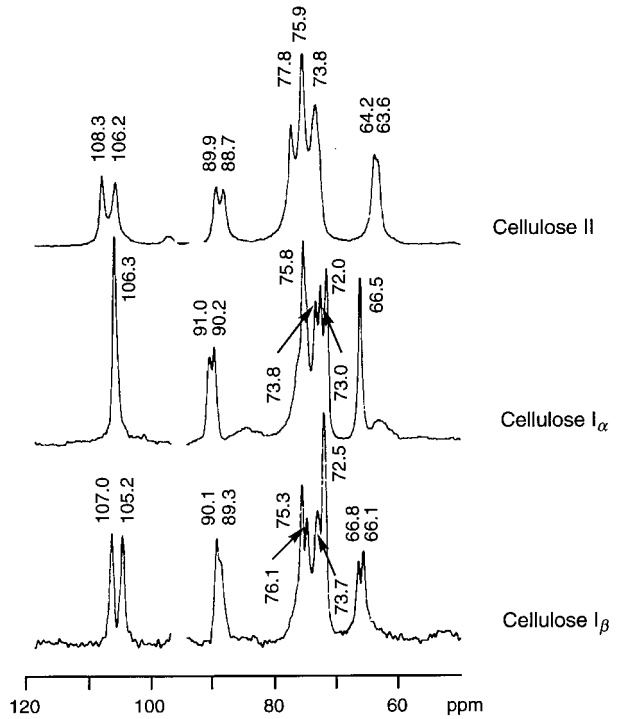

Fig. 14. *Solid-state CP/MAS ^{13}C-NMR spectra of cellulose I_α, I_β, and II* (from [62])

16) The solid-state ^{13}C-NMR spectrum of cellulose I_α was derived from a linear combination of the spectrum of I_α-rich cellulose and that of cellulose I_β, since pure cellulose I_α could not be obtained.

conclusion deduced from the X-ray crystal-structure analysis of cellulose II fibers, postulating a *tg* conformation of the centre chains [12][13]. A recent X-ray crystal-structure analysis of β-cellotetraose hemihydrate [16][17] and molecular-dynamics simulations of cellulose II [18], however, favour a *gt* conformation for all chains of cellulose II, and this has been confirmed by a recent neutron-diffraction analysis of deuteriated cellulose II fibers [19].

Solid-state CP/MAS ^{13}C-NMR spectra of **T-x** and **T-x-x** (**x** = 1–4, 8) are shown in *Figs. 15* and *16*, and their chemical shifts relative to the methyne ^{13}C resonance of

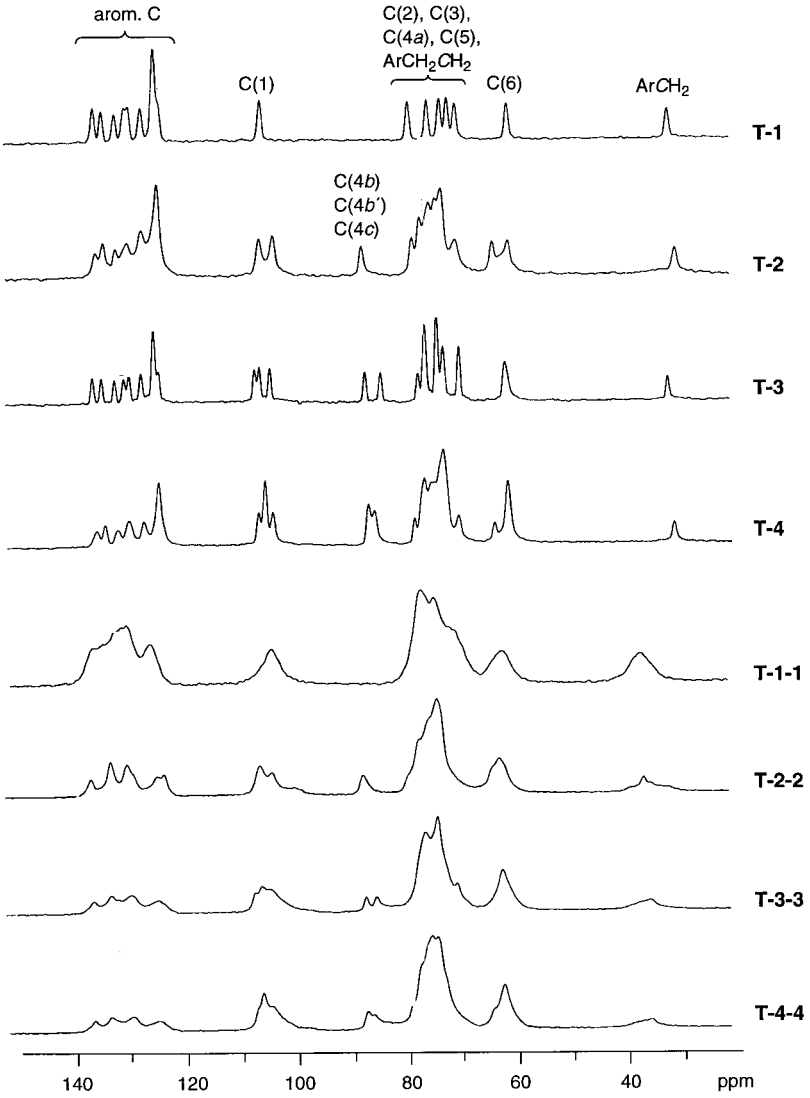

Fig. 15. *Solid-state CP/MAS ^{13}C-NMR spectra of* **T-x** *and* **T-x-x** (**x** = 1–4)

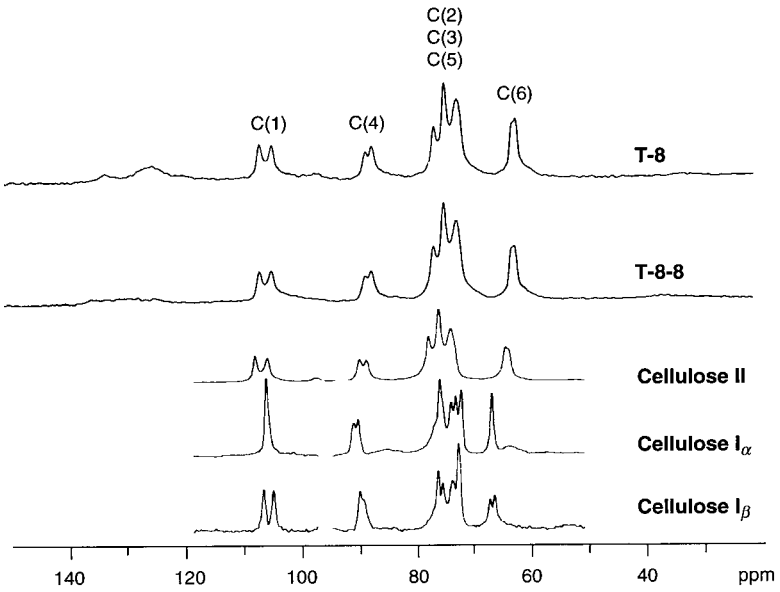

Fig. 16. *Solid-state CP/MAS ^{13}C-NMR spectra of* **T-8**, **T-8-8**, *and cellulose I_α, I_β, and II*

adamantane (38.6 ppm) are listed in *Table 9*. The peak assignment is based on a comparison with the data in D_2O solution and with those of cellodextrins in the solid state [65][66]. The signals of **T-1** and **T-3** are sharp and those of **T-2** and **T-4** slightly broadened (*Fig. 15*). The signals of **T-x-x** (**x** = 1–4) are broad, similar to what has been observed for the corresponding cellodextrins [65]. The relative intensities of the peaks for the benzyl and naphthyl signals at 31.4–32.6 and 136.1–124.3 ppm, respectively, decrease with increasing saccharide chain length. The ranges of the chemical shift for all C(1) to C(6) agree well with the δ values of related cellodextrins [65][66].

The anomeric C(1) of **T-x** (**x** = 1–4) resonate at 107.2–103.8 ppm. Each C(1) of **T-x** (**x** = 1–3) gives rise to a distinct peak, while the four C(1) of **T-4** appear as three peaks with a 1:2:1 intensity. The signal at the highest field of **T-2**, **T-3**, and **T-4** (*ca.* 104 ppm) is best assigned to C(1*c*), similarly as for the corresponding methyl cellosides [66]. The assignment of the resonances at lower field (106.3–107.2 ppm) to C(1*a*), C(1*b*), and C(1*b*′) is in agreement with the data for cellodextrins [65]. The resonances in the range of 79.3–70.2 ppm are assigned to C(2), C(3), C(4*a*), C(5), and $ArCH_2CH_2$. C(6) of **T-1** resonates at 61.5 ppm, and C(6*a*), C(6*b*), and C(6*c*) of **T-3** at 62.0 ppm. Two peaks at 61.4 and 64.1 ppm are observed for the two C(6) of **T-2**, and two peaks with the intensity ratio 3:1 at 61.8 and 64.1 ppm for the four C(6) of **T-4**. The δ values suggest a *gg* conformation for all units of **T-x** (**x** = 1–4), except for one unit of **T-2** and of **T-4**, which possesses the *gt* conformation (δ = 64.1 ppm). It is tempting to correlate the *gt* conformation of one unit with the even number of units in **T-2** and **T-4**, *i.e.*, with the presence of one or two well-defined cellobiosyl moieties (two different ones, *c-b* and *b-a*, are possible in **T-3**) and with the role of cellobiose as repeating unit of celluloses. The

Table 9. *Solid-State CP/MAS ^{13}C-NMR Chemical Shifts* [ppm] *of* **T-x** *and* **T-x-x** (**x** = 1–4, 8)[a])

	C(1)	C(4*b*), C(4*b*′), C(4*c*)	C(2), C(3), C(4*a*), C(5), $ArCH_2CH_2$	C(6)	$ArCH_2$	Arom. C
T-1	106.1	–	79.3, 76.0, 73.7, 72.3, 70.8	61.5	32.6	135.9, 134.4, 132.0, 130.3, 129.6, 127.4, 125.1 (s), 124.1 (sh)
T-2	106.3, 103.8	87.9	78.9, 77.4, 75.7, 74.6, 73.6, 71.0	64.1, 61.4	31.4	135.7, 134.3, 132.1, 130.0, 127.4, 124.6 (s)
T-3	107.2, 106.3, 104.4	87.3, 84.5	77.7, 76.4, 74.3, 73.1, 70.2	62.0	32.6	136.1, 134.5, 132.1, 130.5, 129.6, 127.5, 125.2 (s), 124.3
T-4	106.7, 105.7 (s), 104.2	87.0, 85.9	78.6, 76.9, 75.5, 73.4, 70.7	64.1, 61.8 (s)	32.0	135.8, 134.3, 131.9, 129.9, 127.3, 124.7 (s)
T-8	107.5, 105.5	89.0, 88.0	77.2, 75.2, 73.1	63.0 (br.)	[b])	136–124 (w)
T-1-1	103.8	–	76.9, 74.5, 70.9	62.3	37.1	135.8, 134.0, 131.6, 130.5, 129.7, 125.6
T-2-2	106.3, 104.0	87.4	79.3 (sh), 77.5, 75.8 (sh), 74.6	64.3 (sh), 62.7	37.0	136.4, 132.8, 129.9, 124.5, 123.2
T-3-3	107.2, 106.0, 104.2	87.3, 85.4	76.6, 74.3, 70.8	62.6	36.3	136.1, 133.0, 129.4, 124.6
T-4-4	106.7 (sh), 105.8 (s), 104.3	87.1, 86.0	78.9 (sh), 77.2 (sh), 75.3, 74.3	64.1 (sh), 62.3	35.8	136.1, 133.1, 129.3, 124.5
T-8-8	107.5, 105.5	89.0, 88.0	77.2, 75.2, 73.1	63.0 (br.)	[b])	136–124 (w)

[a]) s: Strong signal, w: weak signal, br.: broad signal, sh: shoulder. [b]) Hidden by the noise.

γ-effect on C(4) in the *gg*, but not in the *gt* conformer[17]), suggests indirectly that unit *a* of **T-4** adopts the *gt* conformation and perhaps also unit *a* of **T-2**. The signals between 84.5 and 88 ppm correspond to C(4) of units *b*, *b*′, and *c*, while C(4*a*) that is not glucosylated resonates between 70 and 80 ppm. The signals at 87.3 and 84.5 ppm of **T-3** must correspond to C(4) of units *b* and *c* with a *gg* conformation, as evidenced by the δ(C(6)) value. One expects a δ value of 87.5–90.3 ppm for C(4) of these units with a *gt* conformation (no γ-effect). None of the signals corresponding to C(4) of unit *b*, *b*′, and *c* of **T-4** resonates in such a position, whereas C(4*c*) of **T-2** resonates just at the lower limit of this range (87.9 ppm), evidencing that unit *a* of **T-4** and perhaps also unit *a* of **T-2** adopt the *gt* conformation. This assignment agrees with the *gg* conformation of unit *c* and the *gt* conformation of unit *a* of methyl β-cellobioside·MeOH complex [72], but not with the *gt* conformation of all units of β-cellotetraose hemihydrate [16][17].

The solid-state CP/MAS ^{13}C-NMR spectrum of **T-4** deviates more strongly from that of cellulose II than that of β-cellotetraose hemihydrate [66], evidencing the influence of the bulky aglycon.

Apart from the lower resolution and the characteristic downfield shift of the signal for $ArCH_2$ ($\Delta\delta$ = 4–5 ppm, as already observed in the solution spectra), the spectra of **T-x-x** (**x** = 1–4) correspond closely to the spectra of the related monochain analogues

---

17) An interpretation of the CP-MAS ^{13}C-NMR and X-ray data in [67–71] on the basis of *Horii*'s assignment [15] shows that the *gg* conformation of glucopyranoses and methyl glucopyranosides leads to an upfield shift for C(4) of *ca.* 3 ppm relative to δ(C(4)) of glucopyranoses and methyl glucopyranosides possessing the *gt* conformation.

(*Table 9* and *Fig. 15*), evidencing that the glycosidic chains in **T-x** and **T-x-x** (**x** = 1–4) possess a similar conformation, and that the chains in **T-x-x** do not significantly interact with each other. There is no significant resemblance of the spectra of **T-x-x** (**x** = 2–4) to those of cellulose I_α, I_β, and II.

Fig. 16 shows the solid-state CP/MAS ^{13}C-NMR spectra of **T-8** and **T-8-8**, together with those of cellulose I_α, I_β, and II. The signals of the template moiety of **T-8** and **T-8-8** are weak and broad. The same is expected for the signals of the units *a* and *c*. Thus, the strong signals of **T-8** and **T-8-8** are due to the central units *b* and *b'*, facilitating a comparison with the spectra of celluloses. The spectra of **T-8** and **T-8-8** strongly resemble each other, showing two peaks for C(1), two for C(4), three for C(2), C(3), and C(5), and a broad peak for C(6). These spectra closely resemble the spectrum of cellulose II, and are clearly different from the spectra of cellulose I_α and I_β. Particularly remarkable is the *gt* conformation of **T-8-8** evidenced by C(6) at 63.0 ppm (*Table 9*). The similarity of the spectra of **T-8**, **T-8-8**, and cellulose II suggests antiparallel packing for **T-8** and, surprisingly, also for **T-8-8**, indicating that the intermolecular H-bonding between antiparallel chains in **T-8-8** is stronger than the intramolecular H-bonding between parallel chains.

The distance of 5.4 or 6.0 Å between the parallel origin and centre chains in cellulose I_β is easily mimicked by **T-8-8**, as schematically shown in *Fig. 17*, *a* and *b* (the O···O distance in crystalline naphthalene-1,8-diethanol is 6.01 Å [1]). One does not expect destabilizing interactions between the two parallel naphthalene units in such a structure, as they are *ca.* 8.2 Å apart. However, the phase shift between the origin and centre chains (*ca.* 2.6 Å in cellulose I_β) is not easily mimicked, and this may be an important factor explaining why **T-8-8** does not adopt a cellulose I_β-like structure. If the axes of the cellooctaosyl chains are parallel to the central bond of the naphthalene moiety (*i.e.*, to the C(4a)–C(8a) bond), a phase shift of 1.5 Å is easily adopted (as observed for crystalline naphthalene-1,8-diethanol), but the phase shift can hardly exceed this value. A larger phase shift in **T-8-8** forces the chain axes to be oblique to the C(4a)–C(8a) bond of the naphthyl moiety.

How can the cellulose II-like structure of **T-8-8** be rationalised? The inversion of the orientation of alternating units in *Fig. 17*, *a* and *b*, does not lead to cellulose II-like structures, since the chains within the sheets of the resulting structures (**A** and **B**, **E** and **F** in *Fig. 17*, *c*, **B** and **G**, **E** and **F** in *Fig. 17*, *d*) are antiparallel. There is no natural precedent for such structures, but, *a priori*, **T-8-8** could adopt such a structure in the solid state.

It is impossible to build a cellulose II-like lattice for **T-8-8** possessing parallel octaosyl chains. To be antiparallel, the chains of **T-8-8** have to be on opposite sides of the naphthalene ring, and the axes of the octaose backbone must be orthogonal to the plane of the naphthyl residue. This is illustrated by the two possible structures in *Fig. 17*, *e* and *f*. They appear to be mimics of cellulose II, since one chain is an origin and the other a centre chain with the required opposite directions, and since the chains within the sheets are parallel (**A**, **B**, and **G** on the one hand; **E** and **F** on the other hand). The phase shift of these chains is readily modulated by the distance between the aromatic moieties along the axis *c*. As the distance between the benzylic C-atoms of crystalline naphthalene-1,8-diethanol is 3.05 Å [1], the structure depicted in *Fig. 17*, *e* (distance of 4.4 Å between the origin and centre chains), appears more probable than the structure depicted in *Fig. 17*, *f* (distance of 7.4 Å).

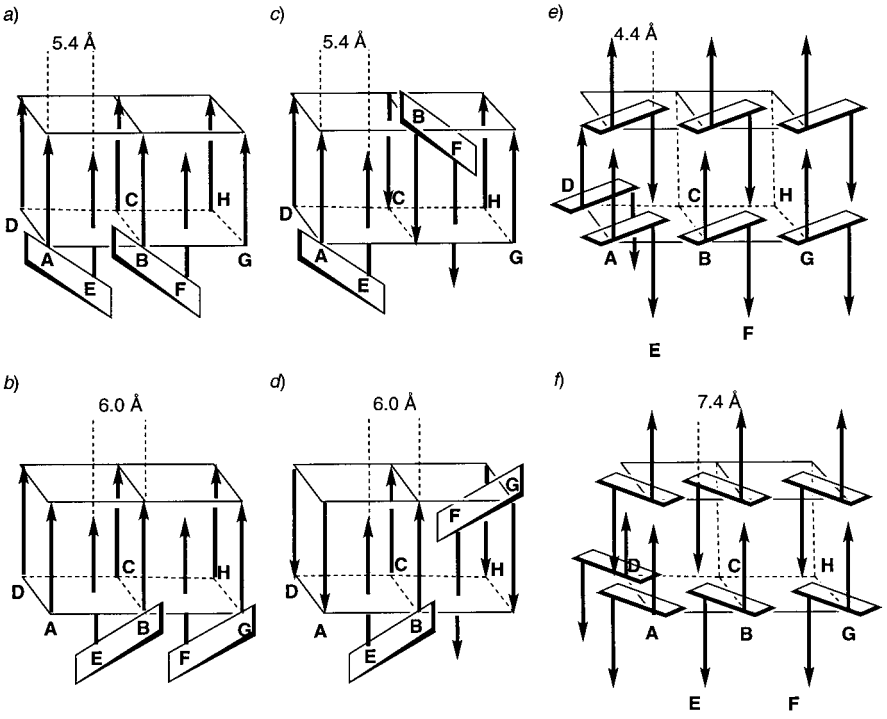

Fig. 17. *Schematic possible packings of* **T-8-8** *in the solid state* (the naphthalene moiety is represented by a rectangle and the octaosyl chains by arrows). a) *and* b) *Parallel packing of molecules possessing parallel-oriented octaosyl chains: models for cellulose* I_β. c) *and* d) *Antiparallel packing of molecules possessing parallel-oriented octaosyl chains.* e) *and* f) *Packing of molecules possessing antiparallel-oriented octaosyl chains: models for cellulose II.*

Conclusion. – A completely persistent inter-residue O(3)–H···O(5′) H-bond and a weakly persistent inter-residue flip-flop H-bond between HO(6) and HO(2′) of **T-x** and **T-x-x** (**x** = 2–4, 8) in (D_6)DMSO, and of **T-3** and **T-3-3** in (D_5)pyridine are evidenced by the analysis of the δ(OH), J(H,OH), and $\Delta\delta$(OH)/ΔT values. Cross-peaks between the signals for H–C(1′) and the signals for each HO(3) and HO(2′) in the ROESY spectra of **T-x** and **T-x-x** (**x** = 4, 8) in (D_6)DMSO, and the additional cross-peaks between the signals for H–C(1′) and the signals for HO(6) in the ROESY spectra of **T-4-4** and **T-8-8** provide further evidence for these inter-residue H-bonds. Weak interchain interactions were, however, only observed for the units closest to the link of **T-x-x** (**x** = 1–4, 8) in (D_6)DMSO, and for parallel units of **T-1-1** and **T-3-3** in (D_5)pyridine. Interchain interactions in **T-x-x** are stronger in (D_5)pyridine and decrease with increasing distance from the link. Thus, the analysis of the solution spectra shows that the cellodextrin chains of **T-x-x** (**x** = 2–4, 8) are not parallel, but slightly divergent, like scissors.

The solid-state CP/MAS ^{13}C-NMR spectra of **T-x** and **T-x-x** (**x** = 1–4) do not resemble those of cellulose I_α, I_β, and II. Particularly noteworthy is the *gg* conformation, except for the *gt* conformation of one unit of **T-x** and **T-x-x** (**x** = 2, 4). The difference between the CP/MAS ^{13}C-NMR spectra of **T-x**/**T-x-x** (**x** = 3, 4) and

celluloses evidences the influence of the bulky aglycon, since the solid-state CP/MAS ^{13}C-NMR spectra of cellotriose and cellotetraose hemihydrate resemble (apart from line broadening) that of cellulose II [65]. The solid-state CP/MAS ^{13}C-NMR spectra of **T-8** and, surprisingly, also of **T-8-8** closely resemble that of cellulose II, showing that a chain length of >4 is required for **T-x** and **T-x-x** to mimic cellulose II. The *gt* conformation of **T-8** and **T-8-8** observed is in keeping with the recently published models of cellulose II obtained from extrapolations of the crystal structure of β-cellotetraose hemihydrate by *Saenger* and co-workers [16], from molecular dynamic calculations of *Kroon-Batenburg* and *Kroon* [18], and from the neutron-diffraction analysis of *Langan et al.* [19]. The strong similarity of the spectra of **T-8-8** and cellulose II is taken as evidence for a similar packing. This can be rationalised by an antiparallel orientation of the cellodextrin chains of **T-8-8** pointing in opposite directions, with chain axes orthogonal to the naphthalene ring. Thus, a flexible template possessing parallel cellodextrin chains does not impose sufficient constraints on the structure of supramolecular assemblies to mimic native celluloses, but leads to a close mimic of cellulose II. With regard to templated models for cellulose I, our results suggest that three conditions have to be fulfilled: the correct distances between the chains, the correct phase shift between the chains, and a low degree of flexibility of the link. A rigid link forcing the cellodextrin chains in a parallel, correctly staggered orientation is probably necessary for a good mimic of native celluloses.

We thank the *Swiss National Science Foundation* and *F. Hoffmann-La Roche, AG*, Basel, for generous support, Dr. *Zhenhong Gan* for recording the CP/MAS solid-state ^{13}C-NMR spectra, Mrs. *B. Brandenberg* for measuring the 500-MHz NMR spectra, and Prof. *B. Jaun* and Dr. *K. V. S. N. Murty* for helpful discussions.

Experimental Part

NMR Experiments with Solutions. D_2O, (D_6)DMSO, and (D_5)pyridine were used as received from *Dr. Glaser AG*, Basel. A fresh ampoule of (D_6)DMSO and (D_5)pyridine was opened for each NMR experiment. The soln. NMR spectra of 10 mM solns. of **T-x-x** (**x** = 1–4), 20 mM solns. **T-x** (**x** = 1–4), and *ca.* 3 mM solns. of **T-3** and **T-4** in D_2O and of **T-8** and **T-8-8** in (D_6)DMSO were recorded on a *Bruker AMX 500* spectrometer or on a *Varian XL 300* spectrometer at 300 K. The ^{1}H-NMR chemical shifts were reported in ppm relative to TMS (0.0 ppm) for (D_6)DMSO and (D_5)pyridine solns., and to acetone (2.15 ppm) for D_2O solns. as internal standard. ^{1}H-NMR Assignments are based on selective homonuclear decoupling experiments (for **T-1**, **T-1-1**, **T-2**, and **T-2-2**), on double-quantum-filtered correlation spectroscopy (DQF-COSY), total correlation spectroscopy (TOCSY), rotation frame *Overhauser* effect spectroscopy (ROESY) (for **T-3** and **T-3-3** in (D_5)pyridine, and for **T-4**, **T-4-4**, **T-8**, and **T-8-8** in (D_6)DMSO). Data matrices were typically 448 real by 4096 complex for DQF-COSY experiments, 512 real by 2048 complex for TOCSY experiments, and 632 real by 2048 complex for ROESY experiments. The mixing time used for all TOCSY and ROESY experiments was 250 ms. The spin-lock field strength used for ROESY experiments was 3 KHz. The samples of **T-1**, **T-1-1**, **T-4**, and **T-4-4** for SIMPLE ^{1}H-NMR experiments in (D_6)DMSO were prepared by the addition of small aliquots of D_2O [43] to the (D_6)DMSO soln. until the required deuteriation ratio (*ca.* 1:1) of the OH groups was reached [43]. The OH/OD ratio was determined by comparison of the integral of the residual OH signals with that of a H–C(1*a*).

Solid-State CP/MAS ^{13}C-NMR Spectroscopy. The solid-state CP/MAS ^{13}C-NMR experiments were performed on a homebuilt NMR spectrometer (75 MHz for ^{13}C at 300 K) equipped with a 4-mm MAS double resonance probe from *Chemagnetics*, Ft. Ciollins, Colorado, USA[18]). For all samples, the spinning frequency was 16 kHz, the contact time for cross polarization 2 ms, and the data acquisition time 41 ms. The radio-frequency field strengths are 100 kHz and 84 kHz for the ^{1}H and the ^{13}C channel, respectively. The numbers of scans

[18]) We thank Dr. *Zhehong Gan* from the group of Prof. *R. R. Ernst*, ETH-Zurich, for measuring the spectra and for helpful discussions.

collected vary from 1000 to 6000 with a repetition of 8 s for all samples. The methyne ^{13}C resonance of adamantane (38.6 ppm) is used as external reference. The peak assignment is based on a comparison with the data in solution (D_2O) and with those for cellodextrins in the solid state [65].

*2-(Naphthalen-1-yl)ethyl β-*D*-Glucopyranoside* (**T-1**). ^1H-NMR (500 MHz, (D_6)DMSO): 8.11 (*dd*, *J* = 1.0, 8.2), 7.91 (*dd*, *J* = 1.5, 8.1), 7.78 (*dd*, *J* = 1.7, 7.5), 7.55 (*ddd*, *J* = 1.5, 6.8, 8.3), 7.50 (*ddd*, *J* = 1.3, 6.8, 8.1), 7.45 (*dd*, *J* = 1.9, 6.9), 7.42 (*t*, *J* ≈ 7.3) (7 arom. H); 4.974 (*d*, *J* = 4.8, HO–C(2^I)); 4.910 (*d*, *J* = 4.8, HO–C(3^I)); 4.874 (*d*, *J* = 5.2, HO–C(4^I)); 4.466 (*t*, *J* = 5.9, HO–C(6^I)); 4.237 (*d*, *J* = 7.8, H–C(1^I)); 4.02 (*ddd*, *J* = 7.0, 8.1, 9.8, $ArCH_2CH$); 3.80 (*ddd*, *J* = 6.8, 8.4, 9.7, $ArCH_2CH$); 3.67 (*ddd*, *J* = 2.1, 5.8, 11.8, H–C(6^I)); 3.43 (*td*, *J* = 5.9, 11.7, H′–C(6^I)); 3.38–3.31 (*AB* of *ABMX*, $ArCH_2$); 3.15 (*dt*, *J* = 4.8, 8.8, H–C(3^I)); 3.11 (*ddd*, *J* = 2.1, 5.9, 9.4, H–C(5^I)); 3.04 (*ddd*, *J* = 5.1, 8.7, 9.5, H–C(4^I)); 2.98 (*ddd*, *J* = 4.8, 7.9, 8.9, H–C(2^I)). ^1H-NMR (500 MHz, (D_5)pyridine): 8.09–8.05 (*m*), 7.89–7.87 (*m*), 7.75 (*dd*, *J* = 2.1, 7.2), 7.48–7.42 (*m*, 2 H), 7.38–7.34 (*m*, 2 H) (7 arom. H); 7.22 (*d*, *J* = 4.3, HO–C(2^I)); 7.17 (*d*, *J* = 4.0, HO–C(3^I)); 7.15 (*d*, *J* = 4.1, HO–C(4^I)); 6.41 (*t*, *J* ≈ 6.2, HO–C(6^I)); 4.93 (*d*, *J* = 7.7, H–C(1^I)); 4.56 (*ddd*, *J* = 2.4, 5.9, 11.7, H–C(6^I)); 4.40 (*ddd*, *J* = 7.8, 8.3, 9.5, $ArCH_2CH$); 4.39 (*ddd*, *J* = 5.4, 6.4, 11.7, H′–C(6^I)); 4.27 (*dt*, *J* = 3.8, 8.9, H–C(3^I)); 4.25 (*dt*, *J* = 4.6, 8.8, H–C(4^I)); 4.09 (*ddd*, *J* = 4.3, 8.1, 8.9, H–C(2^I)); 4.02 (*ddd*, *J* = 7.1, 8.4, 9.7, $ArCH_2CH$); 3.97 (*ddd*, *J* = 2.4, 5.4, 9.2, H–C(5^I)); 3.53–3.44 (*AB* of *ABMX*, $ArCH_2$). ^{13}C-NMR (75 MHz, (D_6)DMSO): 134.79 (*s*, C(1)); 133.53 (*s*, C(4a)); 131.79 (*s*, C(8a)); 128.70, 127.02, 126.91, 126.28 (4*d*, C(2), C(3), C(4), C(5)); 125.76 (*d*, C(6), C(7)); 123.92 (*d*, C(8)); 103.18 (*d*, C(1^I)); 77.02 (*d*, C(5^I)); 76.82 (*d*, C(3^I)); 73.54 (*d*, C(2^I)); 70.13 (*d*, C(4^I)); 69.01 (*t*, $ArCH_2CH_2$); 61.11 (*t*, C(6^I)); 32.74 (*t*, $ArCH_2$).

*2-(Naphthalen-1-yl)ethyl β-*D*-Glucopyranosyl-(1 → 4)-β-*D*-glucopyranoside* (**T-2**). ^1H-NMR (500 MHz, (D_6)DMSO): 8.09 (br. *d*, *J* = 8.4), 7.90 (br. *d*, *J* = 8.0), 7.78 (*dd*, *J* = 1.6, 7.7), 7.55 (*ddd*, *J* = 1.3, 6.8, 8.3), 7.50 (*ddd*, *J* = 1.0, 7.1, 7.5), 7.44 (*dd*, *J* = 2.0, 7.2), 7.42 (*dd*, *J* = 7.1, 7.5) (7 arom. H); 5.199 (*d*, *J* = 4.8, HO–C(2^{II})); 5.127 (*d*, *J* = 5.0, HO–C(2^I)); 4.983 (*d*, *J* = 4.9, HO–C(3^{II})); 4.958 (*d*, *J* = 5.5, HO–C(4^{II})); 4.667 (br. *s*, HO–(3^I)); 4.576 (*t*, *J* ≈ 5.0, HO–C(6^{II})); 4.566 (*t*, *J* = 5.9, HO–C(6^I)); 4.310 (*d*, *J* = 7.9, H–C(1^I)); 4.240 (*d*, *J* = 7.9, H–C(1^{II})); 4.03 (*ddd*, *J* = 7.1, 8.1, 9.8, $ArCH_2CH$); 3.80 (*ddd*, *J* = 6.6, 8.3, 9.7, $ArCH_2CH$); 3.78 (*ddd*, *J* = 2.0, 5.5, 12.0, H–C(6^I)); 3.69 (*ddd*, *J* = 2.1, 5.0, 11.6, H–C(6^{II})); 3.60 (*ddd*, *J* = 4.3, 6.0, 11.9, H′–C(6^I)); 3.40 (*ddd*, *J* = 5.8, 6.4, 11.8, H′–C(6^{II})); 3.37–3.27 (*m*, H–C(3^I), H–C(4^I), H–C(5^I), $ArCH_2$); 3.18 (*ddd*, *J* = 2.0, 6.7, 9.6, H–C(5^{II})); 3.15 (*dt*, *J* = 5.1, 8.8, H–C(3^{II})); 3.05 (*ddd*, *J* = 4.9, 8.0, 9.0, H–C(2^I)); 2.98 (*ddd*, *J* = 5.1, 8.1, 8.7, H–C(2^{II})); 3.03 (*dt*, *J* = 5.7, 9.0, H–C(4^{II})). ^1H-NMR (500 MHz, (D_5)pyridine): 8.06–8.03 (*m*), 7.89–7.87 (*m*), 7.75 (*dd*, *J* = 2.4, 7.0), 7.48–7.42 (*m*, 2 H), 7.38–7.34 (*m*, 2 H) (7 arom. H); 7.0–6.0 (br. *s*, 7 OH); 5.20 (*d*, *J* = 7.8, H–C(1^{II})); 4.86 (*d*, *J* = 7.8, H–C(1^I)); 4.545 (*dd*, *J* = 2.4, 11.7, H–C(6^{II})); 4.54 (*dd*, *J* = 3.5, 11.7, H–C(6^I)); 4.48 (*dd*, *J* = 2.8, 12.1, H′–C(6^I)); 4.34 (*t*, *J* = 9.2, H–C(4^{II})); 4.34 (br. *q*, *J* ≈ 8.1, $ArCH_2CH$); 4.30 (*dd*, *J* = 5.9, 11.6, H′–C(6^{II})); 4.28 (*t*, *J* ≈ 8.8, H–C(3^{II})); 4.21 (*dd*, *J* = 8.3, 8.9, H–C(3^I)); 4.20 (*dd*, *J* = 8.7, 9.3, H–C(4^I)); 4.11 (*t*, *J* ≈ 8.0, H–C(2^{II})); 4.08 (*dd*, *J* = 7.9, 8.7, H–C(2^I)); 4.01 (*ddd*, *J* = 2.5, 5.7, 9.2, H–C(5^{II})); 3.98 (*td*, *J* ≈ 6.7, 9.5, $ArCH_2CH$); 3.90 (*ddd*, *J* = 2.9, 3.8, 9.5, H–C(5^I)); 3.53–3.44 (*AB* of *ABMX*, $ArCH_2$). ^{13}C-NMR (75 MHz, (D_6)DMSO): 134.71 (*s*, C(1)); 133.55 (*s*, C(4a)); 131.79 (*s*, C(8a)); 128.73, 127.01, 126.95, 126.29 (4*d*, C(2), C(3), C(4), C(5)); 125.77 (*d*, C(6), C(7)); 123.88 (*d*, C(8)); 103.31 (*d*, C(1^I)); 102.83 (*d*, C(1^{II})); 80.60 (*d*, C(4^I)); 76.83 (*d*, C(5^{II})); 76.43 (*d*, C(3^{II})); 75.08 (*d*, C(5^I)); 74.97 (*d*, C(3^I)); 73.28 (*d*, C(2^{II})); 73.17 (*d*, C(2^I)); 70.02 (*d*, C(4^{II})); 69.13 (*t*, $ArCH_2CH_2$);61.01 (*t*, C(6^{II})); 60.38 (*t*, C(6^I)); 32.68 (*t*, $ArCH_2$).

*2-(Naphthalen-1-yl)ethyl [β-*D*-Glucopyranosyl-(1 → 4)]$_2$-β-*D*-glucopyranoside* (**T-3**). ^1H-NMR (500 MHz, (D_6)DMSO): 8.10 (br. *d*, *J* = 8.6), 7.91 (*dd*, *J* = 1.5, 7.9), 7.78 (*dd*, *J* = 1.7, 7.3), 7.55 (*ddd*, *J* = 1.5, 6.8, 8.2), 7.51 (*ddd*, *J* = 1.2, 6.8, 8.2), 7.46–7.42 (*m*, 2 H) (7 arom. H); 5.365 (*d*, *J* = 5.0, HO–C(2^{II})); 5.200 (*d*, *J* = 5.0, HO–C(2^{III})); 5.128 (*d*, *J* = 5.0, HO–C(2^I)); 4.990 (*d*, *J* = 5.0, HO–C(3^{III})); 4.960 (*d*, *J* = 5.5, HO–C(4^{III})); 4.712 (*d*, *J* = 1.8, HO–C(3^{II})); 4.638 (*t*, *J* = 6.0, HO–C(6^{II})); 4.595 (*d*, *J* = 1.6, HO–C(3^I)); 4.565 (*t*, *J* = 5.9), 4.561 (*t*, *J* = 5.9 (HO–C(6^I), HO–C(6^{III})); 4.332 (*d*, *J* = 7.9, H–C(1^{II})); 4.310 (*d*, *J* = 7.9, H–C(1^I)); 4.232 (*d*, *J* = 7.9, H–C(1^{III})); 4.03 (*ddd*, *J* = 6.7, 8.2, 9.6, $ArCH_2CH$); 3.80 (*ddd*, *J* = 6.8, 8.2, 9.8, $ArCH_2CH$); 3.78–3.71 (*m*, H–C(6^I), H–C(6^{II})); 3.69 (*ddd*, *J* = 2.3, 5.6, 11.6, H–C(6^{III})); 3.59 (*td*, *J* = 5.6, 11.9), 3.57 (*td*, *J* ≈ 5.6, 11.3), (H′–C(6^I), H′–C(6^{II})); 3.42–3.26 (*m*, H–C(3^I), H–C(3^{II}), H–C(4^I), H–C(4^{II}), H–C(5^I), H–C(5^{II}), H′–C(6^{III}), $ArCH_2$); 3.18 (*ddd*, *J* = 2.0, 6.7, 10.0, H–C(5^{III})); 3.14 (*td*, *J* = 8.8, 5.0, H–C(3^{III})); 3.07–3.01 (*m*, H–C(2^I), H–C(2^{II}), H–C(4^{III})); 2.98 (*ddd*, *J* = 5.0, 8.1, 8.8, H–C(2^{III})). ^1H-NMR (500 MHz, (D_5)pyridine): 8.08–8.05 (*m*), 7.91–7.88 (*m*), 7.79–7.76 (*m*), 7.50–7.44 (*m*, 2 H), 7.41–7.36 (*m*, 2 H) (7 arom. H); 7.77 (*d*, *J* = 4.3, HO–C(2^{II})); 7.52 (*d*, *J* = 4.5, HO–C(2^{III})); 7.36 (*d*, *J* = 4.3, HO–C(2^I)); 7.31 (*d*, *J* = 4.3, HO–C(3^{III})); 7.23 (*d*, *J* = 4.5, HO–C(4^{III})); 6.51 (*t*, *J* = 6.3, HO–C(6^{II}), HO–C(6^{III})); 6.46 (*dd*, *J* = 4.6, 6.5, HO–C(6^I)); 6.39 (*d*, *J* = 1.7, HO–C(3^{II})); 6.19 (*d*, *J* = 1.8, HO–C(3^I)); 5.19 (*d*, *J* = 7.9), 5.15 (*d*, *J* = 7.9), (H–C(1^{II}), H–C(1^{III})); 4.86 (*d*, *J* = 7.8, H–C(1^I)); 4.57–4.48 (*m*, 4 H), 4.47 (*ddd*, *J* = 2.7, 5.7, 12.0) (2 H–C(6^I), 2 H–C(6^{II}), H–C(6^{III})); 4.38–4.30 (*m*, $ArCH_2CH$); 4.34 (*t*, *J* = 9.3), 4.31 (*t*, *J* = 9.4), 4.26 (br. *t*, *J* = 9.1, 2 H)

(H–C(3^{I}), H–C(3^{II}), H–C(4^{I}), H–C(4^{II})); 4.34–4.29 (*m*, H′–C(6^{III})); 4.24–4.17 (*m*, H–C(3^{III}), H–C(4^{III})); 4.11 (*ddd*, *J* = 4.0, 8.1, 9.2, H–C(2^{II})); 4.10 (*ddd*, *J* = 4.3, 8.0, 8.8, H–C(2^{III})); 4.07 (*ddd*, *J* = 4.3, 7.9, 8.8, H–C(2^{I})); 4.04–3.97 (*m*, H–C(5^{II}), H–C(5^{III}), ArCH$_2$C*H*); 3.89 (*ddd*, *J* = 2.9, 3.6, 9.5, H–C(5^{I})); 3.54–3.45 (*AB* of *ABMX*, ArC*H*$_2$). ^{13}C-NMR (75 MHz, (D$_6$)DMSO): 134.68 (*s*, C(1)); 133.51 (*s*, C(4a)); 131.75 (*s*, C(8a)); 128.69, 126.98, 126.90, 126.25 (4*d*, C(2), C(3), C(4), C(5)); 125.75 (*d*, C(6), C(7)); 123.84 (*d*, C(8)); 103.33 (*d*, C(1^{I})); 102.86 (*d*), 102.81 (*d*) (C(1^{II}), C(1^{III})); 80.52 (*d*), 80.43 (*d*) (C(4^{I}), C(4^{II})); 76.83 (*d*, C(5^{III})); 76.50 (*d*, C(3^{III})); 75.06 (*d*, C(5^{I})); 74.95 (*d*, C(3^{II}), C(5^{II})); 74.82 (*d*, C(3^{I})); 73.28 (*d*, C(2^{III})); 73.19 (*d*), 73.06 (*d*) (C(2^{I}), C(2^{II})); 70.05 (*d*, C(4^{III})); 69.09 (*t*, ArCH$_2$*C*H$_2$); 61.04 (*t*, C(6^{III})); 60.33 (*t*, C(6^{I}), C(6^{II})); 32.65 (*t*, Ar*C*H$_2$).

*2-(Naphthalen-1-yl)ethyl [β-*D*-Glucopyranosyl-(1 → 4)]$_3$-β-*D*-glucopyranoside* (**T-4**). ^{1}H-NMR (500 MHz, (D$_6$)DMSO): 8.09 (br. *d*, *J* = 8.6), 7.90 (*dd*, *J* = 1.5, 8.0), 7.78 (*dd*, *J* = 1.7, 7.5), 7.54 (*ddd*, *J* = 1.4, 6.8, 7.3), 7.50 (*ddd*, *J* = 1.3, 6.8, 8.1), 7.45 (*dd*, *J* = 2.0, 7.1), 7.42 (*dd*, *J* = 7.1, 7.5) (7 arom. H); 5.373 (*d*, *J* = 5.0), 5.368 (*d*, *J* = 5.0) (HO–C(2^{II}), HO–C(2^{III})); 5.201 (*d*, *J* = 5.0, HO–C(2^{IV})); 5.132 (*d*, *J* = 5.0, HO–C(2^{I})); 4.993 (*d*, *J* = 5.0, HO–C(3^{IV})); 4.964 (*d*, *J* = 5.4, HO–C(4^{IV})); 4.723 (*d*, *J* = 1.6, HO–C(3^{III})); 4.643 (*d*, *J* = 1.5, HO–C(3^{II})); 4.650 (*t*, *J* = 6.5), 4.641 (*t*, *J* ≈ 6.0) (HO–C(6^{II}), HO–C(6^{III})); 4.600 (*d*, *J* = 1.6, HO–C(3^{I})); 4.570 (*t*, *J* = 5.6, HO–C(6^{I}), HO–C(6^{IV})); 4.325 (*d*, *J* = 7.8), 4.311 (*d*, *J* = 7.8, 2 H) (H–C($1^{I–III}$)); 4.231 (*d*, *J* = 7.8, H–C(1^{IV})); 4.02 (*ddd*, *J* = 6.8, 8.1, 9.8, ArCH$_2$C*H*); 3.82–3.72 (*m*, H–C($6^{I–IV}$), ArCH$_2$C*H*); 3.69 (*ddd*, *J* = 2.4, 4.7, 9.4), 3.64–3.54 (*m*, 2 H) (H′–C($6^{I–III}$)); 3.41–3.27 (*m*, H–C($5^{I–III}$), H–C($4^{I–III}$), H–C($3^{I–III}$), H′–C(6^{IV}), ArC*H*$_2$); 3.18 (*ddd*, *J* = 2.3, 6.8, 9.6, H–C(5^{IV})); 3.14 (*dt*, *J* = 4.9, 8.9, H–C(3^{IV})); 3.09–3.01 (*m*, H–C($2^{I–III}$), H–C(4^{IV})); 2.98 (*ddd*, *J* = 4.9, 8.2, 8.7, H–C(2^{IV})). ^{13}C-NMR (75 MHz, (D$_6$)DMSO): 134.68 (*s*, C(1)); 133.50 (*s*, C(4a)); 131.75 (*s*, C(8a)); 128.69, 126.98, 126.90, 126.25 (4*d*, C(2), C(3), C(4), C(5)); 125.73 (*d*, C(6), C(7)); 123.82 (*d*, C(8)); 103.34 (*d*, C(1^{I})); 102.89 (2*d*), 102.81 (*d*) (C($1^{II–IV}$)); 80.55 (*d*), 80.45 (*d*), 80.40 (*d*) (C($4^{I–III}$)); 76.83 (*d*, C(5^{IV})); 76.50 (*d*, C(3^{IV})); 75.06 (*d*), 74.95 (*d*), 74.84 (4*d*) (C($5^{I–III}$) C($3^{I–III}$)); 73.27 (*d*, C(2^{IV})); 73.19 (*d*), 73.01 (2*d*) (C($2^{I–III}$)); 70.05 (*d*, C(4^{IV})); 69.09 (*t*, ArCH$_2$*C*H$_2$); 61.04 (*t*, C(6^{IV})); 60.29 (*t*, C($6^{I–III}$)); 32.65 (*t*, Ar*C*H$_2$).

*2-(Naphthalen-1-yl)ethyl [β-*D*-Glucopyranosyl-(1 → 4)]$_7$-β-*D*-glucopyranoside* (**T-8**). ^{1}H-NMR (500 MHz, (D$_6$)DMSO): 8.09 (br. *d*, *J* = 8.6), 7.91 (*dd*, *J* = 1.6, 8.0), 7.78 (*dd*, *J* = 1.7, 7.4), 7.55 (*ddd*, *J* = 1.5, 6.8, 8.4), 7.50 (*ddd*, *J* = 1.2, 6.8, 8.0), 7.45–7.40 (*m*, 2 H) (7 arom. H); 5.375 (*d*, *J* = 4.9, HO–C($2^{II–VII}$)); 5.205 (*d*, *J* = 5.0, HO–C(2^{VIII})); 5.131 (*d*, *J* = 5.0, HO–C(2^{I})); 5.000 (*d*, *J* = 4.8, HO–C(3^{VIII})); 4.970 (*d*, *J* = 5.3, HO–C(4^{VIII})); 4.726 (br. *s*, HO–C(3^{VII})); 4.62–4.33 (*m*, HO–C($3^{II–VI}$), HO–C($6^{II–VII}$)); 4.600 (br. *s*, HO–C(3^{I})); 4.569 (*t*, *J* ≈ 5.9, HO–C(6^{I}), HOC(6^{VIII})); 4.314 (*d*, *J* = 7.9), 4.310 (*d*, *J* = 7.6, 6 H) (H–C($1^{I–VII}$)); 4.229 (*d*, *J* = 7.8, H–C(1^{VIII})); 4.03 (*ddd*, *J* = 7.0, 8.4, 9.7, ArCH$_2$C*H*); 3.83–3.66 (*m*, H–C($6^{I–VIII}$), ArCH$_2$C*H*); 3.63–3.52 (*m*, H′–C($6^{I–VII}$)); 3.44–3.26 (*m*, H–C($5^{I–VII}$), H–C($4^{I–VII}$), H–C($3^{I–VII}$), H′–C(6^{VIII}), ArC*H*$_2$); 3.18 (*ddd*, *J* = 2.4, 6.1, 9.0, H–C(5^{VIII})); 3.13 (*dt*, *J* = 4.5, 8.8, H–C(3^{VIII})); 3.09–3.01 (*m*, H–C($2^{I–VII}$), H–C(4^{VIII})); 2.97 (*ddd*, *J* = 4.7, 8.1, 8.7, H–C(2^{VIII})). ^{13}C-NMR (75 MHz, (D$_6$)DMSO): 134.68 (*s*, C(1)); 133.51 (*s*, C(4a)); 131.75 (*s*, C(8a)); 128.69 (*d*), 126.98 (2*d*), 126.23 (*d*) (C(2), C(3), C(4), C(5)); 125.73 (*d*, C(6), C(7)); 123.79 (*d*, C(8)); 102.99 (4*d*), 102.87 (4*d*) (C($1^{I–VIII}$)); 80.42 (*d*, C($4^{I–VII}$)); 76.91 (*d*, C(5^{VIII})); 76.60 (*d*, C(3^{VIII})); 74.84 (*d*, C($5^{I–VII}$), C($3^{I–VII}$)); 73.20 (*d*, C(2^{VIII})); 73.01 (*d*, C($2^{I–VII}$)); 70.05 (*d*, C(4^{VIII})); 60.36 (2*t*), 60.28 (2*t*), 60.22 (2*t*), 60.19 (2*t*) (C($6^{I–VIII}$)); 32.74 (*t*, Ar*C*H$_2$); signal for ArCH$_2$*C*H$_2$ hidden by the noise.

*[(Naphthalene-1,8-diyl)di(ethane-2,1-diyl)] Bis(β-*D*-glucopyranoside)* (**T-1-1**). ^{1}H-NMR (500 MHz, (D$_6$)DMSO): 7.79 (*dd*, *J* = 1.2, 8.1), 7.44 (*dd*, *J* = 1.2, 7.1), 7.38 (*dd*, *J* = 7.2, 7.9) (3 arom. H); 4.982 (*d*, *J* = 4.8, HO–C(2^{I})); 4.900 (*d*, *J* = 4.7, HO–C(3^{I})); 4.861 (*d*, *J* = 5.0, HO–C(4^{I})); 4.421 (*t*, *J* = 5.9, HO–C(6^{I})); 4.219 (*d*, *J* = 7.8, H–C(1^{I})); 3.95 (*dt*, *J* ≈ 6.3, 9.7, ArCH$_2$C*H*); 3.68 (*dt*, *J* ≈ 6.8, 9.7, ArCH$_2$C*H*); 3.64 (*ddd*, *J* = 1.7, 5.6, 11.9, H–C(6^{I})); 3.525–3.43 (*AB* of *ABMX*, ArC*H*$_2$); 3.42 (*td*, *J* = 5.8, 11.9, H′–C(6^{I})); 3.13 (*dt*, *J* = 4.7, 8.7, H–C(3^{I})); 3.09 (*ddd*, *J* = 1.9, 5.6, 9.6, H–C(5^{I})); 3.04 (*ddd*, *J* = 4.8, 8.5, 9.6, H–C(4^{I})); 2.98 (*ddd*, *J* = 4.5, 8.1, 8.7, H–C(2^{I})). ^{1}H-NMR (500 MHz, (D$_5$)pyridine): 7.77 (*dd*, *J* = 1.5, 8.1), 7.36 (*dd*, *J* = 1.5, 7.1), 7.31 (*dd*, *J* = 7.1, 7.9) (3 arom. H); 7.14 (*d*, *J* = 3.9, HO–C(3^{I})); 7.13 (*d*, *J* = 4.5, HO–C(2^{I})); 7.12 (*d*, *J* = 4.4, HO–C(4^{I})); 6.31 (*t*, *J* ≈ 6.3, HO–C(6^{I})); 4.90 (*d*, *J* = 7.7, H–C(1^{I})); 4.54 (*ddd*, *J* = 2.5, 6.0, 11.7, H–C(6^{I})); 4.38 (*ddd*, *J* = 5.5, 6.4, 11.8, H′–C(6^{I})); 4.30 (*dt*, *J* = 6.8, 9.8, ArCH$_2$C*H*); 4.25 (*dt*, *J* = 3.6, 8.7, H–C(3^{I})); 4.21 (*ddd*, *J* = 4.6, 8.9, 9.2, H–C(4^{I})); 4.04 (*dd*, *J* = 4.4, 8.4, H–C(2^{I})); 3.96 (*ddd*, *J* = 2.4, 5.3, 9.2, H–C(5^{I})); 3.93 (*dt*, *J* = 6.4, 9.6, ArCH$_2$C*H*); 3.75–3.65 (*AB* of *ABMX*, ArC*H*$_2$). ^{13}C-NMR (75 MHz, (D$_6$)DMSO): 135.60 (*s*, C(4a)); 134.60 (*s*, C(1)); 131.10 (*s*, C(8a)); 130.53, 128.93 (2*d*, C(2), C(4)); 125.20 (*d*, C(3)); 102.99 (*d*, C(1^{I})); 76.90 (*d*, C(5^{I})); 76.80 (*d*, C(3^{I})); 73.45 (*d*, C(2^{I})); 70.23 (*t*, ArCH$_2$*C*H$_2$); 70.05 (*d*, C(4^{I})); 61.03 (*t*, C(6^{I})); 36.58 (*t*, Ar*C*H$_2$).

*[(Naphthalene-1,8-diyl)di(ethane-2,1-diyl)] Bis[β-*D*-glucopyranosyl-(1 → 4)-β-*D*-glucopyranoside]* (**T-2-2**). ^{1}H-NMR (500 MHz, (D$_6$)DMSO): 7.79 (*dd*, *J* = 1.2, 8.1), 7.44 (*dd*, *J* = 1.3, 7.2), 7.38 (*dd*, *J* = 7.2, 7.9) (3 arom. H); 5.197 (*d*, *J* = 4.9, HO–C(2^{II})); 5.146 (*d*, *J* = 5.2, HO–C(2^{I})); 4.979 (*d*, *J* = 5.0, HO–C(3^{II})); 4.958 (*d*, *J* = 5.5,

HO–C(4^{II})); 4.669 (*d*, *J* = 1.3, HO–C(3^{I})); 4.580 (*dd*, *J* = 5.4, HO–C(6^{II})); 4.530 (*t*, *J* = 6.0, HO–C(6^{I})); 4.297 (*d*, *J* = 7.9, H–C(1^{I})); 4.235 (*d*, *J* = 7.9, H–C(1^{II})); 3.95 (*dt*, *J* ≈ 6.2, 9.7, ArCH$_2$C*H*); 3.72 (*ddd*, *J* = 2.2, 5.7, 12.0, H–C(6^{II})); 3.68 (*ddd*, *J* = 2.1, 5.1, 11.3, H–C(6^{I})); 3.74–3.66 (*m*, ArCH$_2$C*H*); 3.59 (*ddd*, *J* = 4.5, 6.3, 11.4, H′–C(6^{I})); 3.50 (*ddd*, *J* = 5.7, 9.1, 13.6, ArC*H*); 3.42 (*ddd*, *J* = 5.4, 9.3, 13.6, ArC*H*); 3.39 (*td*, *J* = 6.3, 12.0, H′–C(6^{II})); 3.35–3.24 (*m*, H–C(3)), H–C(4^{I}), H–C(5^{I})); 3.19 (*ddd*, *J* = 2.1, 6.6, 9.7, H–C(5^{II})); 3.14 (*dt*, *J* = 4.9, 8.9, H–C(3^{II})); 3.05–3.02 (*m*, H–C(2^{I}), H–C(4^{II})); 2.98 (*ddd*, *J* = 4.9, 8.0, 8.9, H–C(2^{II})). ^{1}H-NMR (500 MHz, (D$_5$)pyridine): 7.77 (*dd*, *J* = 1.5, 8.0), 7.35 (*dd*, *J* = 1.4, 7.1), 7.31 (*dd*, *J* = 7.4, 7.9) (3 arom. H); 7.6–7.4 (br. *s*), 7.5–7.2 (br. *s*, 2 H), 6.6–6.3 (br. *s*, 2 H), 5.2–4.8 (br. *s*, 2 H) (7 OH); 5.17 (*d*, *J* = 7.9, H–C(1^{II})); 4.84 (*d*, *J* = 7.8, H–C(1^{I})); 4.53 (*dd*, *J* = 4.7, 12.2, H–C(6^{I})); 4.52 (*dd*, *J* = 2.6, 11.6, H–C(6^{II})); 4.46 (*dd*, *J* = 2.6, 12.2, H′–C(6^{I})); 4.32 (*t*, *J* = 9.0, H–C(4^{II})); 4.27 (*dd*, *J* = 5.6, 11.2, H′–C(6^{II})); 4.26–4.22 (*m*, ArCH$_2$C*H*); 4.25 (*t*, *J* = 8.9, H–C(3^{II})); 4.20 (*t*, *J* = 8.7, H–C(3^{I})); 4.17 (*dd*, *J* = 8.7, 9.1, H–C(4^{I})); 4.09 (*dd*, *J* = 8.1, 8.6, H–C(2^{II})); 4.04 (*dd*, *J* = 8.1, 8.5, H–C(2^{I})); 4.00 (*ddd*, *J* = 2.7, 5.7, 9.2, H–C(5^{II})); 3.94–3.88 (*m*, ArCH$_2$C*H*, H–C(5^{I})); 3.73–3.63 (*AB* of *ABMX*, ArC*H*$_2$). ^{13}C-NMR (75 MHz, (D$_6$)DMSO): 135.60 (*s*, C(4a)); 134.47 (*s*, C(1)); 131.10 (*s*, C(8a)); 130.52, 128.94 (2*d*, C(2), C(4)); 125.20 (*d*, C(3)); 103.31 (*d*, C(1^{I})); 102.58 (*d*, C(1^{II})); 80.55 (*d*, C(4^{I})); 76.81 (*d*, C(5^{II})); 76.47 (*d*, C(3^{II})); 75.11 (*d*, C(5^{I})); 74.85 (*d*, C(3^{I})); 73.32 (*d*, C(2^{II})); 73.12 (*d*, C(2)); 70.29 (*t*, ArCH$_2$*C*H$_2$); 70.05 (*d*, C(4^{II})); 61.02 (*t*, C(6^{II})); 60.33 (*t*, C(6^{I})); 36.48 (*t*, Ar*C*H$_2$).

*[(Naphthalene-1,8-diyl)di(ethane-2,1-diyl)] Bis{[β-*D*-Glucopyranosyl-(1 → 4)]$_2$-β-*D*-glucopyranoside}* (**T-3-3**). ^{1}H-NMR (500 MHz, (D$_6$)DMSO): 7.79 (*dd*, *J* = 1.2, 8.2), 7.74 (*dd*, *J* = 1.2, 7.3), 7.38 (*dd*, *J* = 7.2, 7.9) (3 arom. H); 5.362 (*d*, *J* = 4.3, HO–C(2^{II})); 5.203 (*d*, *J* = 4.6, HO–C(2^{III})); 5.147 (*d*, *J* = 5.0, HO–C(2^{I})); 4.994 (*d*, *J* = 5.0, HO–C(3^{III})); 4.962 (*d*, *J* = 5.4, HO–C(4^{III})); 4.714 (br. *s*, HO–C(3^{II})); 4.645 (*t*, *J* = 5.4, HO–C(6^{II})); 4.598 (br. *s*, HO–C(3^{I})); 4.567 (*t*, *J* = 5.3, HO–C(6^{III})); 4.529 (*t*, *J* = 6.0, HO–C(6^{I})); 4.311 (*d*, *J* = 8.2, H–C(1^{II})); 4.295 (*d*, *J* = 8.1, H–C(1^{I})); 4.229 (*d*, *J* = 7.9, H–C(1^{III})); 3.95 (*dt*, *J* ≈ 5.9, 9.6, ArCH$_2$C*H*); 3.80–3.66 (*m*, 4 H), 3.59 (*dt*, *J* = 11.4, 5.7), 3.56 (*dt*, *J* = 11.9, 5.9) (2 H–C(6^{I}), 2 H–C(6^{II}), H–C(6^{III}), ArCH$_2$C*H*); 3.53–3.46 (*m*, ArC*H*); 3.46–3.25 (*m*, H–C(3^{I}), H–C(3^{II}), H–C(4^{I}), H–C(4^{II}), H–C(5^{I}), H–C(5^{II}), H′–C(6^{III}), ArC*H*); 3.18 (*ddd*, *J* = 2.1, 6.5, 9.3, H–C(5^{III})); 3.14 (*dt*, *J* = 4.8, 8.9, H–C(3^{III})); 3.06–3.01 (*m*, H–C(2^{I}), H–C(2^{II}), H–C(4^{III})); 2.98 (*ddd*, *J* = 4.5, 8.0, 8.6, H–C(2^{III})). ^{1}H-NMR (500 MHz, (D$_5$)pyridine; assignment based on ^{1}H,^{1}H-COSY, ^{1}H,^{13}C-COSY, and TOCSY): 7.79 (*dd*, *J* = 1.5, 7.9), 7.38 (*dd*, *J* = 1.5, 7.1), 7.34 (*dd*, *J* = 7.4, 7.9) (3 arom. H); 7.71 (*d*, *J* = 4.2, HO–C(2^{II})); 7.50 (*d*, *J* = 4.4, HO–C(2^{III})); 7.30 (*d*, *J* = 3.9, HO–C(3^{III})); 7.26 (*d*, *J* = 4.4, HO–C(2^{I})); 7.22 (*d*, *J* = 4.4, HO–C(4^{III})); 6.46 (*t*, *J* = 6.0), 6.45 (*dd*, *J* = 4.4, 6.4) (HO–C(6^{II}), HO–C(6^{III})); 6.40 (*dd*, *J* = 5.7, 7.5, HO–C(6^{I})); 6.37 (*d*, *J* = 1.8, HO–C(3^{II})); 6.20 (*d*, *J* = 1.8, HO–C(3^{I})); 5.17 (*d*, *J* = 8.0, H–C(1^{II})); 5.14 (*d*, *J* = 7.9, H–C(1^{III})); 4.84 (*d*, *J* = 7.8, H–C(1^{I})); 4.57–4.47 (*m*, H–C(6^{I}), 2 H–C(6^{II}), H–C(6^{III})); 4.45 (*ddd*, *J* = 2.7, 5.7, 12.0, H′–C(6^{I})); 4.34–4.23 (*m*, H–C(3^{I}), H–C(3^{II}), H–C(4^{I}), H–C(4^{II}), H′–C(6^{III}), ArCH$_2$C*H*); 4.23–4.18 (*m*, H–C(3^{III}), H–C(4^{III})); 4.09 (*dt*, *J* ≈ 4.1, 8.3, H–C(2^{II}), H–C(2^{III})); 4.04 (*ddd*, *J* = 4.4, 7.8, 8.7, H–C(2^{I})); 4.03–3.97 (*m*, H–C(5^{II}), H–C(5^{III})); 3.93 (*dt*, *J* ≈ 6.7, 9.5, ArCH$_2$C*H*); 3.90 (*ddd*, *J* = 2.4, 5.6, 9.8, H–C(5^{I})); 3.75–3.65 (*AB* of *ABMX*, ArC*H*$_2$). ^{13}C-NMR (75 MHz, (D$_6$)DMSO): 135.57 (*s*, C(4a)); 134.52 (*s*, C(1)); 131.10 (*s*, C(8a)); 130.49, 128.90 (2*d*, C(2), C(4)); 125.18 (*d*, C(3)); 103.33 (*d*, C(1^{I})); 102.87, 102.63 (2*d*, C(1^{II}), C(1^{III})); 80.11, 79.88 (2*d*, C(4^{I}), C(4^{II})); 77.01 (*d*, C(5^{III})); 76.42 (*d*, C(3^{III})); 75.05 (*d*, C(5^{I})); 74.95 (2*d*), 74.72 (*d*) (C(3^{I}), C(3^{II}), C(5^{II})); 73.28 (*d*, C(2^{III})); 73.11, 73.07 (2*d*, C(2^{I}), C(2^{II})); 70.26 (*t*, ArCH$_2$*C*H$_2$); 69.94 (*d*, C(4^{III})); 60.92 (*t*, C(6^{III})); 60.23 (*t*, C(6^{I}), C(6^{II})); 36.48 (*t*, Ar*C*H$_2$).

*[(Naphthalene-1,8-diyl)di(ethane-2,1-diyl)] Bis{[β-*D*-Glucopyranosyl-(1 → 4)]$_3$-β-*D*-glucopyranoside}* (**T-4-4**). ^{1}H-NMR (500 MHz, (D$_6$)DMSO; assignment based on ^{1}H,^{1}H-COSY and ^{1}H,^{1}H-TOCSY): 7.79 (*dd*, *J* = 1.2, 8.1), 7.43 (*dd*, *J* = 1.0, 7.1), 7.38 (*dd*, *J* = 7.4, 7.8) (3 arom. H); 5.369 (*d*, *J* = 5.0), 5.363 (*d*, *J* = 4.9) (HO–C(2^{II}), HO–C(2^{III})); 5.200 (*d*, *J* = 4.9, HO–C(2^{IV})); 5.146 (*d*, *J* = 5.1, HO–C(2^{I})); 4.992 (*d*, *J* = 4.9, HO–C(3^{IV})); 4.963 (*d*, *J* = 5.4, HO–C(4^{IV})); 4.722 (*d*, *J* = 1.6, HO–C(3^{III})); 4.640 (*d*, *J* = 1.5, HO–C(3^{II})); 4.653 (*t*, *J* = 5.7), 4.638 (*t*, *J* = 6.4), (HO–C(6^{II}), HO–C(6^{III})); 4.600 (br. *s*, HO–C(3^{I})); 4.570 (*t*, *J* = 5.3, HO–C(6^{IV})); 4.530 (*t*, *J* = 6.0, HO–C(6^{I})); 4.314 (*d*, *J* = 7.8), 4.308 (*d*, *J* = 7.8) (H–C(1^{II}), H–C(1^{III})); 4.297 (*d*, *J* = 7.8, H–C(1^{I})); 4.229 (*d*, *J* = 7.8, H–C(1^{IV})); 3.95 (*dt*, *J* ≈ 6.3, 9.6, ArCH$_2$C*H*); 3.81–3.66 (*m*, H–C(6$^{I–IV}$), ArCH$_2$C*H*); 3.63–3.24 (*m*, H′–C(6$^{I–IV}$), H–C(5$^{I–III}$), H–C(4$^{I–III}$), H–C(3$^{I–III}$), ArC*H*$_2$); 3.18 (*ddd*, *J* = 2.3, 6.9, 9.3, H–C(5^{IV})); 3.14 (*dt*, *J* = 4.8, 8.7, H–C(3^{IV})); 3.06–3.01 (*m*, H–C(4^{IV}), H–C(2$^{I–III}$)); 2.98 (*ddd*, *J* = 4.9, 8.1, 8.7, H–C(2^{IV})). ^{13}C-NMR (75 MHz, (D$_6$)DMSO; assignment based on ^{1}H,^{13}C-COSY): 135.59 (*s*, C(4a)); 134.47 (*s*, C(1)); 131.09 (*s*, C(8a)); 130.51, 128.94 (2*d*, C(2), C(4)); 125.20 (*d*, C(3)); 103.34 (*d*, C(1^{I})); 102.91 (2*d*), 102.81 (*d*) (C(1$^{II–IV}$)); 80.51, 80.45, 80.38 (3*d*, C(4$^{I–III}$)); 76.83 (*d*, C(5^{IV})); 76.49 (*d*, C(3^{IV})); 75.06 (*d*), 74.84 (5*d*) (C(5$^{I–III}$), C(3$^{I–III}$)); 73.27 (*d*, C(2^{IV})); 73.01 (*d*, C(2$^{I–III}$)); 70.31 (*t*, ArCH$_2$*C*H$_2$); 70.05 (*d*, C(4^{IV})); 61.02 (*t*, C(6^{IV})); 60.29 (*t*, C(6$^{I–III}$)); 36.25 (*t*, Ar*C*H$_2$).

[(Naphthalene-1,8-diyl)di(ethane-2,1-diyl)] Bis{[β-D-Glucopyranosyl-(1 → 4)]$_7$-β-D-glucopyranoside} (**T-8-8**). ^{1}H-NMR (500 MHz, (D_6)DMSO): 7.79 (br. *d*, *J* = 8.2), 7.46–7.41 (*m*), 7.40–7.35 (*m*) (3 arom. H); 5.37 (*d*, *J* = 4.9, HO–C($2^{II–VII}$)); 5.200 (*d*, *J* = 5.0, HO–C(2^{VIII})); 5.323 (*d*, *J* = 4.4, 0.3 H), 5.146 (*d*, *J* = 5.2, 0.4 H), 5.096 (*d*, *J* = 5.3, 0.15 H), 4.772 (*d*, *J* = 5.3, 0.15 H) (HO–C(2^I)); 4.994 (*d*, *J* = 4.8, HO–C(3^{VIII})); 4.962 (*d*, *J* = 5.4, HO–C(4^{VIII})); 4.722 (*s*, HO–C(3^{VII})); 4.69–4.61 (*m*, 0.4 HO–C(3^I), 0.25 HO–C(6^I), HO–C($3^{II–VI}$), HO–C($6^{II–VII}$)); 4.596 (*s*, 0.4 H), 4.459 (br. *s*, 0.2 H) (0.6 HO–C(3^I)); 4.565 (*t*, *J* = 5.3, HO–C(6^{VIII})); 4.529, 4.527 (2*t*, *J* ≈ 5.9, 0.55 H), 4.435 (*t*, *J* = 6.1, 0.2 H) (0.75 HO–C(6^I)); 4.31 (*d*, *J* = 7.7, H–C($1^{I–VII}$)); 4.229 (*d*, *J* = 7.7, H–C(1^{VIII})); 3.99–3.92 (*m*, $ArCH_2CH$); 3.82–3.66 (*m*, H–C($6^{I–VIII}$), $ArCH_2CH$); 3.63–3.24 (*m*, H′–C($6^{I–VIII}$), H–C($5^{I–VII}$), H–C($4^{I–VII}$), H–C($3^{I–VII}$), $ArCH_2$); 3.19 (*ddd*, *J* = 1.9, 6.5, 9.7, H–C(5^{VIII})); 3.14 (*dt*, *J* = 5.0, 8.9, H–C(3^{VIII})); 3.09–3.01 (*m*, H–C(4^{VIII}), H–C($2^{I–VII}$)); 2.98 (*ddd*, *J* = 5.2, 8.1, 8.6, H–C(2^{VIII})). ^{13}C-NMR (75 MHz, (D_6)DMSO): 135.60 (*s*, C(4a)); 134.50 (*s*, C(1)); 131.09 (*s*, C(8a)); 130.50, 128.90 (2*d*, C(2), C(4)); 125.14 (*d*, C(3)); 103.0 (*d*, C($1^{I–VIII}$)); 80.45 (*d*, C($4^{I–VII}$)); 76.84 (*d*, C(5^{VIII})); 76.52 (*d*, C(3^{VIII})); 74.84 (*d*, C($5^{I–VII}$), C($3^{I–VII}$)); 73.35 (*d*, C(2^{VIII})); 73.01 (*d*, C($2^{I–VII}$)); 70.35 (*t*, $ArCH_2CH_2$); 70.06 (*d*, C(4^{VIII})); 60.3 (*t*, C($6^{I–VIII}$)); 36.56 (*t*, $ArCH_2$).

Acetylation of **T-8-8**. A soln. of **T-8-8** (21 mg) and LiCl (30 mg) in *N*,*N*-dimethylacetamide (1 ml) was treated with Ac_2O (0.5 ml) and pyridine (1 ml), and stirred at r.t. for 16 h. Evaporation, workup (AcOEt), and FC (hexane/AcOEt/MeOH 10 : 10 : 1 → 20 : 20 : 3) gave the peracetate of **T-8-8** [1] (33 mg).

REFERENCES

[1] J. Xu, A. Vasella, *Helv. Chim. Acta* **1999**, *82*, 1728.
[2] J. Sugiyama, T. Imai, *Trends Glycosci. Glycotechnol*. **1999**, *11*, 23.
[3] T. Kondo, in 'Polysaccharides, Structural Diversity and Functional Versatility', Ed. S. Dumitriu, Marcel Dekker Inc., New York, 1998, p. 131.
[4] G. Meshitsuka, A. Isogai, in 'Chemical Modification of Lignocellulosic Materials', Ed. D. N.-S. Hon, Marcel Dekker Inc., New York, 1996, p. 11.
[5] T. Imai, J. Sugiyama, T. Itoh, F. Horii, *J. Struct. Biol*. **1999**, *127*, 248.
[6] J. Sugiyama, T. Okano, H. Yamamoto, F. Horii, *Macromolecules* **1990**, *23*, 3196; J. Sugiyama, J. Persson, H. Chanzy, *Macromolecules* **1991**, *24*, 2461; J. Sugiyama, R. Vuong, H. Chanzy, *Macromolecules* **1991**, *24*, 4168.
[7] E. M. Debzi, H. Chanzy, J. Sugiyama, P. Tekely, G. Excoffier, *Macromolecules* **1991**, *24*, 6816.
[8] K. H. Gardner, J. Blackwell, *Biopolymers* **1974**, *13*, 1975.
[9] C. Woodcock, A. Sarko, *Macromolecules* **1980**, *13*, 1183.
[10] D. P. Miller, A. Li, in 'Cellulose and Wood Chemistry and Technology', Ed. C. Schuerch, John Wiley, New York, 1989, p. 139.
[11] V. L. Finkenstadt, R. P. Millane, *Macromolecules* **1998**, *31*, 7776.
[12] F. J. Kolpak, J. Blackwell, *Macromolecules* **1976**, *9*, 273.
[13] A. J. Stipanovic, A. Sarko, *Macromolecules* **1976**, *9*, 851.
[14] H. A. Krässig, in 'Cellulose Structure, Accessibility and Reactivity', Ed. M. B. Huglin, Gordon and Breach Science Publishers, Yverdon, 1992, p. 6.
[15] F. Horii, A. Hirai, R. Kitamaru, *Polym. Bull*. **1983**, *10*, 357.
[16] K. Gessler, N. Krauss, T. Steiner, C. Betzel, A. Sarko, W. Saenger, *J. Am. Chem. Soc*. **1995**, *117*, 11397; K. Gessler, N. Krauss, T. Steiner, C. Betzel, C. Sandmann, W. Saenger, *Nature* **1994**, *266*, 1027.
[17] S. Raymond, A. Heyraud, D. Tran Qui, A. Kvick, H. Chanzy, *Macromolecules* **1995**, *28*, 2096.
[18] L. M. J. Kroon-Batenburg, J. Kroon, *Glycoconjugate J.* **1997**, *14*, 677.
[19] P. Langan, Y. Nishiyama, H. Chanzy, *J. Am. Chem. Soc*. **1999**, *121*, 9940.
[20] G. A. Jeffrey, W. Saenger, 'Hydrogen Bonding in Biological Structures', Springer-Verlag, Berlin, 1991.
[21] G. Tuchscherer, M. Mutter, *J. Biotechnol*. **1995**, *41*, 197.
[22] J. P. Schneider, J. W. Kelly, *Chem. Rev*. **1995**, *95*, 2169.
[23] L. J. J. Hronowski, W. A. Szarek, G. W. Hay, A. Krebs, W. T. Depew, *Carbohydr. Res.* **1991**, *219*, 33.
[24] A. R. Vaino, W. T. Depew, W. A. Szarek, *Chem. Commun*. **1997**, 1871.
[25] R. R. Schmidt, K. Jankowski, *Liebigs Ann. Chem*. **1996**, 867.
[26] T. M. Herrington, A. D. Pethybridge, B. A. Parkin, M. G. Roffey, *J. Chem. Soc., Faraday Trans. 1* **1983**, *79*, 845.
[27] M. L. Wolfrom, J. C. Dacons, *J. Am. Chem. Soc*. **1952**, *74*, 5331.
[28] C. L. McCormick, P. A. Callais, J. B. H. Hutchinson, *Macromolecules* **1985**, *18*, 2394.
[29] J. M. Harvey, M. C. R. Symons, R. J. Naftalin, *Nature (London)* **1976**, *261*, 435.
[30] L. Poppe, H. van Halbeek, *J. Am. Chem. Soc*. **1991**, *113*, 363; S. Sheng, H. van Halbeek, *Biochem. Biophys. Res. Commun*. **1995**, *215*, 504.

[31] L. Poppe, H. van Halbeek, *Struct. Biol.* **1994**, *1*, 215.
[32] B. Adams, L. E. Lerner, *Magn. Reson. Chem*. **1994**, *32*, 225.
[33] B. R. Leeflang, J. F. G. Vliegenthart, L. M. J. Kroon-Batenburg, B. P. van Eijck, J. Kroon, *Carbohydr. Res.* **1992**, *230*, 41.
[34] B. Bernet, A. Vasella, *Helv. Chim. Acta* **2000**, *83*, 2055.
[35] L. M. J. Kroon-Batenburg, J. Kroon, B. R. Leeflang, J. F. G. Vliegenthart, *Carbohydr. Res.* **1993**, *245*, 21.
[36] M. Ikura, K. Hikichi, *Carbohydr. Res.* **1987**, *163*, 1.
[37] Y. Nishida, H. Hori, H. Ohrui, H. Meguro, *J. Carbohydr. Res.* **1988**, *7*, 239.
[38] K. Bock, J. O. Duus, *J. Carbohydr. Chem*. **1994**, *13*, 513.
[39] B. Bernet, A. Vasella, *Helv. Chim. Acta* **2000**, *83*, 995.
[40] B. Gillet, D. Nicole, J.-J. Delpuech, B. Gross, *Org. Magn. Reson*. **1981**, *17*, 28.
[41] J. C. Christofides, D. B. Davies, *J. Am. Chem. Soc*. **1983**, *105*, 5099.
[42] B. N. Craig, M. U. Janssen, B. M. Wickersham, D. M. Rabb, P. S. Chang, D. J. Oleary, *J. Org. Chem*. **1996**, *61*, 9610.
[43] J. C. Christofides, D. B. Davies, *Magn. Reson. Chem*. **1985**, *23*, 582.
[44] A. Bax, D. G. Davis, *J. Magn. Reson*. **1985**, *64*, 533.
[45] A. A. Bothner-By, R. L. Stephens, J. Lee, *J. Am. Chem. Soc*. **1984**, *106*, 811.
[46] C. J. Bauer, T. A. Frenkiel, A. N. Lane, *J. Magn. Reson*. **1990**, *87*, 144.
[47] W. R. Croasmun, R. M. K. Carlson, 'Two-Dimensional NMR Spectroscopy', VCH Publishers, New York, 1994, p. 341.
[48] B. R. Leeflang, J. B. Bouwstra, J. Kerekgyarto, J. P. Kamerling, J. F. G. Vliegenthart, *Carbohydr. Res.* **1990**, *208*, 117.
[49] F. Mohamadi, N. G. J. Richards, W. C. Guida, R. Liskamp, C. Caufield, M. Lipton, G. Chang, T. Hendrickson, W. C. Still, *J. Comput. Chem*. **1990**, *11*, 440.
[50] M. J. Kamlet, J. L. M. Abboud, M. H. Abraham, R. W. Taft, *J. Org. Chem*. **1983**, *48*, 2877; M. J. Kamlet, J. F. Gal, P. C. Maria, R. W. Taft, *J. Chem. Soc., Perkin Trans. 2* **1985**, 1583.
[51] H. Sugiyama, T. Usui, *Agric. Biol. Chem.* **1980**, *44*, 3001.
[52] K. Koike, C. Bevelle, S. K. Talapatra, G. Cordell, N. R. Farnsworth, *Chem. Pharm. Bull*. **1980**, *28*, 401.
[53] T. Nohara, Y. Ito, H. Seike, T. Komori, M. Moriyama, *Chem. Pharm. Bull*. **1982**, *30*, 1851.
[54] T. Miyase, K. Yamaki, S. Fukushima, *Chem. Pharm. Bull*. **1984**, *32*, 3912; Y. Inose, T. Miyase, A. Ueno, *Chem. Pharm. Bull*. **1991**, *39*, 2037.
[55] K. Ori, Y. Mimaki, K. Mito, Y. Sashida, T. Nikaido, *Phytochemistry* **1992**, *31*, 2767.
[56] Y. Shao, B. Zhou, L. Lin, G. A. Coedell, *Phytochemistry* **1995**, *38*, 927.
[57] T. Miyase, M. Kuroyanagi, T. Noro, A. Ueno, S. Fukushima, *Chem. Pharm. Bull*. **1985**, *33*, 4445.
[58] P. R. Muddasani, E. Bozo, B. Bernet, A. Vasella, *Helv. Chim. Acta* **1994**, *77*, 257.
[59] P. Sohàr, 'Nuclear Magnetic Resonance Spectroscopy', CRC Press, Florida, 1983, p. 97.
[60] C. A. Fyfe, P. J. Stephenson, R. P. Veregin, G. K. Hamer, R. H. Marchessault, *J. Carbohydr. Chem*. **1984**, *3*, 663.
[61] A. Isogai, M. Usuda, T. Kato, T. Uryu, R. H. Atalla, *Macromolecules* **1989**, *22*, 3168.
[62] R. H. Atalla, D. L. VanderHart, *Science* **1984**, *223*, 283.
[63] F. Horii, A. Hirai, R. Kitamaru, 'Cross-Polarization/Magic Angle Spinning ^{13}C-NMR Study: Molecular Chain Conformation of Native and Regenerated Cellulose', in 'Polymers for Fibers and Elastomers', Ed. J. J. C. Arthur, Am. Chem. Soc. Washington, D. C., 1984, ACS Symp. Series, No. 260, p. 27.
[64] P. T. Larsson, K. Wickholm, T. Iversen, *Carbohydr. Res.* **1997**, *302*, 19.
[65] R. L. Dudley, C. A. Fyfe, P. J. Stephenson, Y. Deslandes, G. K. Hamer, R. H. Marchessault, *J. Am. Chem. Soc*. **1983**, *105*, 2469.
[66] B. Henrissat, S. Perez, I. Tvaroska, W. T. Winter, in 'The Structures of Cellulose', Ed. R. H. Atalla, American Chemical Society, Washington, DC, 1987, ACS Symposium Series 340, p. 38.
[67] G. M. Brown, H. A. Levy, *Acta Crystallogr., Sect. B* **1979**, *35*, 656.
[68] R. C. G. Killean, W. G. Ferrier, D. W. Young, *Acta Crystallogr*. **1962**, *15*, 911.
[69] H. M. Berman, S. H. Kim, *Acta Chem. Scand., Ser. B* **1968**, *24*, 897.
[70] W. G. Ferrier, *Acta Crystallogr*. **1963**, *16*, 1023.
[71] G. A. Jeffrey, S. Takagi, *Acta Chem. Scand., Ser. B* **1977**, *33*, 738.
[72] J. T. Ham, D. G. Williams, *Acta Crystallogr., Sect. B* **1970**, *26*, 1373.

Received June 14, 2000